Evaluation of alternatives for hydraulic analysis of sanitary sewer systems

by

George Adrian van Heerden

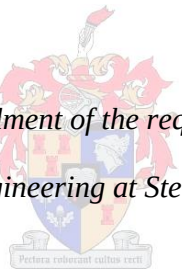

Thesis presented in partial fulfilment of the requirements for the degree of

Master of Science in Engineering at Stellenbosch University

Supervisor: Prof. H.E. Jacobs

April 2014

Declaration

By submitting this thesis electronically, I declare that the entirety of the work contained therein is my own, original work, that I am the sole author thereof (save to the extent explicitly otherwise stated), that reproduction and publication thereof by Stellenbosch University will not infringe any third party rights and that I have not previously in its entirety or in part submitted it for obtaining any qualification.

Name: George Adrian van Heerden

Number: .....

Signed: .....

Date: .....

Sinopsis

Hierdie navorsing projek is gefokus op riool dreineringsisteme. Wanneer ŉ analise van ŉ riool dreineringsisteem met bekende beperkinge onderneem word, moet ŉ geskikte model gekies word afhangende van die doelwitte van die analise. Onbekendes is ook teenwoordig in die analise van riool dreineringsisteme. Dit word belangrik dat die onsekerhede en die foute in hidroliese modelle moet verstaan en oorweeg word. Die verwagte vlak van akkuraatheid en die tipe hidroliese probleem wat opgelos moet word mag die ingewikkeldheid van die hidroliese probleem, wat gebruik word om ŉ rioolsisteem op te los, verander. Die wye verskeidenheid van beskikbare simulasie modelle bemoeilik verder die keuse van ŉ model. Met etlike modelle beskikbaar vir seleksie, is die mees geskikte model vir ŉ spesifieke dreineringsisteem simulasie belangrik.

Die verskeie modelle vir riool dreineringsisteem analise kan op verskillende wyses gekategoriseer word. Byvoorbeeld, dit is moontlik om modelle te kategoriseer volgens hulle doel, wat evaluasie, ontwerp en beplanning kan wees. Evaluasiemodelle word hoofsaaklik gebruik om te toets of huidige of beplande sisteme voldoende is en of hulle die hoogs moontlike hidroliese besonderhede benodig. Ontwerpmodelle word gebruik om die grootte van ŉ leipyp binne ŉ rioolsisteem te bepaal en benodig matige vlakke van hidroliese besonderhede. Beplanningsmodelle word hoofsaaklik gebruik vir strategiese beplanning en besluitneming vir stedelike en landelike rioolsisteme en benodig die laagste vlak van hidroliese data. ŉ Begrip van die beskikbare modelle is nodig om ŉ keuse te maak rakende die mees geskikte simulasie model vir die verlangde doelwit.

Sommige modelle is afkomstig van die Saint-Venant vergelykings van vloei. Die mees gedetailleerde modelle word tipies na verwys as die volledige dinamiese golf modelle en benut alle komponente van die Saint-Venant vloei vergelykings. Deur die verwydering van terme van die Saint-Venant vergelykings kan ŉ kinematiese golf model daargestel word. Sommige minder gekompliseerde modelle ignoreer die basiese beginsels van hidrologie om aannames te maak wat die proses van golf simulering vereenvoudig. In hierdie tesis is drie verskillende modelle vergelyk; ŉ gedetailleerde model wat volledige dinamiese vloeivergelykings gebruik; ŉ vereenvoudigde model wat kinematiese golfvergelykings gebruik en ŉ basiese model wat bydraende hidroliese versending vergelykings. Vir die dreineringsisteem analise was SWMM-EXTRAN gebruik as die volledige dinamiese

golfmodel, SWMM-TRANSPORT was gebruik as die kinetiese golfmodel en SEWSAN was gebruik as die bydraende hidroliese model.

Twee dreineringsisteme in Suid-Afrika was gebruik as gevallestudies en word na verwys as Dreineringsisteem A en Dreineringsisteem B. Die werklike vloeikoers was aangeteken by twee punte met vloeimeters, een in elk van die sisteme. Die vloeikoers was deurlopend opgeteken met 1 uur tussenposes vir die periode 1 Julie 2010 tot 9 Julie 2010 in Dreinering Sisteem A sowel as Dreinering Sisteem B. Dieselfde inset parameters was gebruik vir elke model wat dit moontlik gemaak het dat die gemoduleerde vloeikoerse met die gemete vloeikoerse vergelyk kon word.

Die modelle het spits vloeiresultate voorsien wat binne 2% van die gemete spits vloeikoerse was en, in die meeste situasies, dat die gemoduleerde gemiddelde vloei binne 8.5% van die gemete gemiddelde vloei was. Wanneer vinnig varierende vloei voorgekom het, die kinetiese golf and bydraende hidrograaf modelle konserwatiewe resultate gelewer het, aangesien hulle nie in staat was om hidroliese effekte soos versnelling te verklaar nie. Die effek van versnelling was op sy duidelikste stroomopwaarts en stroomafwaarts onder valstrukture en by gedeeltes waar die helling aansienlik verander het. Die kinetiese golf en bydraer hidrograaf modelle was gevolglik nie in staat om oorladingsomstandighede akkuraat te simuleer nie.

Die resultate wys dat die volledige dinamiese vloeimiddel gebruik kan word in alle omstandighede. Die kinematiese vloeimiddel kan gebruik word vir ’n ontwerp analise indien geen hidroliese struktuur in die sisteem voorkom nie. Die bydraer hidrograaf model behoort nie gebruik te word vir ’n evaluerings analise nie, maar kan gebruik word vir ’n ontwerp analise indien ’n relatiewe hoë vlak van vertroue in die parameter stel bestaan en geen area van vinnig veranderende vloei of hidroliese strukture binne die sisteem bestaan nie.

Synopsis

This research project focuses on sanitary sewer systems. When performing an analysis of a sewer drainage system with known constraints, an appropriate model needs to be chosen depending on the objectives of the analysis. Uncertainties are also present in the analysis of sewer drainage systems. The uncertainties and the errors in hydraulic models need to be understood and considered. The required level of accuracy and the type of hydraulic problem that needs to be solved may alter the complexity of the hydraulic model used to solve a drainage system. The wide variety of available simulation models further complicates model selection. With various models available, selecting the most appropriate model for a particular drainage system simulation is important.

The various models for sewer drainage system analysis can be categorised in different ways. For example, it is possible to categorise models according to their purpose, which could be evaluation, design or planning. Evaluation models are mainly used to test whether existing systems or planned systems are adequate and require the highest hydraulic detail. Design models are used to determine the size of conduits within a drainage system and require moderate levels of hydraulic detail. Planning models are primarily used for strategic planning and decision making for urban or regional drainage systems and require the least amount of hydraulic detail. An understanding of the available models is required in order to choose the most suitable simulation model for the desired purpose.

Some models are derived from the Saint-Venant equations of flow. The most detailed models are typically referred to as fully dynamic wave models and utilise all the components of the Saint-Venant flow equations. By removing terms from the Saint-Venant equations a kinematic wave model can be created. Some less complex models ignore basic principles of hydraulics in order to make assumptions that simplify the process of simulating flows. In this thesis three different models were compared: a detailed model using fully dynamic flow equations, a simplified model using kinematic wave equations and a basic model using contributor hydrograph routing equations. For the drainage system analysis SWMM-EXTRAN was used as the fully dynamic wave model, SWMM-TRANSPORT was used as the kinematic wave model and SEWSAN was used as the contributor hydrograph model.

Two drainage systems situated in South Africa were used as case studies and are referred to as Drainage System A and Drainage System B in this thesis. The actual flow rate was

recorded at two points with flow loggers, one in each of the two systems. The flow rate was continually recorded at 1 hour intervals for the period 1 July 2010 to 9 July 2010 in Drainage System A as well as in Drainage System B. The same input parameters were used for each model allowing the modelled flow rates to be compared to the measured flow rates.

The models provided peak flow results that were within 2% of the measured peak flow rates and the modelled mean flows were within 8.5% of the measured mean flows in most situations. However, when rapidly varied flows occurred the kinematic wave and contributor hydrograph models returned conservative results as they were unable to account for hydraulic effects such as acceleration. The effect of acceleration became most pronounced up and downstream of drop structures and sections where the slope changed considerably. The kinematic wave and contributor hydrograph models were therefore unable to accurately simulate surcharge conditions.

The results suggest that the fully dynamic wave model can be used in all scenarios. The kinematic wave model can be used for a design analysis if no hydraulic structures occur in the system. The contributor hydrograph model should not be used for an evaluation analysis, but can be used for a design analysis if a relatively high level of confidence in the parameter set exists and no areas of rapidly varying flow or hydraulic structures exist within the system.

Acknowledgements

Firstly, I would like to thank my wife, Caroline, for her unending support without which my thesis would never have come this far. Secondly, I would like to thank Prof. Heinz Jacobs for his support and tireless proofreading of my thesis. If it were not for his efforts this thesis would not be what it is today. I would like to thank Dr. Alex Sinske, Altus de Klerk, and Kerry Fair for their valued input and support. I would also like to thank GLS Consulting for allowing me the opportunity to pursue post-graduate studies. Finally, I would like to thank my family for their never ending support.

Contents

List of equations

List of figures

List of tables

List of symbols

A	Cross-sectional area of flow normal to x
$\bar{A}$	Average cross-sectional area of flow within the conduit
AADD	Average Annual Daily Demand
β	Boussinesq momentum flux correction coefficient
g	Gravitational acceleration
h	Depth of flow along Y
h_L	Local energy loss per unit length
K	Local loss coefficient
K_n	Manning formula conversion constant (1.486 for imperial and 1.0 for SI units).
k_s	Nikuradse pipe roughness
ℓ	Litres
t	Time
θ	The angle between the conduit and the horizontal plane
n	Manning's roughness coefficient
Q	Discharge
R	Hydraulic radius
$\bar{R}$	Average hydraulic radius
Re	Reynolds number
S_f	Friction slope
S_O	Slope of the conduit
V	Flow velocity
$\bar{V}$	Average flow velocity

X	Flow direction of the sewer
Y	Direction normal to x on the vertical plane
Y_i^{obs}	Observed flow at time *i*
Y_i^{sim}	Modelled flow at time *i*
Y^{mean}	Mean of the observed flow

List of abbreviations

AADD	Average annual daily demand
ISS	Illinois Storm Sewer System Simulation
SWMM	Storm Water Management Model
SWMM-EXTRAN	SWMM Extended Transport Block
SWMM-TRANSPORT	SWMM transport block
SEWSAN	Sewer and sanitation model
CAREDAS	Calcul des Reseaux d'assainissement (Calculation of sewage networks)
MOUSE	Model for urban sewers
SOGREAH	Societe Grenobloise d'Etudes et d'Applications Hydrauliques

1. Introduction

1.1. Background

Unknowns are present in the analysis of sewer systems. These unknowns might be socio-economic, environmental, structural, hydrologic or hydraulic in nature. Uncertainties in describing parameters as well as errors resulting from hydraulic models can be substantial. Decisions based on hydraulic models are becoming increasingly common, and the results obtained from simulations affect decision making. It has therefore become vital that the uncertainties and the errors in hydraulic models be understood and considered.

A drainage system accounts for a large portion of the overall expense of waste disposal. Substantial savings could theoretically be effected with improved designs of systems. Design procedures involve balancing pipe slope and size to provide sufficient peak flow capacity while also maintaining sufficient scouring flow velocities at average or minimum flows. Various scenarios are considered, and a least-cost scenario is generally chosen. The effectiveness of the procedure depends on the experience of designers, and inexperience often results in an optimal scenario not being reached.

The required level of accuracy and the type of hydraulic problem that needs to be solved may alter the complexity of the hydraulic model used to solve a drainage system. Hydraulic problems in the case of drainage systems can broadly be separated into three types: planning, design and evaluation.

When designing drainage systems, all the various components, including conduits and other facilities such as pumps, need to be sized optimally. In South Africa sewer systems should be designed to separate storm water from sewage, though some ingress may occasionally occur. In other countries where combined sewer and storm water drainage systems are constructed, engineers need to take rainfall or design storms into account. When sanitary sewers are being designed, the runoff from residential, commercial and industrial stands over the life of a drainage system should be considered.

Due to large numbers of differing and often complex flows, drainage systems have not always been analysed by means of complex hydraulic models. Simplified models have been employed to save computational time and to reduce errors. The wide variety of possible

simulation models can often lead to confusion. A proper understanding needs to be gained in order to choose the optimal simulation model for the desired level of results.

1.2. Terminology

Commonly used terms in the thesis are defined as follows:

- *Drainage system* refers to the total sewer system, including topology and loads, which can be the physical real-world system or a simplified representation of the system used for analysis purposes.
- *Drainage system topology* refers to the physical layout of a drainage system as well as the dimensions of conduits and manholes, which can be the real-world topology or a simplified representation for analysis purposes.
- *Drainage system loads* refers to the flows that come into the system, which can be physical inflows and ingress into a drainage system or simplified representations of inflows for analysis purposes.
- *Model* refers to a mathematical method of calculating the flows within a drainage system.
- *Software* refers to a computer program that is capable of analysing the hydraulic model of a drainage system.
- *Simulation* refers to the act of using a model to analyse a drainage system in order to obtain the flows.
- *Design* refers to the general layout and sizing of conduits of the drainage system and does not extend to the detailed design of hydraulic structures.
- *Conduit* refers to any structure, be it an open channel or a closed pipe, which transports flow downstream in a drainage system. In sewer systems, a conduit is usually a closed pipe or tunnel and is connected at either end to a manhole.
- *Rising main* refers to a pipe that transports flows within a drainage system by making use of pumps instead of relying on gravitational forces.
- *Manhole* refers to structures that are situated at the start and end of conduits or rising mains.
- *Dendritic layout* refers to a drainage system that does not split into multiple downstream routes.
- *Stand* refers to a plot of land that is serviced by a drainage system.

1.3. Problem statement

When performing an analysis of a sewer drainage system with known constraints or parameter set, it is often not known which model would be appropriate and would provide the proper results. Uncertainties as well as the objective of an analysis are intrinsic to the dilemma of choice. The level of uncertainty varies and stems from a range of sources used to compile a theoretical drainage system of the actual system being simulated. For example, uncertainties could be present in data obtained for the sole purpose of calibrating a system. Uncertainty may be reduced, but can never be fully removed.

The process of designing drainage systems, such as storm water or sewer systems, requires that flow within each conduit of the system be analysed. Numerous models with which to analyse dry- or wet-weather flows are available. Models vary in complexity and accuracy. The influence that selected models and corresponding parameters have on the results of an analysis was the focus of this research. The manner in which assumptions and simplifications affect results need to be understood in order to accurately address the problem.

1.4. Motivation

This study investigated a few available models used to analyse gravity-induced flow within urban drainage systems in order to aid the process of choosing an appropriate model for a given problem. A comparison would allow various strengths and shortcomings of models to be highlighted, allowing a basic outline to be provided that could aid modellers when analysing an urban drainage system. Though the fundamentals of modelling storm water and sewer systems are similar, the focus of this study was on sewer systems.

Often modellers have to decide which of the models best suit their needs, and a decision should not be made without proper understanding of the various shortcomings of each model. More importantly, it should be understood how shortcomings will impact the results of the analysis. Decisions impact the quality and accuracy of results, as well as the costs incurred due to time spent on design and data acquisition. This study provides a reference point for model selection so that a suitable model for a design purpose can be chosen..

1.5. Research objectives

The following research objectives were set for this study:

- To provide a detailed literature review of previous work done on drainage system analysis, models of partially full pipe flow, uncertainty with regard to modelling large drainage systems and available software packages.
- To provide an exposition of a few available models.
- To select three models to compare with one another. Each of the three models had to be of differing hydraulic sophistication to allow for a comparison of models or philosophies.
- To compare the various models against two large, physical drainage systems.
- To perform a sensitivity analysis of the model parameters.
- To provide an outline to show when a model will provide reasonable results.

1.6. Case study selection

As part of this research, the result sets for each of the three selected model types: the fully dynamic wave model, the kinematic wave and the contributor hydrograph model were compared to sewage flow measurements from actual drainage systems. Two drainage systems were selected for this purpose from one of South Africa's largest urban areas. The longitudinal sections chosen represented the outfall conduits of the drainage systems and excluded small-diameter conduits. The conduits were mostly rectangular brick tunnels with depths greater than a metre. The theoretical results were then compared to recorded flows near the lowest point of each drainage system.

The flow capacities from the models were subsequently compared in certain conduits where one or more models indicated surcharge conditions. Such cases occurred where flow structures were found or where the slope rapidly changed within the system. The results were then compared statistically, and a sensitivity analysis was performed to determine which factors affected the resultant hydrographs the most, allowing for a comparison between models and objectives.

1.7. Methodology

Figure 1:1 illustrates the process followed to verify the results from the models chosen. Two physical drainage systems were chosen. Flow rates which were measured at two points, one within each drainage system, were used to verify modelled flow hydrographs. The drainage system was simplified to create a theoretical drainage system that could be coupled with a mathematical model to produce modelled flow hydrographs. The modelled flows were then compared to the measured flow hydrographs and the results verified with the use of statisical equations. The results were then compiled and discussed.

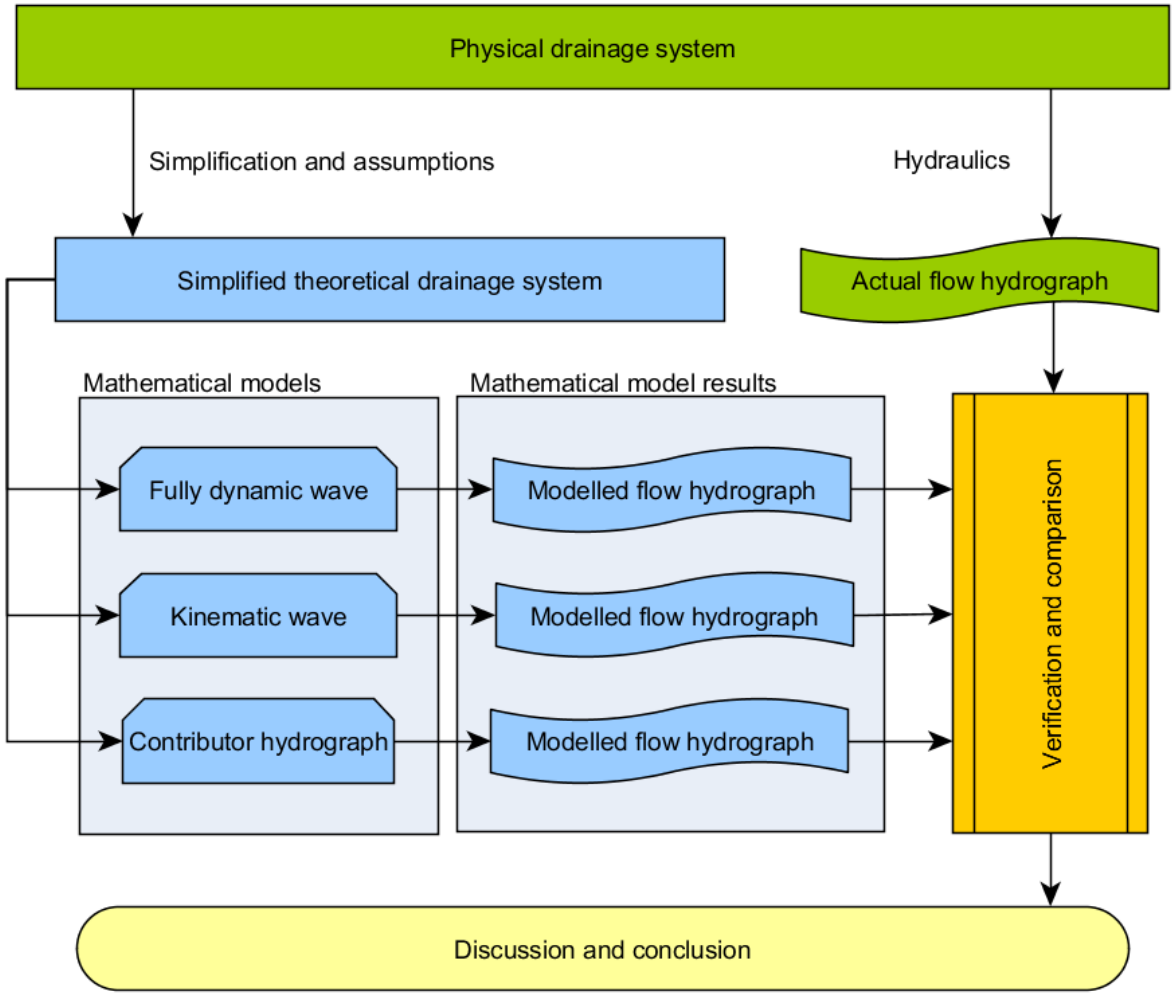

Figure 1:1: Schematic of testing methodology

Figure 1:2 adds further detail to Figure 1:1 with regards to the mathematical models and how the flow hydrographs were calculated in order to provide data for verification and comparison. Figure 1:2 illustrates which models were chosen and the software used for each.

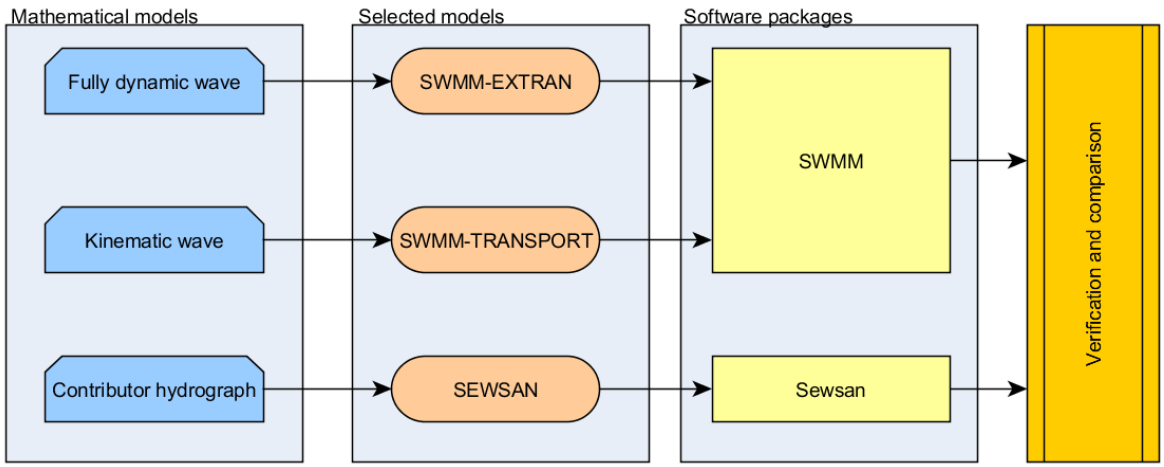

Figure 1:2: Schematic diagram of models and software used

1.8. Scope and limitations

The study included steady and unsteady flow conditions. Complex aspects of hydraulics, such as aeration, were not considered. The effects of pumps and rising mains were not investigated as part of this research, because the same theory typically applies to all models. A list of models was considered after which three models were selected for investigation. The results could be extrapolated to a certain extent when considering other models that rely on similar mathematical equations. Optimisation routines and sedimentation were considered beyond the scope of this study.

The research also excluded a few unconventional types of sewer systems, briefly discussed in the sub-sections below.

1.8.1. Combined sewer systems

Systems that are designed to transport both sewage and storm water through a single system of pipes are known as combined sewer systems (CSSs). When little or no rain falls, the CSS is able to transport all sewage to downstream wastewater treatment plants. During times of wet-weather flow (WWF), the system may reach its design capacity and become unable to deliver all sewage, resulting in overflows known as combined sewer overflows (CSOs) (Water Environment Federation, 1999).

Storm water systems often use retention storage facilities that are able to capture and dispose of storm water through evaporation, infiltration, percolation and other means. Detention storage as used by CSOs stores any overflow before releasing flows back into the sewerage system at a lower rate.

1.8.2. Pressure sewer systems

Pump stations and pressure mains have been used for a long time within sewer systems. Clift (1968) was one of the first to report on pressure systems in a case study of 42 houses. The case study was abandoned due to equipment issues. There were, however, no major obstacles surrounding the concept.

1.8.3. Vacuum sewer systems

Vacuum sewers use an air pressure differential to move waste water through a system of pipes. A source is required to constantly maintain a vacuum throughout the system. In order to maintain a vacuum, valves are required at all points of entry into the system. The valves are designed to open when a certain waste level has been achieved. The difference in pressure drives the waste through the system.

The benefits of vacuum sewers are small conduit sizes, no required manholes, shallower conduits, shallow depths requiring narrower trenches, high velocities that reduce the risk of blockages, maintenance crews that are not subjected to the dangers of hydrogen sulphide gases, leaks that cannot go unnoticed, a single required source of power and reduced cost of treatment plants.

Models used to describe vacuum sewers are notably different from those for waterborne sewers, and thus were excluded from this study.

1.8.4. Small bore sewer systems

Small bore sewers are also called solids-free sewers or effluent sewers. In this text the notation by Little (2004) is adopted. Effluent sewers can be divided into two groups: those using gravity, called septic tank effluent gravity (STEG) systems, and those using pressure, called septic tank effluent pumping (STEP) systems.

Effluent sewers consist of small-diameter collector conduits or mains that feed into interceptor tanks. Collectors are designed to transfer only the liquid portion of waste to a treatment works or standard sewer system. Solids or any objects that could possibly cause

blockages are separated from the liquid portion in the interceptor tanks where they are periodically removed.

By removing solids, an effluent sewer system has some distinct advantages. The velocity requirements are lower due to solids not needing to be transported. Excavation costs are reduced as no minimum velocities need to be catered for. Material costs are lower as interceptor tanks provide surge protection and fewer manholes are required. Treatment works have reduced requirements because a large amount of waste has been removed by the interceptor tanks. Smaller and longer conduits reduce infiltration into the system due to fewer leaks, which are further reduced by conduits being shallower.

The major drawback of effluent sewers is the high degree of maintenance required as regular inspections need to be made and tanks need to be pumped throughout the entire system. These systems can only be used when sustainable procedures can be implemented (Water Environment Federation, 1999).

2. Literature review

2.1. Uncertainty

Guo & Song (1989) state that a lack of understanding of hydraulics while planning and designing drainage systems is the cause of problems within constructed drainage systems. They state that problems include eventual overflow, flooding of streets, manhole and drop shaft covers being blown off and structural damages. Willems (2012) also states that it has become vital that uncertainties and errors found in hydraulic models be understood and considered. Thorndahl et al. (2008) state that the design standards of sewer systems are largely uncertain and even though they have good objectives and simplified design procedures, they could still result in overdimensioning. The inexperience of drainage system designers can further aggravate the problem (Argaman, Shamir and Spivak, 1973). Unknowns in models can therefore easily result in underdimensioned or overdimensioned systems, resulting in problems.

Deletic et al. (2012) state that the first logical step in the process of providing an accurate theoretical drainage system is to understand the principles of uncertainty. Uncertainty forms an integral part of any theoretical model and is intrinsic to the entire process. The authors continue by saying that no matter the level of accuracy of data used or the confidence felt in the process, uncertainty will always remain part of any analysis performed. Since such elements cannot be removed, uncertainties need to be assessed and then reduced. It becomes important to fully understand the sources of information and the impact the information has on predictions made by the model. Beven (2006) notes that there are numerous sources of uncertainty, such as the data obtained or the assumptions made by mathematical simulation models, many of which could react nonlinearly with the modelling process. Uncertainties cannot always be quantified to acceptable levels.

Willems (2012) asserts that insufficient knowledge, also termed ignorance, is an uncertainty that cannot easily be quantified and that ignorance comes into existence when vital knowledge is lacking. The shortcoming in knowledge can be divided into two types of ignorance. Willems mentions that the first can be viewed as accepted or recognised ignorance by which one acknowledges a lack of knowledge and properly declares shortcomings and prepares for the deficiencies. The second is total ignorance and occurs when there is no knowledge of the fact that something is ignored. No preparations can thus be made. Willems continues to say that knowledge regarding a model can vary from certainty (may be referred

to as determinism) to ignorance (zero confidence or indeterminacy). It should be noted that no matter what level of confidence is placed in a model or solution, the results may be incorrect or even correct due to ignorance.

Johnson (1996) comments that uncertainties in parameters are the inability to represent a parameter exactly. Required parameters are not always available, or they are unobtainable due to lack of time or money. Parameters would be defined as uncertain and estimated and may result in inaccurate results.

Kuczera and Parent (1998) mention that large drainage systems may result in numerous input parameter sets, all of which are plausible and provide logical results according to calibration data obtained. The conflicting logical results may reduce confidence in the predictions of the model.

Deletic et al. (2012) state that a large number of publications that have investigated uncertainties of model parameters and the impact of the parameters on the model exist. Such investigations are often referred to as a sensitivity analysis, and they can be used to provide parameter probability distributions. Johnson (1996) states that the distributions can be used to determine the sensitivity of a model to changes in specific parameters, which can then be used to provide an estimated confidence level around the outputs of the model.

The effect of calibration data and the accuracy of models have often concentrated on the usefulness of calibration and the verification of the data (Deletic et al., 2012). Articles that discuss the number of events of a calibration process and a verification process of a model and how the process affects uncertainty have been published (Mourad, Bertrand-Krajewski and Chebbo, 2005). There are, however, few reports on measured data and how the uncertainty can be determined. Deletic et al. (2012) point out that large uncertainties have been reported with measured discharges of urban drainage systems and that this is a known problem.

It has been discussed that various calibration methods result in different parameter sets, each of which produces a resultant set with a respectable fit when comparing measured and modelled data (Gaume, Villeneuve and Desbordes, 1998). This becomes increasingly evident as the complexity of the model increases (Silberstein, 2006). Therefore, calibration algorithms, especially in complex models, cannot always provide a good solution.

Calibration data for drainage systems are quite rare for nonresearch models as measurements tend to be very expensive to obtain. As a result, many consulting engineers rely on default settings and best choice parameters. Default parameters will almost certainly lead to the results being uncertain. Schaarup et al. (2005) have shown that there could be pronounced differences between a well-calibrated urban drainage model and one that is not. Johnson (1996) mentions that the differences can be compounded by the fact that parameters within a drainage system, such as conduit roughness coefficients, conduits slopes and shear stresses, are known to vary greatly.

Mays (2001) also states that as in all engineering designs, uncertainties or unknowns are present in the design of sewer drainage systems and that unknowns might be socio-economic, environmental, structural, hydrologic or hydraulic. Uncertainties might fall in a single category, but usually a project will have uncertainties in more than one if not all the mentioned categories.

In conclusion, it can be stated that uncertainty is a lack of complete knowledge about events and the steps involved. Since knowledge can never be said to be complete, uncertainties will always be present. However, uncertainties can be reduced by gradually increasing the knowledge and understanding of each aspect of sewer system analysis through obtained data, hydraulics, system parameters, simulation models or processes. Uncertainties as well as errors resulting from hydraulic models can be substantial and need to be understood. Decisions based on hydraulics models are becoming more common, and the results obtained from simulations affect decision making.

2.2. Optimisation

Optimisation of a drainage system relies on an understanding of drainage system analysis. By understanding the inherent differences among different models, a designer will be able to better decide which design scenario provides the best solution after all aspects of a design project have been considered.

Mays (2001) claims that when system designers take uncertainties into account, they tend to view the design of a system in a conservative manner, which might include an increase in the value of safety factors or an artificial reduction in system capacities. Such measures have generally been determined in a subjective manner, which involves the experience of

individual designers. Mays also states that such an approach might lead to a safer design but would probably result in a trade-off between an optimised system and the costs of the project.

Argaman et al. (1973) state that drainage systems account for large portions of the overall expense of waste disposal, including solid waste such as rubbish. Substantial savings could theoretically be effected with improved system designs. The authors mention that procedures to achieve better designs may involve balancing pipe slopes and sizes to provide sufficient peak flow capacity within conduits while also maintaining sufficient scouring flow velocities during peak flow conditions. Though various scenarios are usually considered, a least cost scenario is generally chosen. The authors argue that the effectiveness of the procedure often depends on the experience of the designers. An optimal scenario may not be reached.

The process of finding a better solution for a drainage system can be divided into two parts, as explained by Argaman et al. (1973). First, the layout can be improved. Second, the design parameters can be optimised for a fixed layout. It would be best if both parts were considered simultaneously during an optimisation process because together they form the design problem.

Individual experience on the part of a system designer contributes greatly to the final design of a drainage system. The quality of the final system is also affected by inherent uncertainties: the greater the level of uncertainty the lower the probable level of the solution. Better understanding of the different models may limit one or more areas of uncertainty. Reduced uncertainty will improve the quality of a drainage system and lower the final costs of a project by avoiding construction of unnecessary structures or overly large conduits.

2.3. Overview of sewer drainage system components

Sewer systems comprise various components or auxiliary hydraulic structures, including manholes, conduits, weirs, pumps, siphons, valves, gates, drop shafts and structures, transition structures and outlet controls.

2.3.1. Conduits

The most common building block of any waterborne drainage system is the conduit between two manholes. Conduits transport flows downstream by gravitational acceleration and include conduits that are surcharged.

2.3.2. Pressurised conduits

Pressurised conduits, also referred to as rising mains, operate under pressure and the flow is controlled by pumps within pumping stations. These stations are required to pump waste from one drainage system into another where treatment plants are available.

2.3.3. Manholes

Manholes, or junctions, form the connection points among various conduits. Hydraulically, manholes create backwater effects to conduits flowing into them. In addition to backwater effects, a manhole also provides temporary storage, distribution and dissipation of energy. Temporary storage or overflow can be discharged into the system once downstream conduits have sufficient capacity. Manholes also mix as well as transfer momentum of the flow, which affects sediment and pollutants. Actual hydraulic analysis of a manhole is complex due to energy losses, mixing, turbulence and separation. It is important to take the hydraulics into account in realistic, reliable simulations of drainage systems (Mays, 2001).

2.3.4. Pumps

Pumps, coupled with pressurised conduits, push waste from topological lows to higher points in adjacent drainage systems. Pumps are usually housed within a fixed structure and are linked to a single conduit. Pumps are required to provide additional energy in order to overcome changes in elevation and resultant energy losses (Mays, 2001).

2.3.5. Diversion structures

Conduits usually flow into one another and combine their flows into a single downstream conduit. On rare occasions, the flow might be split as conveyance is usually dendritic. Such splits or diversions occur often where an existing conduit has insufficient capacity and it is decided to lay a new relief conduit parallel to the old conduit instead of replacing the original (Mays, 2001).

Weirs are used for flow diversions. Side weirs can be used to divert high flows. Weirs are usually parallel to the conduit with enough depth to prevent dry-weather flows to be discharged. Transverse weirs are generally placed across conduits and operate almost like a dam. They can be used to direct low flows to a diversion conduit or relief sewer.

An orifice structure may be used as a diversion structure. The structure allows flow to move through a rectangular or circular orifice and into another conduit. The orifice can be horizontally orientated at the conduit invert or vertically on the sides of conduits.

2.3.6. Drop structures

Drop structures are used in areas with steep elevation drops. They aid with energy dissipation in order to avoid erosion and structural failures; hydraulic instabilities, such as surcharging; and pneumatic problems, such as noise, air binding, flow instabilities and increased friction.

2.3.7. Siphons

Siphons are often used to move flows across depressions, such as canals, roads or valleys. They work by themselves and require no external mechanisms (Mays, 2001).

2.4. Sedimentation

Manenti et al. (2012) state that the process of siltation from sediment in flows reduces the original storage capacity of conduits. Sedimentation within a drainage system adversely affects hydraulic performance. Ashley et al. (1992) mention that sedimentation leads to problems such as overflows, surcharging, blockages, increased concentration of pollutants and costly removal. Mays (2001) mentions that the increase in possible concentration of pollutants comes from sediment being eroded, resulting in a large influx of pollutants that had once been trapped. Pollutant levels can exceed estimated concentrations. Heavy metals and hydrocarbons attach themselves to solid particles, which are abundant in sewer systems. Periodic releases from sewer overflows often contain sediments and as a result trapped pollutants. Release of the pollutants is viewed as a source of pollution in urban areas. Ota and Nalluri (2003) assert that by not accounting for sedimentation and instead relying on the concept of self-cleansing conduits results in underdesigned sewer conduits.

2.5. Sewage flow

Flow within a partially full conduit is similar to that of an open channel (Chadwick, Morfett and Borthwick, 2006). A key characteristic is that a surface that is not in contact with the conduit exists. A free surface, however, does exist during surcharge conditions.

2.5.1. Types of flow

Mays (2001) states that sewage flow is usually turbulent, unsteady, nonuniform and subcritical. When flows vary slowly over time in such a manner that the travel time through the length of conduit is considerably smaller than the duration of the rising hydrograph, the flow can be treated as stepwise steady flow without committing too great an error. Flow within a system can also be divided into three major regions: the entrance into a conduit, the flow within a conduit and the exit from a conduit. This study was concerned mainly with the flow within a conduit.

Figure 2:1 below shows 10 differing cases of nonuniform flow within a conduit. The cases vary depending on whether the flow is subcritical, supercritical or surcharged.

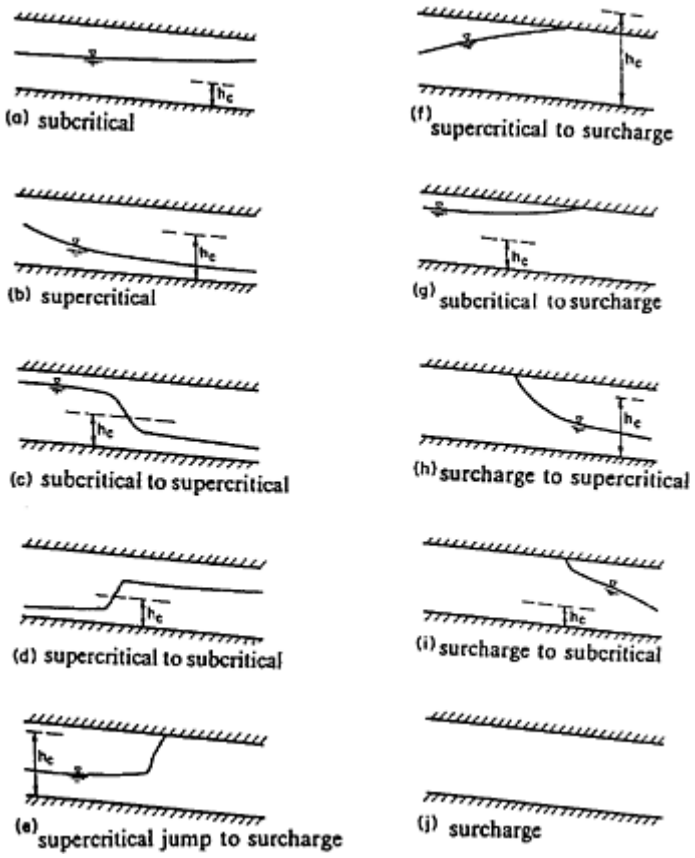

Figure 2:1: Flow classification within a sewer pipe (Chadwick, Morfett and Borthwick, 2006)

Entrance conditions into a conduit can be divided into four cases, as shown in Figure 2:2 below. The first case illustrates downstream control. The second case illustrates upstream control. In the third case, the flow beneath the pocket of air can be subcritical, supercritical or even transitional. In the fourth case, the flow may be controlled by downstream as well as upstream conditions (Yen, 2004).

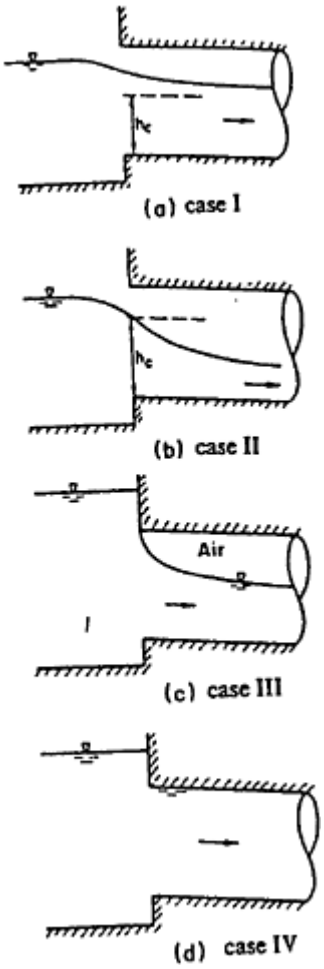

Figure 2:2: Entrance flow conditions (Yen, 1986)

Exit conditions, illustrated in Figure 2:3, can be divided into four groups as well. The first case illustrates outlet control. The second case illustrates upstream control if the flow is supercritical and downstream control if the flow is subcritical. The third case illustrates upstream control while the water surface at the junction is under downstream control. The fourth case is usually under downstream control. The flow can, however, be under both downstream and upstream control (Mays, 2001).

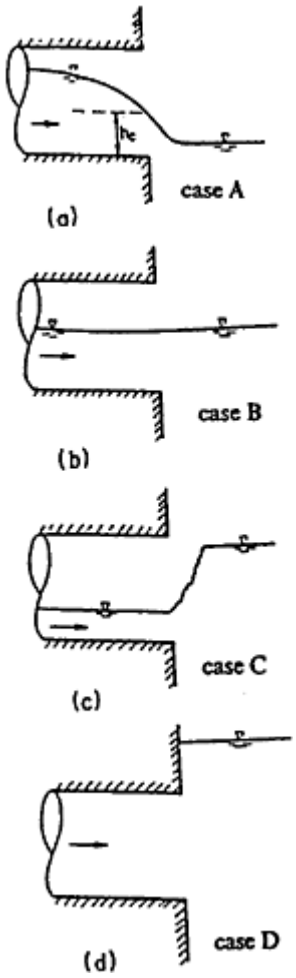

Figure 2:3: Pipe exit conditions (Yen, 1986)

Due to large numbers of differing and often complex flows, drainage systems have not always been analysed with complex hydraulic models. With improvements in the understanding of hydraulics and advances in computational capabilities, a more realistic or detailed analysis of drainage systems is now attainable (Mays, 2001).

2.6. Surcharge

Yen (1980) defines surcharge as the time when a conduit is flowing full and gravity-induced flow is no longer prevalent. A few common reasons for surcharges include:

- Under design of a system, which might have resulted from parameter uncertainties.
- Inflow risks, as the probability always exists that design flows can be exceeded.
- Material deviations and construction faults.
- Changing conditions within the system, such as blockages, sedimentation and deformation of conduits.
- Basins that changed after construction and design.

When surcharging occurs, the flow cross-sectional area and therefore the flow depth can no longer increase as the limits of the geometry of the conduit have been reached. Despite the depth being unable to increase, flow discharge may continue to increase. This is a result of the increasing difference in hydraulic head upstream and downstream of the conduit. Figure 2:4 below illustrates the problem.

Figure 2:4(a) shows the flow depth within the conduit at various times (t). Flow depths at various times are shown in cross-section c-c in Figure 2:4(b). Depths are reflected in Figure 2:4(c) where they are shown as a depth graph, in direct comparison with the actual discharge of the conduit in Figure 2:4(d). Despite the depth being capped between times t4 and t5, the discharge continues to increase and is the result of increased pressure head (Yen, 1986).

Flow usually remains nonuniform during surcharge conditions, despite the sewer diameter remaining constant. Flow is influenced by the upstream and downstream conditions as well as entrance and exit conditions that result in nonparallel streamlines (Yen, 2004).

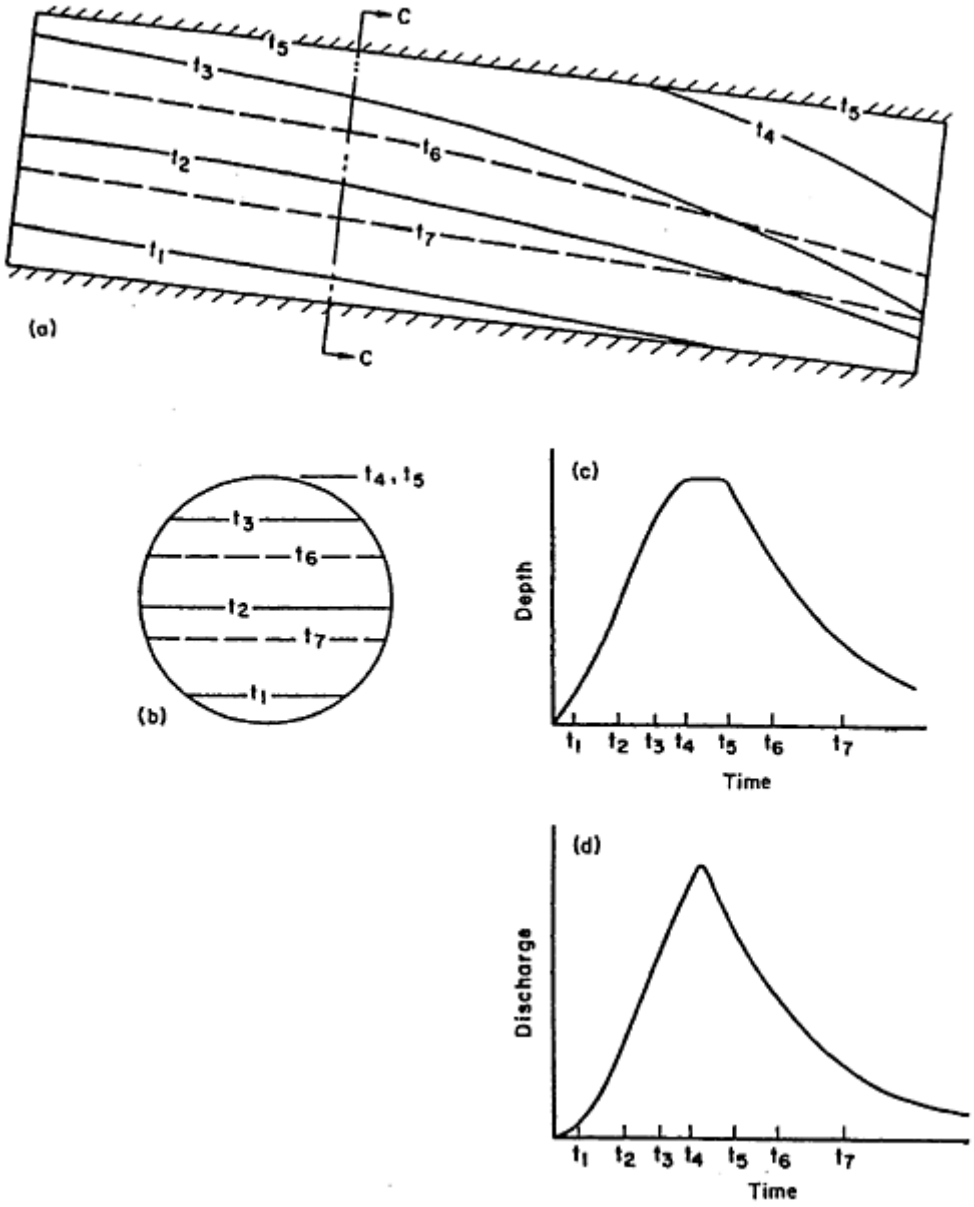

Figure 2:4: Surcharge and variation in discharge and depth (Yen, 1986)

2.7. Depth-discharge relationship

As a result of the flow being mostly nonuniform and unsteady, the relationship between the depth and discharge of a conduit is nonunique. Steady and uniform flow, which is an approximation, also results in a nonlinear relationship between depth and discharge.

When considering a circular pipe in ideal conditions, the nondimensional curve in Figure 2:5 can be drawn to compare depth and discharge. Figure 2:5 illustrates that for a circular conduit, peak flow and velocities do not occur when the conduit is flowing full, but at approximately 96% and 80% flow depth, respectively.

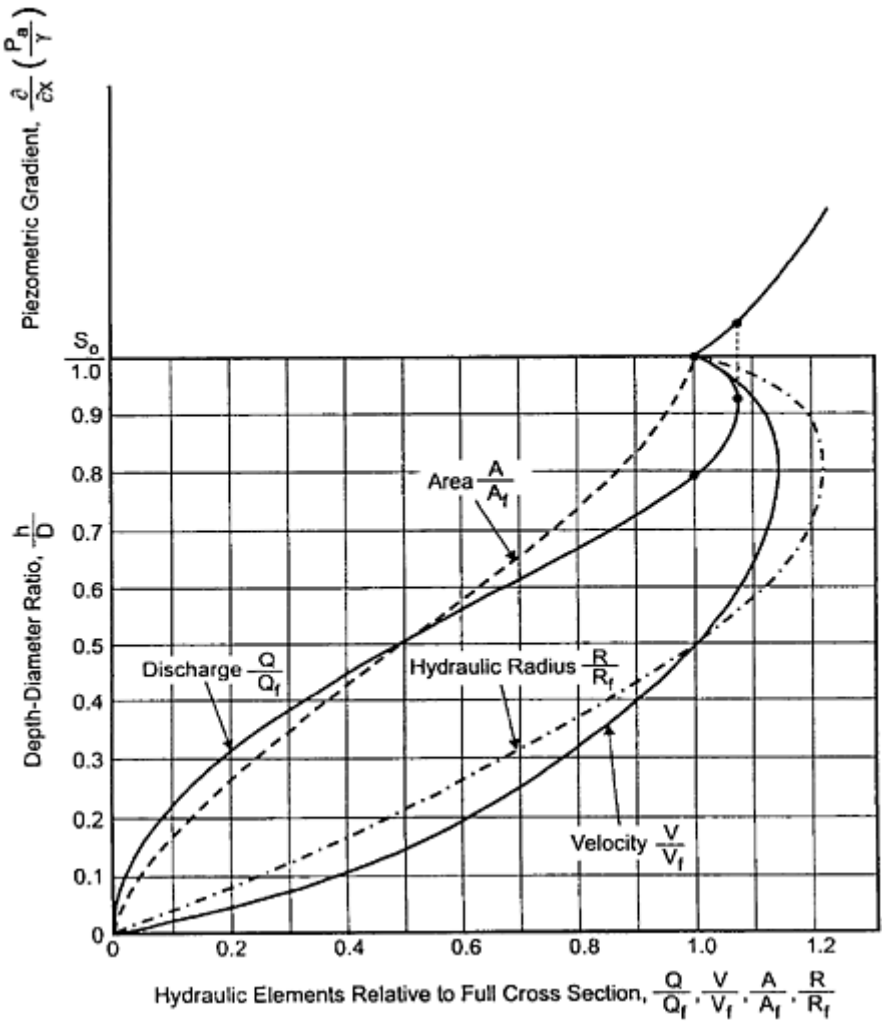

Figure 2:5: Ideal depth versus discharge curve of a circular pipe (Mays, 2001)

2.8. Sewer hydraulic flow equations

Hydrodynamic flow equations allow both existing and future drainage systems to be investigated (Joliffe, 1984). Through the use of equations, mathematical models that analyse the flow within drainage systems can be created. Some models make use of unsteady flow equations while others simplify the equations to create less sophisticated hydraulic models.

2.8.1. Saint-Venant flow equations

The attenuation and translation of a hydrograph can be represented by using the complete Saint-Venant flow equations (Blandford and Ormsbee, 1993) and are represented by the conservation of mass and the conservation of momentum equations.

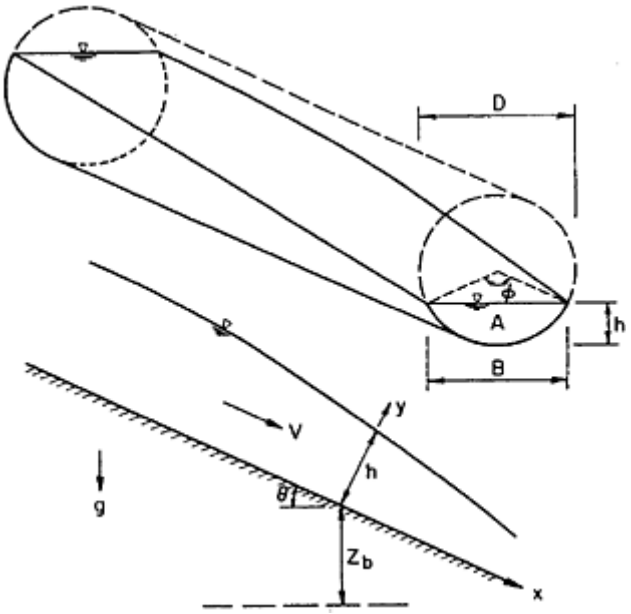

Figure 2:6: Unsteady flow with a free surface (Mays, 2001)

Using Figure 2:6 the momentum equation can be written in the conservative form as follows in terms of discharge (Yen, 2004):

$$\frac{1}{gA}\frac{\partial Q}{\partial t}+\frac{1}{gA}\frac{\partial}{\partial x}\left(\frac{\beta Q^2}{A}\right)+\cos\theta\frac{\partial h}{\partial x}-S_O+S_f=0$$

Equation 2.1: Momentum equation (conservative form)

Where:

- x is the flow direction of the sewer.
- A is the cross-sectional area of flow normal to x.
- y is the direction normal to x on the vertical plane.
- h is the depth of flow along y.
- Q is the discharge.
- S_O is the slope of the channel (equal to $\sin\theta$).
- θ is the angle between the conduit and the horizontal plane.
- S_f is the friction slope.
- g is gravitational acceleration.
- t is time.

The Boussinesq momentum flux correction coefficient is included in Equation 2.1 to represent nonuniform flow velocity distributions (Yen, 2004).

$$\beta = \frac{A}{Q}\int_A \bar{u}^2\, dA$$

Equation 2.2: Boussinesq momentum flux

Where:

- $\bar{u}$ is the x-component of the local velocity averaged over turbulence.

Furthermore, the continuity equation (Equation 2.3) is required to describe the flow. The term q_1 represents any lateral inflows (Blandford and Ormsbee, 1993).

$$\frac{\partial A}{\partial t} + \frac{\partial Q}{\partial x} = q_1$$

Equation 2.3: Continuity equation

When the momentum equation (Equation 2.1) is described, the first part is the inertial term resulting from local acceleration. The second term is the inertial term resulting from convective acceleration. The third term is the pressure as a result of the water surface gradient. The fourth term is the body force or conduit slope. The fifth term is the resistance force or friction slope. When uniform flow is considered, the first three terms are removed and only S_o and S_f are retained ($S_o = S_f$). The continuity equation paired with the momentum equation where $\beta = 1$ is usually referred to as the Saint-Venant equations or otherwise the fully dynamic wave equations.

Yen (2004) mentions the shortcomings of the above mentioned approach. The first is to assume hydrostatic pressure distribution over the cross-sectional area. The second assumption is that there is a uniform velocity distribution over the cross-sectional area, thus $\beta = 1$. The final assumption is that the spatial gradient of forces due to internal stresses is negligible.

2.8.2. Flow resistance

The friction slope, denoted by S_f in the momentum equation, can usually be determined or estimated by using semi-empirical methods, such as the Manning formula (Equation 2.4) or the Darcy-Weisbach formula (Equation 2.5).

$$S_f = \frac{n^2 Q|Q|}{K_n^2 A^2} R^{-4/3}$$

Equation 2.4: Manning's equation (Chadwick, Morfett and Borthwick, 2006)

Where:

- n is the Manning's roughness coefficient.
- K_n is a conversion constant (1.486 for imperial and 1.0 for SI units).
- R is the hydraulic radius.

$$S_f = \frac{f}{8gR} \frac{Q|Q|}{A^2}$$

Equation 2.5: Darcy-Weisbach equation (Chadwick, Morfett and Borthwick, 2006)

Where:

- f is the Weisbach resistance coefficient.

Flow reversal is accounted for by use of the absolute value signs in both the equations. The values for *n* and *f* are dependent on the roughness of the conduit, the form of the conduit (especially if sediments are present), the Reynolds number, the Froude number, as well as the steadiness and uniformity of flow (Rouse, 1965). For unsteady and nonuniform flows, the pipe slope, energy gradient, total head gradient and hydraulic gradient are different from the friction slope. They are only equal to one another when steady uniform flows occur.

The steady uniform values for the two coefficients are usually approximated in literature. The values for the Weisbach coefficient can be read from the Moody diagram or calculated from the Colebrook-White formula.

$$\frac{1}{\sqrt{f}} = -2.0 \log \left[\frac{k_s}{14.83} + \frac{2.52}{4Re\sqrt{f}} \right]$$

Equation 2.6: Colebrook-White formula (Colebrook, 1938)

Where:

- k_s is the Nikuradse pipe roughness.
- Re is the Reynolds number.

Rouse (1965) identified a few problems with the Colebrook-White formula. The first is that the formula pertains to full-pipe flow conditions while most sewers flow partially full. The second problem is that the formula is implicit and requires iterations to determine an approximate value. The third is that for any pipe and surface roughness, the value of *f* varies constantly, not only with flow depth but also with the geometry of the cross-sectional area of flow. As a result, the value will need to be constantly recomputed for each variation in flow depth. In an attempt to reduce the first two problems, Yen (1991) proposed Equation 2.7:

$$f = \frac{1}{4}\left[-\log\left(\frac{k_s}{12R} + \frac{1.95}{Re^{0.9}}\right)\right]^{-2}$$

Equation 2.7: Simplified Colebrook-White coefficient (Yen, 1991)

Values for Manning's *n* can be obtained from tables and have been derived empirically. A thorough list can be found in Chow (1959). The main advantage of Manning's coefficient is that the coefficient is nearly constant when the Reynolds's number is sufficiently high with a set surface roughness in a prismatic channel.

2.8.3. Unsteady flow equations

The dynamic wave equation can be a solution (and is sometimes viewed as being a total solution) as the equation contains the elements of all the dynamic terms that affect unsteady flow in an open channel. Mays (2001), however, points out that the dynamic wave model is not a total solution due to the assumptions made, as has already been discussed. Despite the simplifications, the fully dynamic wave equation remains computationally expensive to analyse, which becomes even more so for larger drainage systems and has resulted in various simplified models.

When the $\partial Q/\partial t$ term is dropped, a new form of the equation is formed, which is called the quasi-steady dynamic wave equation (Equation 2.11). Removing both the local and convective acceleration terms results in the noninertia approximation (Equation 2.12). Furthermore, if the $\partial h/\partial x$ term is removed in conjunction with the two inertia terms, the kinematic wave approximations are achieved (Equation 2.13).

The dynamic wave equation can be expressed as follows after some manipulation (Mays, 2001):

$$Q = CA\sqrt{S_O - \cos\theta\frac{\partial h}{\partial x} - (2\beta - 1)\frac{V}{g}\frac{\partial V}{\partial x} - \frac{1}{g}\frac{\partial V}{\partial t} + \frac{\beta - 1}{g}\frac{VB}{A}\frac{\partial h}{\partial t}}$$

Equation 2.8: Reordered dynamic wave equation

Where:

- C is dependent on the friction slope formula used.
- B is the width of the surface flow.
- A is the cross-sectional area of flow.

When using Manning's formula, the following (Equation 2.9) can be used to solve for C:

$$C = {}^{K_n}/_{n}\, R^{2}/_{3}$$

Equation 2.9: Coefficient for Manning's formula

When using Darcy-Weisbach's formula, the following (Equation 2.10) can be used to solve for C:

$$C = \left(\frac{8gR}{f}\right)^{\frac{1}{2}}$$

Equation 2.10: Coefficient for Darcy-Weisbach formula

When terms are removed from the fully dynamic wave equation to simplify the equation, various approximate formulas can be derived. By removing the last term as stated, the quasi-steady dynamic wave equation is obtained (Equation 2.11).

$$Q = CA\sqrt{S_O - \cos\theta\frac{\partial h}{\partial x} - (2\beta - 1)\frac{V}{g}\frac{\partial V}{\partial x} - \frac{1}{g}\frac{\partial V}{\partial t}}$$

Equation 2.11: Quasi-steady dynamic wave

Removing the next two terms results in the noninertia formula (Equation 2.12).

$$Q = CA\sqrt{S_O - \cos\theta \frac{\partial h}{\partial x}}$$

Equation 2.12: Non-inertia formula

Finally, after removing the last term, the kinematic wave formula is obtained (Equation 2.13).

$$Q = CA\sqrt{S_O}$$

Equation 2.13: Kinematic wave formula

When Manning's value for C is substituted into the kinematic wave equation, the Manning formula for flow is obtained (Equation 2.14). The result of all the simplifications is evident as the original fully dynamic wave equation can be used for nonuniform unsteady flows, while the Manning formula is used for uniform flow.

$$Q = \frac{k}{n} R^{2/3} \sqrt{S_o}$$

Equation 2.14: Manning's formula for uniform flow

2.9. Instability of flows

In sewers there are various transitional flow instabilities; the hydraulics of sewer flow is rather complex. Yen (1978) mentions five instabilities that occur in sewer conduits, each of which will be discussed in more detail:

1. The transition between free-surface flow and full flow.
2. During the free-surface phase when flow transitions between super- and subcritical flow.
3. Water-surface roll-wave instability of supercritical free-surface flow.
4. Approaching dry-bed flow.
5. Surcharge.

2.9.1. Transition between free-surface flow and full flow

The first is relevant to any study where surcharge takes place. Factors affecting instabilities are the following:

- Nonunique discharge versus depth relationship when the flow depth approaches the full depth of the conduit.
- Lack of air to supply the pocket of air at the conduit entrance as well as the air within the conduit.
- Conduit geometry.
- Geometry and flow conditions at the entrance and exit of the conduit.
- Surface waves.
- The phenomena of hydraulic jump directly to surcharge conditions as well as hydraulic jump from surcharge.

All the factors may work together to create instabilities within a drainage system or individual conduit (Mays, 2001).

2.9.2. Subcritical-supercritical transitional instabilities

The transition between subcritical and supercritical flows can be separated into hydraulic jump, when flow moves from supercritical to subcritical flow, and hydraulic drop, when flow moves from subcritical to supercritical flow.

2.9.3. Roll and surface waves

The first type of surface wave found in sewers is air-water interfacial waves. Surface waves are created through the shear forces between the air and water flow against one another. The phenomenon is found in both subcritical and supercritical flow conditions. Killen and Anderson (1969) state that the frequency of the waves is high and that the amplitude of the waves is small. As a result of the waves being small, they can only force transition into surcharge conditions when the flow depth is already very near to the full depth of the conduit, and this usually occurs when the flow is greater than 90% of the full depth (Killen and Anderson, 1969). Figure 2:7 illustrates surface waves (Yen, 1986).

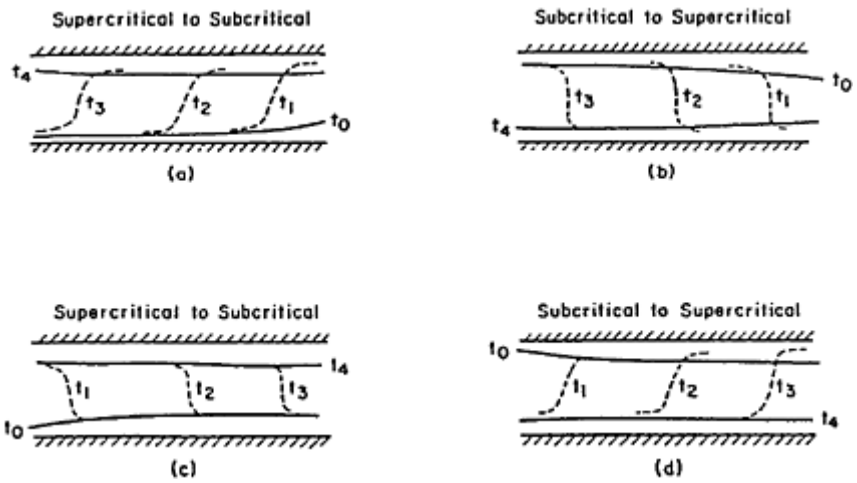

Figure 2:7: Surface waves

Another type of wave found during supercritical flows is the roll wave, which occurs when the Froude number exceeds two in circular conduits (Yen, 1980). Unlike the surface waves that are created by shear between the air and water, the roll wave is more closely related to the friction of the conduit bed. The phenomenon occurs from the interaction between the fast-moving flow near the free surface and the much slower moving flow near the conduit bed. The difference may result in instability. In comparison with surface waves, roll waves are more regular and periodic as well as having larger amplitudes (Mays, 2001).

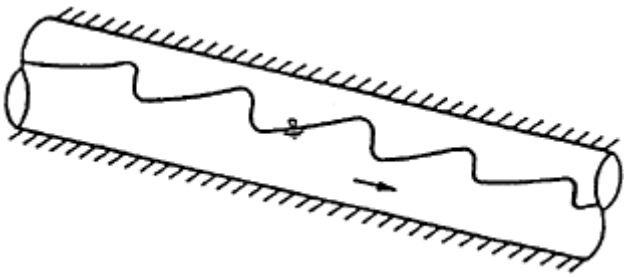

Figure 2:8: Roll waves (Yen, 1980)

2.9.4. Dry-bed instabilities

Dry-bed instabilities occur when the flow within a conduit is very low and surface tension begins to play a role (Yen, 1980). Low flows may occur during the initial or final stages of flow through a conduit.

When a tiny amount of water is placed in a conduit, water might not flow downstream. Instead, small pockets will form as a direct result of surface tension. The small pockets will gradually increase as more water is added. As the pockets increase in size and depth, the gravitational force will increase and the relative force of surface tension will decrease.

Eventually water will begin to move and small pockets will merge, allowing thin-film flow. Thereafter the pools disappear and regular flow conditions take over.

Dry-bed instabilities are more important to mechanical and chemical engineers and do not play any practical role in the civil engineering design of sewer systems (Mays, 2001).

2.9.5. Surcharge

As discussed previously, sewers can flow full and flow under pressure. Such surcharge conditions usually occur during rainstorms or when a conduit has been insufficiently designed. There are two established methods of simulating surcharge (Mays, 2001): the hypothetical piezometric open-slot approach and the standard transient pipe flow approach.

If the standard transient pipe flow method is used, the flow within the conduit is considered as pressurised transient pipe flow. The flow cross-sectional area is equal to the full flow of the conduit; therefore, the change in area over the change in distance is zero (Yen, 2004).

The hypothetical slot, which is continuous and narrow, is added to the crown of the conduit and runs the entire length of the conduit (Song, Cardle and Leung, 1983). The philosophy behind the approach is to simulate surcharge as if a conduit was still an open channel. The additional pipe capacity granted by the open slot is negligible. The process, however, is computationally expensive.

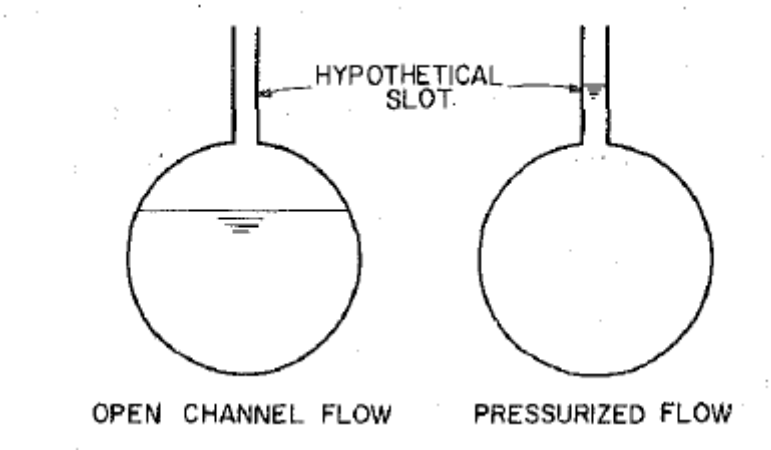

Figure 2:9: Hypothetical (Song, Cardle and Leung, 1983)

Due to a lack of physical data, neither method has been proven to be accurate in simulating a single conduit or an entire system (Mays, 2001). Numerical testing has been performed on the two methods, and neither performed markedly better than the other. In sewer systems where a large portion of the duration is under surcharge, the standard approach would probably save

computational time. However, in cases where flow might transition frequently between open-channel and surcharge conditions, the hypothetical slot approach would be advised.

2.10. Unit hydrographs

A unit hydrograph is a simplified model to analyse the response of inflow hydrographs into a catchment or sewer system (Chadwick, Morfett and Borthwick, 2006). In storm water applications, a unit hydrograph is generally defined as a hypothetical unit response of a drainage area to a unit influx of rainfall (Mays, 2001). A unit hydrograph can also be called a direct runoff hydrograph that results from one unit of rainfall that occurred uniformly across a drainage area. A unit hydrograph describes the direct runoff portion of a hydrograph, thus a separate base flow portion might be required.

The initial intuitive concept of a unit hydrograph was developed in 1932 and is attributed to Sherman (Jain, Singh and Bhunya, 2006). The concept outlines that a drainage system or watershed reacts in a similar manner to a linear reservoir (Mays, 2001). Effective rainfall from storms with near-constant intensity and similar duration can be shown to result in runoff hydrographs of similar durations and peaks. If the relative ordinates of the hydrograph can be determined for one unit of rain, the resulting ordinates of any other rainfall intensity can be determined if the duration remains constant.

Despite there being various methods to develop synthetic unit hydrographs for the use of modelling (Jain, Singh and Bhunya, 2006), Mays (2001) states that no method can be defined as being better or worse than another. He also adds that the manner in which a unit hydrograph was developed does not impact the way in which the unit hydrograph is used. The application of unit hydrographs remains identical. An analyst needs to choose the methods that provide answers reflecting the area in which the unit hydrographs are to be implemented.

A unit hydrograph, however, represents a singular event. Drainage systems often rely on multiple input sources of varying intensity. The concept of unit hydrographs thus needs to be expanded.

2.11. Contributor hydrographs

As discussed, a unit hydrograph represents a single event. A sewer drainage system can consist of an almost endless number of events that influence the inflow into the system. The events could be as small as a flushing toilet or leaking cistern. The events could also be

grouped together to create an event that represents a stand. The stands could then be grouped together to create an event for a street or region. The contributor hydrograph makes use of unit hydrograph theory to produce inflow hydrographs that can be used to populate the boundary conditions of a model. This section will describe the components that make up a contributor hydrograph.

Shaw (1963) states that a contributor hydrograph for a sewer system can be defined as the hydrograph of sewer flow originating from a contributory hydrograph unit. The contributory unit could be expressed as a unit of length, area or pipe infiltration. The unit may even be a household, a person or a set number of fixture units. The hydrograph can be either synthetic or real. A synthetic hydrograph is usually developed to ensure that certain design allowances are met (Shaw, 1963).

In essence, the contributor hydrographs of a sewer system are similar to the unit hydrographs used in the design of storm water systems (Shaw, 1963). For the purposes of this study, a contributory unit consists of a 24-hour flow hydrograph.

2.11.1. Components of the contributor hydrograph

Flows into sewer systems do not only include domestic and trade effluents (Shaw, 1963). Other components also play an important role in the development of a contributory unit. The components of flow that make up a contributory unit are summarised below:

- Domestic sewage: Daytime variation that conforms to fairly general patterns and usually includes one main peak, as well as one or more minor peaks, and low night flows. Domestic sewage is affected by the average annual daily demand (AADD).
- Trade effluents: The rate and quantity of discharge varies, but usually also conforms to a fairly regular weekly pattern.
- Infiltration:
    - Groundwater: Is a constant day-and-night inflow during dry months and occurs where conduits are below the permanent water table.
    - Subsurface: Is an inflow coupled with rainstorms. Inflow into the system increases immediately after a storm and then decreases gradually.
- Water entry: Results in high peaks that result from direct inflow into the sewer system during storms.

- Local inflow and leaks: Form part of domestic sewage and trade effluents as it is difficult to distinguish between them. Inflows and leaks may also form a significant portion of night-time flows.

2.11.2. Inflow from land uses

The inflow is the direct result of land uses that are serviced directly by the conduit. The flow contributed by each of the land uses along the conduit is usually assumed to enter the system at each of the manholes (Fair, 2008 a). Each land use type is associated with a certain unit hydrograph. The unit hydrograph combined with the demand from the land use creates a hydrograph that is assigned to the nearest manhole.

2.11.3. Leakage

A portion of any flow within a system is generated by leaks and is generally generated from leaking cisterns or other leaks. Leakage can generally be assumed to be constant throughout the course of a year. A rate of around 0.15 l/min/land unit has been suggested (Stephenson and Hine, 1982). The value can, however, be increased or decreased depending on the age of a system, with newer developments tending to be less wasteful. Leakage could also be increased with increased property size (Fair, 2008 a).

2.11.4. Groundwater and subsurface infiltration

Similar to leakage, infiltration from groundwater will cause an increase in flow into the system (Fair, 2008 b). Infiltration often occurs at joints and other connections at manholes and land units. Instead of the inflow being determined from the land use, the rate of infiltration is determined by the length and diameter of the conduit.

Infiltration also varies among different regions. Areas where conduits are closer to the ground water level will have increased infiltration. Some areas are also moister than others, leading to an increased inflow.

2.11.5. Storm water ingress

Rainwater can enter a system during storms. The ingress from such storms into each pipe is a percentage of the precipitation on a contributing area (Fair, 2008 a). A hydrograph (which describes a storm), an ingress percentage and the contributing area need to be specified. The inflow percentage can vary widely.

2.11.6. Inflow hydrograph

The hydrographs from all surrounding land uses are summated to generate a composite inflow hydrograph (Fair, 2008 a). The leakage and ground water infiltration constants are

added to the hydrograph. Finally, a storm water hydrograph is added. The combination of all the factors creates a composite hydrograph that can then be routed downstream of the manhole, the integral of which provides the total daily flow into the system.

2.11.7. Type-area hydrographs

Shaw (1963) states that inflow hydrographs can be grouped into various type-area hydrographs, with each type-area hydrograph representing a certain inflow characteristic. Each would therefore define a single contributor hydrograph. The actual number of defined type-areas depends on the required amount of detail as well as the reliability of any available data (Shaw, 1963).

The type-areas can also be expanded to include other inflow factors such as leakage, storm water entry as well as infiltration. Therefore, all the mentioned factors of inflow, including legitimate sewage, into a sewer system could be included in a single contributory hydrograph (Shaw, 1963).

2.12. Simulating drainage systems

The act of simulating a drainage system is a way to mathematically represent a natural event that occurs continuously within systems (Hydrosim CC, 2001). Usually, knowing the design peak discharge of a conduit within a system suffices (Mays, 2001). However, in the case of operations or planning runoff volumes, flow state or even flow hydrographs may be required. Determining peak flows within a conduit may only require simple and traditional hydraulic and hydrologic methods. Yen (2004) mentions that determining flow hydrographs at certain points within a system requires more complex hydraulic models. Hydraulic simulations employ energy or momentum equations, or simplified variations, as well as the continuity equation. Simulations can be further simplified in certain cases, which will be discussed in later sections.

Flows within conduits and junctions interact with one another in drainage systems (Mays, 2001). In order for simulation results to be accurate or reliable, the conduits and junctions should be considered as a system. The underlying hydraulics of drainage systems has been discussed in previous sections. Accordingly, many drainage system models have been developed.

With various differing models available, selecting the most appropriate model for a particular drainage system simulation can be a difficult task. Some factors affecting a selection are listed below (Mays, 2001):

- Final objective of the simulation.
- Required detail and accuracy of the simulation.
- Required input data include readily available data that still needs to be acquired. The greater the complexity of the model, the more detailed the required information becomes. Such information can be very costly. Existing data may also not be required for the level of accuracy.
- Hardware and software required to perform simulations.
- Efficiency, such as running time and costs of using a model to perform the simulations.
- Availability of support when problems arise when operating the model.
- Budget.
- Available time.

Before the various models available are described, a brief overview of the differing mathematical models is given. Over the years, many models have been developed and they could possibly be organised as follows:

1. Group models according to their purpose
    a. Design
        i. Design
        ii. Optimisation
        iii. Risk
    b. Evaluation
    c. Planning
2. Group models according to the project objective
    a. Flood
    b. Pollution
3. Group models according to the extent of the space
    a. Only the sewer system
    b. The sewer system as well as the overland flows
4. Group models by the nature of the wastewater
    a. Sanitary sewer
    b. Storm or combined storm and sewer
5. Group models according to water quality and quantity
    a. Quantity

   b. Quality
   c. Quantity and quality
6. Group models according to time consideration of rainfall
   a. Single-event models (usually less than a week)
   b. Multiple-event models (longer than a week)
7. Group models according to probability considerations
   a. Deterministic
   b. Probabilistic
   c. Purely statistical
   d. Stochastic
8. Group models according to the systems concept
   a. Lumped system
   b. Distributed system
9. Group models according to hydrologic principles
   a. Hydrologic (mass conservation)
   b. Hydraulic (mass, momentum and energy)

For the purposes of this study, only the first group is applicable.

2.12.1. Evaluation analysis

Evaluation models are used primarily on drainage systems that have already been built as well as systems that have already been fixed, which include diameters, slopes and position. The models are mainly used to test whether existing systems or planned systems are adequate. Evaluation models often require the highest level of hydraulic accuracy and are used when reliable flow data is required. Many simplified models do exist, however (Yen and Sevuk, 1975).

2.12.2. Design analysis

Models are used to help determine the size of conduits within a drainage system (Yen, 2004). Models can also be used to determine the slopes and layouts of new systems as well as to make upgrades to existing infrastructure and to optimise the system design in terms of cost or other objectives. Design models are used when planning according to certain events, which could be a design peak flow or other specific event. Due to the fixed sizes of commercial conduits, models often require only moderate levels of hydraulic accuracy.

2.12.3. Planning analysis

Planning models are primarily used for strategic planning and decision making for urban or regional drainage systems. The models are often applied to larger spatial and time frames than design or evaluation models (Yen and Sevuk, 1975). Planning models can often consider longer continuous periods of flow, which may often cover various events including multiple

storms or peak dry-weather flow scenarios. Therefore, planning models usually use the most simplified hydraulic models of flow. In some cases a simplified water balance may be sufficient.

Hydraulic models can also be grouped by the level of hydraulics. The groups could include dynamic wave, noninertia, nonlinear kinematic wave and linear kinematic wave (Mays, 2001). Other models that use much simplified levels of hydraulics than the models listed can be added to the list, such as the contributor hydrograph model or SWMM's runoff model (steady-state).

Figure 2:10 depicts how required hydraulic sophistication decreases from evaluation analyses to planning analyses. Hydraulic sophistication of models also increases from basic models to detailed models. The boundaries of where the requirements of an analysis and the abilities of a model intersect are not always evident.

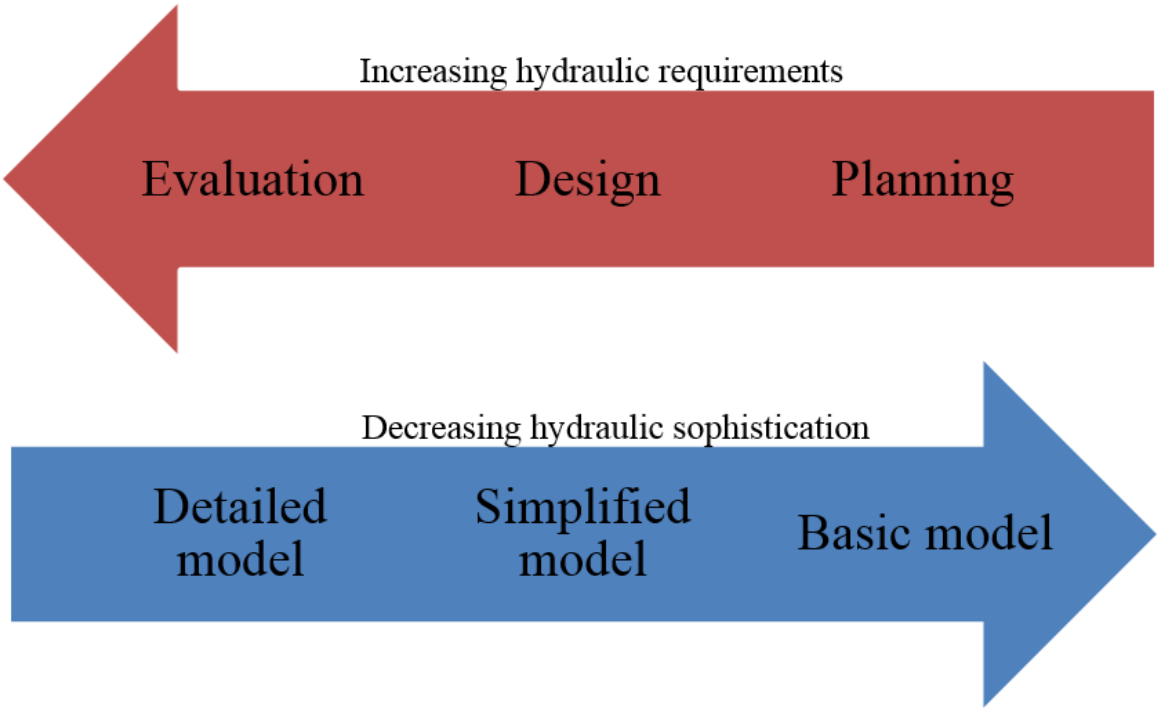

Figure 2:10: Purpose and sophistication of model

2.13. Comparison of available models

The design of any sewer system is impacted by the mathematical model used (Zhong, 1998). The results obtained from an analysis can be used from planning, design, to operations. Aspects of any simulation model are the speed of analysing, the size of models that can be used, the stability of the model and, importantly, the accuracy. The various aspects are of importance to any engineer, and the weighting of each will differ depending on project requirements.

Two types of numerical simulation models are available: explicit and implicit schemes. Explicit schemes, being simpler, can be used on general systems, but require smaller time steps as well as conduits of a minimum length, as enforced by the Courant criteria (Equation 2.15).

$$\frac{\Delta x}{\Delta t} \geq V \sqrt{gA/B}$$

Equation 2.15: Courant criteria

In sewer systems, the Δx is generally much smaller than for rivers and results in a very small Δt being required. The time step can be less than 30 seconds or even as small as one or two seconds. The small time step usually limits the speed with which models can be analysed. The various shortcomings of the explicit schemes have resulted in numerous implicit schemes to be developed. Indications from research have shown that implicit schemes are better for analysing looped systems (Zhong, 1998).

One-dimensional flow equations in which a free surface occurs can be defined using the continuity and momentum equations. The mass balance is described using the continuity equation while the force balance under dynamic conditions is described using the momentum equation. Newton's second law of conservation of energy, when assuming hydrostatic pressure and ignoring acceleration in the vertical direction, is used to formulate the momentum equation. The principle of conservation of mass, whereby the rate of inflow and outflow is always equal to the rate of change of storage, is used to determine the continuity equation.

Boundary conditions need to be set when solving two partial differential equations. Conditions in a sewer system are usually defined by a rating curve between the flow depth

and flow. Incoming lateral flow from other conduits is not a boundary condition as lateral inflow is already taken into account within the continuity equation (Zhong, 1998).

There are a few well-known models that employ the most sophisticated hydraulics, such as the dynamic wave model, and were developed to analyse flows instead of designing sewer or storm water systems. Two models, the Illinois Storm Sewer System Simulation (ISS) and the Storm Water Management Model's Extended Transport Block (SWMM-EXTRAN), have manuals available. The ISS can, however, only handle open-channel flows. Other models such as Calcul des Reseaux d'assainissement (CAREDAS), UNSTDY, HYDROWORKS and Model for urban sewers (MOUSE) are proprietary models (Yen, 2004). A brief overview of a few models is given, where after a model from each hydraulic purpose – evaluation, design and planning – is investigated further.

2.13.1. Fully dynamic wave models

Amongst models, the fully dynamic model is often described as the highest hydraulic level, fully utilising the complete Saint-Venant flow equations' dynamic wave routing to produce the most accurate theoretical results, and was initially developed for flow simulation rather than sewer system analysis (Mays, 2001). Dynamic wave equations make use of both continuity and momentum equations for conduits and junctions use volume continuity equations (Rossman, 2006). The junction conditions and surcharge conditions, assuming that surcharge conditions apply, are required for accurate flow simulations (Water Environment Federation, 1999).

With fully dynamic wave routing, pressurised flow, which occurs when full flow has been exceeded within a conduit and has become full, can be simulated. Dynamic wave routing can also simulate storage within conduits, backwater, friction losses at entrances and exits, and reversal of flow. Dynamic wave routing can be applied to any drainage system layout, even if there are multiple downstream diversions or loops within a system and is often the simulation model of choice where flow restrictions or flow regulators such as weirs or orifices occur downstream.

The price for such accuracies lies in having to use much shorter time steps that may be a few minutes or less. Software such as SWMM will reduce time steps so that numerical stability may be retained. Most models rely on Manning's equation, or similar, to relate the rate of flow with the depth and the friction slope. Pressurised flow, however, requires either the Darcy-Weisbach or the Hazen-Williams equations (Rossman, 2007).

CAREDAS

One the earlier models developed by Societe Grenobloise d'Etudes et d'Applications Hydrauliques (SOGREAH). It uses a Preismann slot for surcharge conditions and was the first model to do so. The model first checks the system for conduits that are steep enough where the kinematic wave equations would be sufficient. The dynamic wave equations are then only applied to flatter sections of the system (Yen, 2004).

HYDROWORKS

The model can handle looped systems and development was based on an earlier model called SPIDA. Inertia portions of the Saint-Venant equation are gradually phased out in a linear fashion between Froude values of 0.8 and 1.1. For supercritical flows, a noninertia approximation is used. When flows become pressurised, the hypothetical slot approach is used (Yen, 2004).

ISS

The model can handle only open-channel flows, though the model could be adapted to use the Preismann slot.

MOUSE

The model is an implicit, finite-difference model using Saint-Venant equations of momentum and continuity. Supercritical and subcritical flows can be modelled, and the model takes into account backwater and surcharges.

Surcharge, or pressurised flow conditions, is modelled using a Preismann slot, which allows both free-surface and pressurised flow conditions to be analysed. The model allows smoother transitions between the two types of flow condition (DHI Software, 2004).

SWMM-EXTRAN

The model is supported by the United States Environmental Protection Agency and is one of the most widely used sewer models. The EXTRAN block was added to SWMM to provide the package with a dynamic wave model.

SWMM-EXTRAN is an explicit scheme and with the explicit difference formulation solves flow using a single sweep. As a result, simultaneous solutions of sewers within the system are not required. Though relatively easy to program, assumptions made with surcharge conditions combined with convergence and stability problems of the explicit scheme of the model mean that EXTRAN is inferior to other dynamic wave models (Mays, 2001).

UNSTDY

The model makes use of a four-point noncentral implicit scheme in order to solve the Saint-Venant flow equations when subcritical flows are examined. When flows become supercritical, the model reverts to kinematic wave approximations. UNSTDY can also solve looped systems (Yen, 2004).

2.13.2. Kinematic wave models

Kinematic wave models are a simplified form of the dynamic wave equation and use a simplified derivative of the fully dynamic wave equation along with the continuity equation. The momentum equation, however, assumes that the slope of the water surface is always equal to the slope of the conduit.

The full normal flow is the maximum flow that can be passed through the conduit. Excess flows can either pond or are lost to the system. Ponded flows can re-enter the system as and when there is spare capacity in the system.

Kinematic wave models allow areas and flows to vary with both time and space inside a conduit. Flows can be delayed and attenuated although backwater effects, flow reversal, entrance and exit losses and pressurised flows are not accounted for in full. The model also restricts the system to a dendritic layout. Numeric stability can generally be maintained even with a large time step (5–15 minutes). If the listed shortcomings are not expected within a system, the results can be accurate and efficient (Rossman, 2007).

HYDROSIM

The model was developed as part of the doctoral research of Dr Ian Green. HYDROSIM has been continually expanded to its current state. The overland flow algorithm is HYDROSIM's major element and is based on one-dimensional kinematic wave flow equations. Overland flows accumulate at nodes and are then routed downstream through conduits, open channels, overflow channels and reservoirs.

SWMM-TRANSPORT

The model forms part of the SWMM package, which also provides the SWMM-EXTRAN model and the SWMM-RUNOFF model. The SWMM-TRANSPORT model was the initial routing model used by SWMM (Huber and Dickinson, 1998) and is a drainage system model used to analyse sewage and storm water flow quality and quantity.

2.13.3. Other models

Other models are simplified models that do not necessarily use Saint-Venant flow equations of momentum or continuity.

SEWSAN

The model was designed to simulate flows within a sewer system. The model is based on the contributor hydrograph model developed by Shaw (1963) (GLS Software, 2013). In essence SEWSAN is similar to unit hydrograph theory from storm water. Contributory units, 24-hour flow hydrographs, flow into the system. The units are accumulated and routed downstream by making use of a time-lag routing scheme.

SWMM-RUNOFF

The model's method of routing is a simpler form of flow routing. The model assumes that flow is steady and uniform within each computational time step (Water Environment Federation, 1999). Drainage systems, as discussed, are generally unsteady and consist of nonuniform flow. Hydrographs, however, may span several hours, and flow within a single conduit is generally within minutes. Unsteady flow intervals are often in the range of seconds. Unsteady flows can be treated as steady flows without losing too much accuracy. The model shifts flow into a conduit downstream without delay or change in shape. Flow rate and flow area are found using normal flow equations.

Rossman (2006) mentions that this model of routing ignores channel storage, backwater, losses at inlets and outlets, reversal of flow and pressurised flow. The model is limited to dendritic conveyance drainage systems, which implies that each junction is required to have only a single outflow conduit. Multiple downstream conduits can be accommodated when a junction is a divider, thus allowing the model to divide the flow among various downstream conduits. Generally the model is not very sensitive to the time step used and is better suited to long-term continuous simulations or preliminary studies (Rossman, 2006).

2.14. Model selection

It was discussed that simulating a drainage system could fall within one of three categories: design, evaluation and planning. Each of the categories requires differing levels of hydraulic detail. A planning analysis requires the least amount of hydraulic sophistication, a design analysis requires moderate levels of sophistication, while an evaluation analysis requires the highest level of sophistication. It can be deduced that each of the mentioned types of analysis would probably benefit from a different model. Using the most sophisticated model on a planning analysis would, therefore, be a waste of resources while using the most basic of models on an evaluation analysis would probably provide inconclusive or unreliable results. As a result, an appropriate model needs to be coupled with each analysis type (refer to Figure 2:11).

Figure 2:11 shows that assumptions made about the actual drainage system simplify obtained results. Each level further removes the results from the physical system. Assumptions can be made with regard to the physical topology, the physical loads and also in the model used to analyse a system.

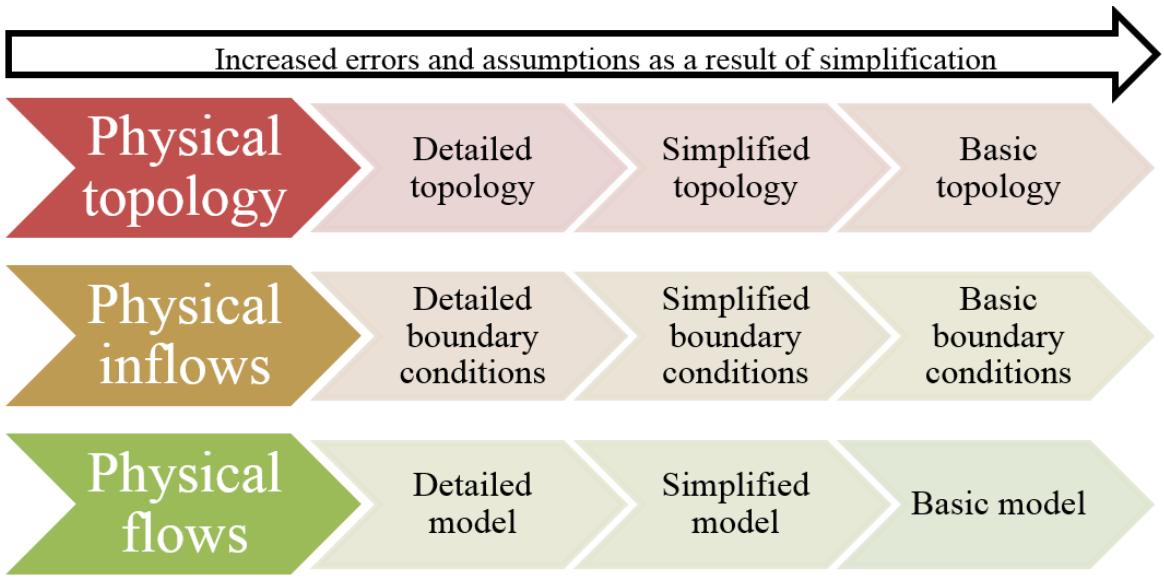

Figure 2:11: Levels of model simplification

3. Selected models

In this research project, three models were selected for evaluation, each with different levels of sophistication, and the simulation results compared (refer to Figure 2:10). Fully dynamic wave models provide the highest level of hydraulic sophistication and can be coupled with an evaluation analysis. Other models that do away with basic hydraulic principles, such as water balance, offer the most primitive levels of hydraulic sophistication and can be coupled with a planning analysis. For design analysis, a middle-ground model needs to be chosen. Any of the simplified dynamic wave models could do, but for the purposes of this study, the kinematic wave model was chosen as the model represents the lowest form of sophistication discussed that still utilises hydraulic principles. Deciding which models to choose can become a fiercely debated subject as each model has both advantages and disadvantages. The choice often becomes one of personal preference.

SWMM-EXTRAN, which is a dynamic wave model that is recognised worldwide. Similarly SWMM-TRANSPORT, which is a kinematic wave model, was chosen. Finally it was decided to also use SEWSAN, as the model makes use of a large number of assumptions and ignores basic hydraulics.

Other well-known models such as MOUSE and SWMM-RUNOFF could just as easily have been chosen. The aim of this study was not to determine which software program was the best but rather to investigate differing simulation philosophies and to determine if they are able to provide reasonable results.

As such three different means to analyse a drainage system were evaluated: SWMM-EXTRAN, SWMM-TRANSPORT and SEWSAN. An understanding of the underlying theory behind each model will aid in understanding the differences among the various models and in determining the effectiveness of each under different circumstances. In order to analyse various models for simulating a drainage system, a thorough understanding of the hydraulics behind the flow of water is needed. Some statistical equations that will allow the resulting flow hydrographs of the various models to be compared against actual measured flow data are also reviewed in this chapter.

3.1. Description of models

This section will discuss the most basic model, the contributor hydrograph model, then the kinematic wave model and the finally dynamic wave model. The design philosophies included in this study. The model used is stated in brackets:

- The contributor hydrograph model (SEWSAN).
- The kinematic wave model (SWMM-TRANSPORT).
- The dynamic wave model (SWMM-EXTRAN).

Models can assist engineers or designers in solving problems within sewer systems. All models are based on assumptions in order to analyse physical problems (Yen, 2004).

3.1.1. The contributor hydrograph model

This subsection will detail how the contributor hydrograph model, used by SEWSAN, routes flow through a drainage system. The model, as stated previously, uses a simplified approach for analysing a system. The model is not widely used, and little has been written or published on SEWSAN.

The process of designing or evaluating a drainage system requires that the flow in individual conduits be determined. With flow in conduits in mind, the contributor hydrograph theory was developed. At its core, contributor hydrograph theory is very similar to hydrographs that are used for storm water system designs. A contributing unit, such as a single conduit in a system, contributes a 24-hour flow hydrograph. The flow hydrograph within the conduit is then required to be routed downstream of the contributing unit until the hydrograph reaches the end of the drainage system. The model is also limited to dendritic conveyance drainage systems and, like steady-state models, requires dividers at junctions in order to accommodate multiple downstream conduits (Fair, 2008 a).

Similar to steady-state flow models, the contributor hydrograph model does not allow for the damping of flows, thus the flow peak never flattens and the shape of the hydrograph remains constant downstream of the system except where the peak is shifted. Hydraulic factors such as momentum and energy conservation do not play a role in the final results (Fair, 2008 a).

The first assumption made by the contributor hydrograph model has to do with velocity and how the hydrograph flows through a conduit towards the following downstream structure. Unlike more detailed models, the flow velocity is assumed to be the full flow velocity of the conduit (Fair, 2008 b), which results in a constant hydraulic radius. The full flow velocity is

calculated by using flow equations such as those of Manning or Chezy. The flow velocity can then be used to calculate the time taken for the hydrograph to flow through a conduit towards the following downstream structure.

It can be deduced that the velocity within each conduit is a constant that is dependent on the slope, diameter and roughness of the pipe. If the velocity is a constant, the time taken for any portion of a hydrograph to flow between two specific structures along a conduit is also constant. The constant time can then be used to shift a hydrograph from an upstream structure to a downstream structure.

Hydrographs will reach downstream structures at different times and will therefore be out of phase with one another due to the time-lag effect introduced by routing hydrographs downstream. The hydrographs cannot be summed in a linear fashion to obtain a specific peak flow. As a result of the time-lag effect, the peaks appear to become attenuated (Fair, 2008 a).

To simplify any hydraulic model, hydrographs are stored in a finite number of set time intervals. For example, a flow hydrograph could be made up of 24 points, in other words a flow at each hour, which does not constitute a major problem for boundary conditions. However, the fixed amount of hydrograph ordinates becomes a limitation downstream of the initial structure as the time-lag effect of routing shifts the hydrograph out of phase. Linear interpolation among the various points of the hydrograph is required to create a new hydrograph (Fair, 2008 a).

An important part of any simulation or design is determining the peak flow within a conduit that is required to be transported downstream. It becomes important to capture peak flows as accurately as possible. Linear interpolation between points may result in peak flows being reduced. An example of a reduction is when a peak occurs between time x and y. The new maximum flow will be the flow at either time x or y. As the peak lies between the two time points, the actual maximum flow will be reduced. The reduction in peak flow can be compounded when combining various flow hydrographs at a downstream structure (Fair, 2008 a).

The reduction in peak flows could be ignored, but by taking a conservative approach, a method of shifting the peaks in the model that allows the maximum flow to be retained at all times is adopted (Fair, 2008 a).

An important part of the contributor hydrograph model is the shifting of the peak flow since there are a finite number of time steps. A time step might be minutes or even hours. The time taken for a hydrograph to flow between manholes is often less than the time step.

Refer to the figures below and the given example for how flows are routed downstream. The first three cases will look at a three hypothetical points on a flow hydrograph.

Figure 3:1 illustrates Case A. The flow at Time Step 1 is less than the flow at Time Step 2, which in turn is less than the flow at Time Step 3. In Case A, the flow at Time Step 1 for the structure is determined by linear interpolation between time steps 1 and 2.

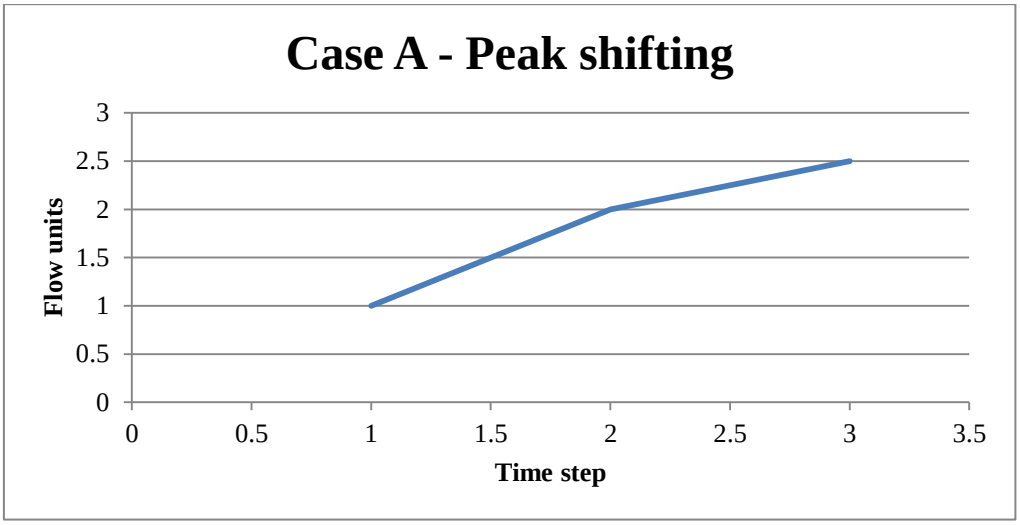

Figure 3:1: Case A: Peak shifting

Figure 3:2 illustrates Case B. The flow at Time Step 1 is less than the flow at Time Step 2, which in turn is greater than the flow at Time Step 3. Thus the hydrograph is concave down with Time Step 2 being the peak. If the new flow hydrograph is calculated using linear interpolation between Time Step 1 and Time Step 2, the peak flow will be reduced. To compensate for the peak, the flow at Time Step 1 is made equal to the flow at Time Step 2.

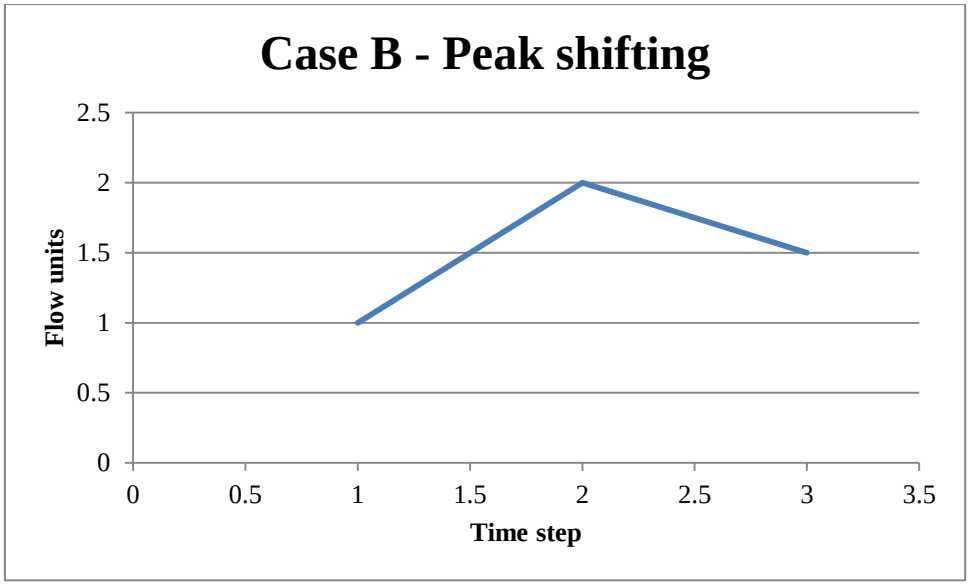

Figure 3:2: Case B: Peak shifting

Figure 3:3 illustrates Case C. The flow at Time Step 1 is greater than the flow at Time Step 2, which in turn is greater than the flow at Time Step 3. In Case C, the flow at Time Step 1 for the structure is determined by linear interpolation between time steps 1 and 2.

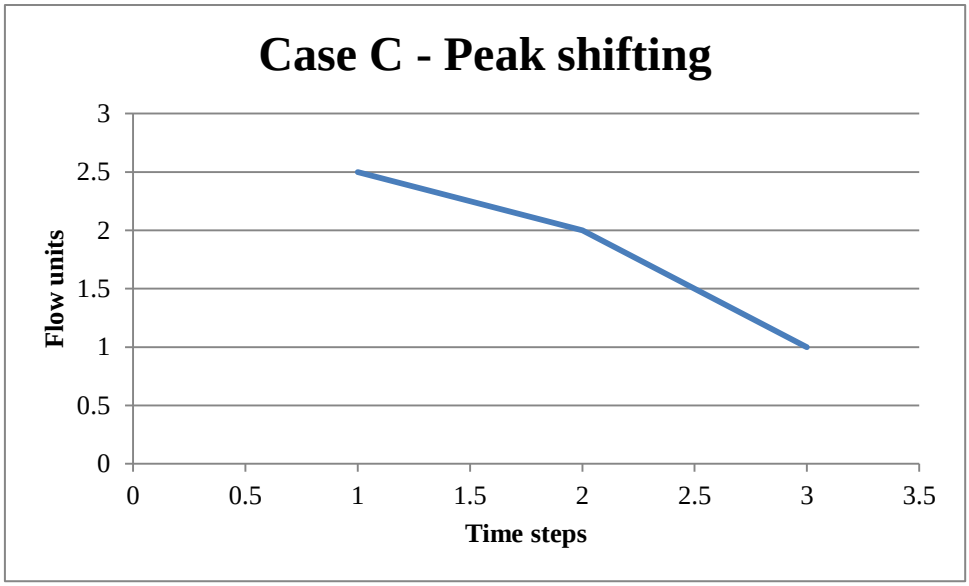

Figure 3:3: Case C: Peak shifting

Each manhole in a system has a base inflow hydrograph at the current time. The first part of determining flows throughout a system is to time route the base inflow from each manhole to the manhole's respective end manhole. This can be done since the flow lag from the manhole to the end manhole is known from assumptions that have been made. The new hydrograph

shall be called the end hydrograph. This is analogous to taking a manhole's present flow and converting it to a manhole's future flow.

The end hydrograph is then routed downstream of the initial manhole. As a result the flow at each manhole between the initial manhole and the end manhole becomes a representation of how the flow hydrograph of each manhole would appear at the end manhole if no other flows existed in the system. This is analogous to storing a manhole's future flow at each downstream manhole.

Since the flow lag is known from each manhole to the end manhole the stored hydrographs at each manhole can then be time shifted back to produce the actual flow hydrograph at the manhole. This is analogous to converting the stored future flow into a present flow at each manhole.

The following example demonstrates how flow shifting works in the contributor hydrograph model. The example makes use of a conduit that will be refered to as Conduit A . Infiltration has been ignored in the example.

The lag in flow downstream of Conduit A to the end manhole is 35.9 minutes (0.599 h). This is calculated by summing the flow lag from each conduit downstream of Conduit A. Table 3.1 and Table 3.2 show how the flow exiting Conduit A is calculated. The interpolated flow is then calculated by linear interpolation between Flow 1 and Flow 2 from Time 1 to the arrival time (Tn) at the end manhole. Making use of this information the flow hydrograph exiting Conduit A can be calculated by time shifting the hydrograph to the current time.

The interpolated flow is then calculated by linear interpolation between Flow 1 and Flow 2 from Time 1 to the arrival time (Tn) at the end manhole. This gives the first estimate at the new flow hydrograph at the downstream manhole. This aligns flows at Time 2 and Time 3 with the flow at Time 1. This makes it easier to calculate the three cases from Figure 3:1, Figure 3:2 and Figure 3:3.

The original peak flow into the conduit was 0.9680 m^3/s. The peak flow exiting the conduit after interpolation is 0.9658 m^3/s. Therefore the peak flow has been reduced by 2.22 ℓ/s or 0.23%. This might not seem significant, but the effect will increase with the amount of conduits in the drainage system.

In order to maintain the peak flow the following criteria is followed. From Figure 3:1 the first criteria tested is that Flow 2 must be greater than Flow 1. The second criterion tested is that Tn plus the time step length, which is 1 hour in this scenario, must be greater than Time 2. This is always the case in this scenario. The final criterion is that Flow 3 must be less than Flow 2. If all three of the criteria are met then the flow at the downstream manhole is made equal to Flow 2, which represents a peak. Figure 3:4 shows the result of the peak shift.

Table 3.1: Breakdown of flow and flow times

Time (h)	End manhole representation of flow into Conduit A (m^3/s)	Time 1	Flow 1 (m^3/s)	Time 2	Flow 2 (m^3/s)	Time 3	Flow 3 (m^3/s)
0	0.59250	0	0.59	1	0.57	2	0.54
1	0.56940	1	0.57	2	0.54	3	0.50
2	0.54290	2	0.54	3	0.50	4	0.45
3	0.50340	3	0.50	4	0.45	5	0.40
4	0.45220	4	0.45	5	0.40	6	0.36
5	0.39900	5	0.40	6	0.36	7	0.34
6	0.36090	6	0.36	7	0.34	8	0.35
7	0.34250	7	0.34	8	0.35	9	0.41
8	0.35080	8	0.35	9	0.41	10	0.53
9	0.41020	9	0.41	10	0.53	11	0.74
10	0.53250	10	0.53	11	0.74	12	0.97
11	0.73600	11	0.74	12	0.97	13	0.96
12	0.96800	12	0.97	13	0.96	14	0.95
13	0.96430	13	0.96	14	0.95	15	0.93
14	0.95210	14	0.95	15	0.93	16	0.89
15	0.92850	15	0.93	16	0.89	17	0.83
16	0.88820	16	0.89	17	0.83	18	0.78
17	0.83030	17	0.83	18	0.78	19	0.75
18	0.77960	18	0.78	19	0.75	20	0.74
19	0.75400	19	0.75	20	0.74	21	0.71
20	0.73840	20	0.74	21	0.71	22	0.66
21	0.71490	21	0.71	22	0.66	23	0.62
22	0.66470	22	0.66	23	0.62	24	0.59
23	0.61780	23	0.62	24	0.59	1	0.57
24	0.59250	24	0.59	1	0.57	2	0.54

Table 3.2: Calculating flow at downstream manhole

Arrival time (Tn) at the end manhole (h)	Interpolated out flow from Conduit A (m^3/s)	If Flow 2 > Flow 1	If Tn+1 > Time 2	If Flow 3 < Flow 2	Time (h)	Resultant out flow from Conduit A (m^3/s)
0.60	0.5787	0	1	1	0	0.5787
1.60	0.5535	0	1	1	1	0.5535
2.60	0.5193	0	1	1	2	0.5193
3.60	0.4727	0	1	1	3	0.4727
4.60	0.4203	0	1	1	4	0.4203
5.60	0.3762	0	1	1	5	0.3762
6.60	0.3499	0	1	0	6	0.3499
7.60	0.3475	1	1	0	7	0.3475
8.60	0.3864	1	1	0	8	0.3864
9.60	0.4834	1	1	0	9	0.4834
10.60	0.6543	1	1	0	10	0.6543
11.60	0.8749	1	1	1	11	0.9680
12.60	0.9658	0	1	1	12	0.9658
13.60	0.9570	0	1	1	13	0.9570
14.60	0.9380	0	1	1	14	0.9380
15.60	0.9044	0	1	1	15	0.9044
16.60	0.8535	0	1	1	16	0.8535
17.60	0.7999	0	1	1	17	0.7999
18.60	0.7643	0	1	1	18	0.7643
19.60	0.7447	0	1	1	19	0.7447
20.60	0.7243	0	1	1	20	0.7243
21.60	0.6848	0	1	1	21	0.6848
22.60	0.6366	0	1	1	22	0.6366
23.60	0.6027	0	1	1	23	0.6027
24.60	0.5931	0	1	1	24	0.5931

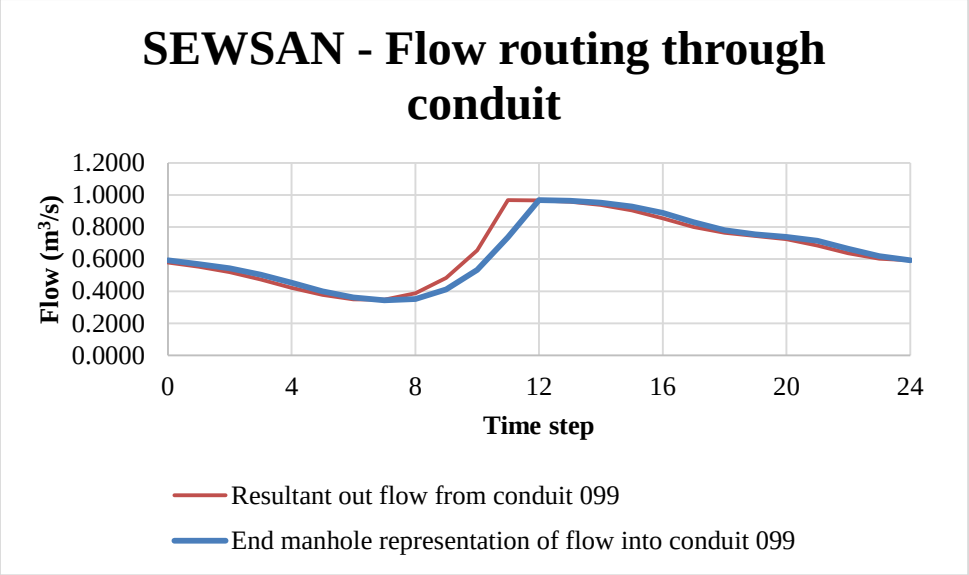

Figure 3:4: SEWSAN - Flow routing through conduit

It should be noted that shifting peaks has some undesired effects on the results of the model. The first and probably the most notable difference is the shape of the simulated hydrographs. The shape of the hydrograph affects any flow volume calculations. Because no allowances have been made for flood attenuation, the peak flows should also be greater than those found in fully hydrodynamic models. An overall decrease in the time step used to simulate a model should result in improved accuracy (Fair, 2008 a). Furthermore, the lag calculated for each conduit is independent of upstream and downstream conduits. This means that the actual invert levels of a conduit are not important, only the individual conduit slope is required. This does, however, allow systems to be analysed where invert levels are unknown and slopes are assumed.

3.1.2. The kinematic wave model

The SWMM-TRANSPORT model uses a modified nonlinear kinematic wave model and is a drainage system model used to analyse sewage and storm water flow quality and quantity. This study, however, only investigated the flow quantity. The SWMM-TRANSPORT model forms part of the SWMM package, which also provides the SWMM-EXTRAN model and the SWMM-RUNOFF model.

The continuity equation is initially normalised by using ‘just-full’ steady uniform flow and area. The equation is then written in finite differences and shown as a linear function of normalised unknowns. The unknowns are A/Af and Q/Qf at points $x = (1 + i)dx$ and $t = (n + 1)dt$ and can be expressed as shown in Equation 3.1 (Yen, 2004).

$$(Q/Q_f)_{i+1,n+1} + C_1(A/A_f)_{i+1,n+1} + C_2 = 0$$

Equation 3.1: SWMM-TRANSPORT

C1 and C2 are functions of determined quantities. According to the assumptions made by kinematic wave models, flow is related to depth. In order to find a relationship between the depth of flow and the flow, Manning's equation is used (Clemmens and Strelkoff, 2011).

$$(Q/Q_f) = AR^{2/3}/A_f R_f^{2/3} = f(A/A_f)$$

Equation 3.2: SWMM-TRANSPORT discharge

A normalised curve showing the relationship between Q/Qf and A/Af, Equation 3.2, for steady uniform flow in conduits of varying geometry is generated. According to the kinematic wave model, only a single boundary condition is required. The required boundary condition is the upstream inflow, thus the downstream boundary condition is not a requirement and as a result, no backwater effects can be calculated even if the flow is subcritical. The SWMM-TRANSPORT model, however, uses a friction slope of the previous time values at spatially forward points, resulting in backwater effects partially being taken into account. When routing unsteady nonuniform flow by using the above two equations, the value of Q_f is not determined as steady uniform full flow. It is, however, adjusted by making use of the following assumption (Mays, 2001):

$$S_f = S_o - \frac{\partial h}{\partial x} - \frac{V}{g}\frac{\partial V}{\partial x} = S_o - \frac{h_{i+1,n} - h_{i,n}}{\Delta x} - \frac{V_{i+1,n}^2 - V_{i,n}^2}{2g\Delta x}$$

Equation 3.3: SWMM-TRANSPORT discharge adjustment

SWMM-TRANSPORT also makes a further assumption in order to improve the stability of the model. It is assumed that for iteration k, Q_{fk} is the average of current and previous values (relaxation factor of 0.5).

$$Q_{fk} = \frac{1}{2}Q_{f(k-1)} + \frac{K_n}{2n\sqrt{\Delta x}}A_f R_f^{2/3} \times [S_o\Delta x + h_{i(k-1)} - h_{1+1(k-1)} + \frac{V_{i(k-1)}^2}{2g} - \frac{V_{i+1(k-1)}^2}{2g}]^{1/2}$$

Equation 3.4: SWMM-TRANSPORT flow adjustment

The values of head and velocity are at the previous time step n(dt). Use of Equation 3.3 yields results closer to a quasi-steady dynamic wave model. Making further use of Equation 3.4 results in downstream backwater effects being partially taken into account (Yen, 2004).

The adjustment makes SWMM-TRANSPORT a more desirable kinematic wave model than other nonlinear kinematic models. The backwater effect, however, is only effective if flows do not change rapidly. No hydraulic jumps or drops are allowed. It should be remembered, however, that the downstream boundary condition is never really accounted for. Yen (2004) also states that a comparison between SWMM-TRANSPORT and SWMM-EXTRAN (following model) has not been reported.

If the slope of the conduit is very steep, and flow approaches critical flow depths, floods may be moved through a conduit without time lag. Small manholes are handled as point-type manholes where the change in storage with respect to time is zero.

Huber and Dickinson (1998) state that surcharge is treated by merely storing flows that are unable to be transported downstream. The excess is stored at the upstream manhole until the downstream conduit has sufficient capacity. The model does not attempt to model pressurised flow nor whether any overland flow occurs.

3.1.3. The dynamic wave model

SWMM's Extended Transport Block (SWMM-EXTRAN) was developed to be used on systems where it cannot be assumed that steady flows, for backwater calculations, are sufficient. As stated before, SWMM-EXTRAN uses fully dynamic wave equations for gradually varying flows. The program also uses an explicit solution to step along in time. Wave celerity in short conduits therefore governs the solution to the time step analysis.

The model uses a link to node design that allows the use of a non-dendritic drainage system. As a result, the model allows for greater flexibility. Drainage system components that can be added to the model are the following (Roesner and Aldrich, 1992):

- Parallel conduits
- System loops
- Lateral diversions/weirs
- Orifices
- Pumps
- Partial surcharge conditions

Since SWMM-EXTRAN is versatile, some designers have developed a tendency to analyse entire drainage systems using SWMM-EXTRAN while other more simplified models, such as SWMM's SWMM-RUNOFF or SWMM-TRANSPORT, would have sufficed. Hydraulically less sophisticated models, in systems where complex flows such as surcharge or backwaters are not required, could have provided savings in unrequired data and computer solving time. SWMM-EXTRAN does, however, have its limitations. If the limitations are not understood, incorrect results for heads and flows for a system can be produced. Some of the limitations are the following (Roesner and Aldrich, 1992):

- Head loss is not accounted for at junctions, areas of contraction or expansions, bends, and so forth. It is assumed that losses are accounted for in the Manning *n* value of the conduits, where such losses may possibly occur.
- The change in head in areas of rapid contractions or expansions is not accounted for. In areas of rapid expansion, head loss will try to equalise the heads, while in areas of rapid contraction, head loss might further aggravate problems.
- Where inverts of two connecting conduits are not similar, such as a drop manhole, errors will be generated during surcharge conditions if the crown of the lowest conduit lies beneath the invert of the higher conduit. The error will increase the greater the difference in height is.
- Instabilities in the model may occur at manholes with weirs when the manhole is under surcharge conditions and the weir has become submerged to such a degree that the upstream head equals or has become less than the downstream head.
- EXTRAN is also incapable of simulating water quality.

Governing equations

The model is based on the principles of conservation of mass and momentum. The principles govern unsteady flow through conduits, known as the Saint Venant equations, as shown below in equations Equation 3.5 and Equation 3.6 (Rossman, 2007).

$$\frac{\partial A}{\partial t} + \frac{\partial Q}{\partial x} = 0$$

Equation 3.5: SWMM-EXTRAN continuity equation

$$\frac{\partial Q}{\partial T} + \frac{\partial (Q^2/A)}{\partial x} + gA\frac{\partial H}{\partial x} + gAS_f + gAh_L = 0$$

Equation 3.6: SWMM-EXTRAN momentum equation

Where:

- x is current distance of the conduit.
- t is time.
- A is the cross-sectional area.
- Q is the rate of flow.
- H is hydraulic head.
- S_f is the friction slope.
- h_L is the local energy loss per unit length.
- g is gravitational acceleration.

The friction slope, Equation 3.7, can be obtained by rewriting the Manning equations; refer to the section about hydraulics in the literature review.

$$S_f = \frac{n^2 V|V|}{K_n^2 R^{4/3}}$$

Equation 3.7: Manning's friction slope

Where:

- n is Manning's coefficient.
- V is the flow velocity.
- R is the hydraulic radius.
- K_n is a constant (1.49 for US units and 1.0 for metric units).

Local losses can be expressed as shown in Equation 3.8:

$$h_L = \frac{KV^2}{2gL}$$

Equation 3.8: Local losses

Where:

- K is the local loss coefficient.
- L is the length of the conduit.

If the cross-sectional area is a known entity, as within a sewer system, the flow depth can be determined from the hydraulic head. Therefore, the dependent variables of the above equations are the flow rate and head, both of which are functions of time and distance (Rossman, 2007).

Another continuity relationship is required at nodes connecting two or more conduits when simulating a drainage system. SWMM-EXTRAN assumes a continuous water surface between the surface level at a node and the entering or exiting conduits. The approach of the model to the dynamic routing model also takes into account stored water.

To take continuity into account, the change in hydraulic head at any node needs to be determined, which can be done with Equation 3.9:

$$\frac{\partial H}{\partial t} = \frac{\sum Q}{Astore + \sum As}$$

Equation 3.9: SWMM-EXTRAN change in hydraulic head with respect to time

Where:

- Astore is the cross-sectional area of the node.
- $\sum As$ is the surface area of the contributing counduits.
- $\sum Q$ represents the net inflow at the node (i.e. inflow minus outflow).

General solution

To solve the abovementioned equations, they need to be converted into an explicit series of finite difference equations, which computes the flow within a conduit and the head at a node. The values are computed for time t + dt for known values at time t.

In order to solve the momentum and continuity equations shown above, boundary conditions need to be set. Initial conditions are required for head and flow at time 0. Boundary conditions are required at x = 0 and x = L at all times.

The flow within each conduit within the drainage system can be expressed as follows:

$$Q_{t+\Delta t} = \frac{Q_t + \Delta Q_{gravity} + \Delta Q_{inertial}}{1 + \Delta Q_{friction} + \Delta Q_{losses}}$$

Equation 3.10: SWMM-EXTRAN explicit flow within conduit

Each of the separate components of the explicit flow formula is defined as follows:

$$\Delta Q_{gravity} = \frac{g\bar{A}(H_1 - H_2)\Delta t}{L}$$

Equation 3.11: SWMM-EXTRAN explicit dQ gravity

$$\Delta Q_{inertial} = 2\bar{V}(\bar{A} - A_t) + \frac{\bar{V}^2(A_2 - A_1)\Delta t}{L}$$

Equation 3.12: SWMM-EXTRAN explicit dQ inertial

$$\Delta Q_{friction} = \frac{gn^2|\bar{V}|\Delta t}{k^2\bar{R}^{4/3}}$$

Equation 3.13: SWMM-EXTRAN explicit dQ friction

$$Q_{losses} = \frac{\sum_i K_i|V_i|\Delta t}{2L}$$

Equation 3.14: SWMM-EXTRAN explicit dQ losses

Where:

- $\bar{A}$ is the average cross-sectional area of flow within the conduit.
- $\bar{R}$ is the average hydraulic radius.
- $\bar{V}$ is the average flow velocity.
- V_i is the local flow velocity at position i in the conduit.
- K_i is the local loss coefficient at position i in the conduit.
- H_1 is the head at the upstream node.
- H_2 is the head at the downstream node.

- A_1 is the cross-sectional area at the upstream entrance of the conduit.
- A_2 is the cross-sectional area at the downstream exit of the conduit.

In order to solve the head at each node, the following equation is used:

$$H_{t+\Delta t} = H_t + \frac{\Delta Vol}{(A_{store} + \sum A_s)_{t+\Delta t}}$$

Equation 3.15: SWMM-EXTRAN explicit head at node

Where:

$$\Delta Vol = 0.5 \left[(\sum Q)_t + (\sum Q)_{t+\Delta t} \right] \Delta t$$

Equation 3.16: SWMM-EXTRAN explicit change in volume through node

SWMM-EXTRAN solves Equation 3.10 and Equation 3.15 by using a modified Euler method, which is equivalent to the second-order Runge-Kutta method. Flow is calculated for new flows in each conduit using half time steps, dt/2. The process uses the previously computed values of velocity, head and area at time t. The subsequent values computed are substituted into Equation 3.15 in order to compute head, again using half time steps (Rossman, 2006).

Full-step flows are calculated by using Equation 3.10. However, the full time step dt is used. It also uses the velocities, head and areas computed for the half-step solution. Further, new heads are determined for the full time step by solving Equation 3.15 again using the full-step flows.

3.1.4. Model limitations

Table 3.3 lists basic flow conditions that occur in sewer systems that can be modelled by the three models. The table indicates that the detailed model, SWMM-EXTRAN, is capable of taking all flow conditions into account. The simplified model, SWMM-TRANSPORT, can take gradually varied flows into account as the model partially takes backwater effects into account. The greater the rate of flow change the less effective the model becomes in handling backwater effects, the model could theoretically compensate for rapidly varied flow in a very limited manner. The basic model, SEWSAN, always assumes full flow conditions in the conduit. As a result it cannot take gradually varying flows into account.

Table 3.3: Model limitations

Flow conditions	SWMM-EXTRAN	SWMM-TRANSPORT	SEWSAN
Surcharge	X		
Rapidly varying flows	X	Very limited	
Gradually varying flows	X	X	
Constant flow	X	X	X

3.2. Model boundary and initial conditions

Boundary conditions must be set in order for any model to produce a unique set of results. Boundary conditions could be fixed inflows at junctions or hydrographs that represent inflow with respect to time.

Yen (2004) states that initial conditions differ from boundary conditions and represent the state of a model before the simulation begins (t = 0). It is thus the velocity V(x, 0) and the discharge Q(x, 0) that are paired with the depth h(x, 0). For storm water systems, initial conditions might all be zero as dry-bed conditions exist. For sewer systems, the initial conditions will probably represent base flow or dry-weather flow.

Furthermore, zero initial conditions could cause problems for numeric simulations. Either a small depth or a small discharge is usually assumed. For dry-bed situations, the assumption is valid as dry-bed film flow will exist and flow does not start gradually. Considering dry-bed flow instabilities, an initial depth of less than 5 mm is acceptable (Yen, 2004).

For sewers the initial depth could be insufficient as negative depths may be obtained after the first time step has been completed. The continuity equation requires volumes much greater than the volume of water in the conduit with a small depth. Therefore, an initial discharge that allows the simulation to commence is assumed.

3.3. Verification procedure

When analysing physical drainage systems, the results will firstly be compared using the following three criteria (Butler and Graham, 1995):

- $Peak\ flow = \frac{predicted\ peak\ flow - actual\ peak\ flow}{actual\ peak\ flow}$
- $Mean\ flow = \frac{predicted\ mean\ flow - actual\ mean\ flow}{actual\ mean\ flow}$
- $Peak\ time = \frac{predicted\ time - actual\ time}{actual\ time}$

The peak flow is mostly used when determining pipe capacities and is useful when designing a system for a certain peak design flow. The mean flow and peak time can be used to determine the size and other requirements of a waste water treatment plant.

The following values were suggested for the verification of British urban sewer drainage systems (Green and Drinkwater, 1985):

- Peak flows should be in the order of 10%.
- Mean flows should be in the order of 10%.
- Timings should be in the order of 10 minutes.

Butler and Graham (1995) also propose a fourth criterion, the root mean square method. Instead of using their proposed equation it was decided to use three other, more accepted, statistical equations to compare the flow hydrographs (Moriasi et al., 2006):

- Nash-Sutcliffe efficiency (NSE).
- Percent bias (PBIAS).
- RMSE-observations standard deviation ratio (RSR).

3.3.1. Nash-Sutcliffe efficiency

NSE (Equation 3.17) is an indicator for the agreement between the calibrated (observed) flow and the modelled (simulated) flow hydrographs (Moriasi et al., 2006). The value can range from -∞ to 1.0, with an NSE value of 1.0, suggesting perfect alignment of the two hydrographs. Values between 0.0 and 1.0 are considered perfectly acceptable. Values less than zero, however, suggest unacceptable performance of the simulated values. NSE is recommended by American Society of Civil Engineers (ASCE) (1993) and is commonly used. It was also found to be the objective factor that best reflected the overall fit between two hydrographs.

$$NSE = 1 - \frac{\sum_{i=1}^{n}(Y_i^{obs} - Y_i^{sim})^2}{\sum_{i=1}^{n}(Y_i^{obs} - Y^{mean})^2}$$

Equation 3.17: NSE equation

Where:

- Y_i^{obs} is the observed flow at time i.
- Y_i^{sim} is the modelled flow at time i.

- Y^{mean} is the mean of the observed flow.

3.3.2. Percent bias

PBIAS (Equation 3.18) gives an indication whether the modelled flow hydrograph tends to be larger or smaller than the measured flow hydrograph. If the value is greater than zero, the modelled hydrograph underestimated the flow. If the value is less than zero, the modelled hydrograph overestimated the flow. A value of zero is optimal, suggesting similar flow. Values approaching zero indicate higher accuracy. PBIAS was also recommended by ASCE (1993) and is often used in determining water balance errors and to indicate poor model performance (Moriasi et al., 2006).

$$PBIAS = \frac{\sum_{i=1}^{n}(Y_i^{obs} - Y_i^{sim})}{\sum_{i=1}^{n}(Y_i^{obs})} \times 100$$

Equation 3.18: PBIAS equation

3.3.3. RMSE-observations standard deviation ratio

RMSE (Equation 3.19) is an error index used in statistics. It is accepted that the lower the RMSE value is, the better a model performs in comparison to observed model flows. Singh et al. (2004) developed the RMSE-observations standard deviation ratio (RSR). RSR is calculated by dividing the RMSE value by the standard deviation of the observed flows. Zero is the optimal value for model performance. It can increase to a large positive number. The greater the number, the lower the model performance (Moriasi et al., 2006).

$$RSR = \frac{RMSE}{STDEV_{obs}} = \frac{\sqrt{\sum_{i=1}^{n}(Y_i^{obs} - Y_i^{sim})^2}}{\sqrt{\sum_{i=1}^{n}(Y_i^{obs} - Y^{mean})^2}}$$

Equation 3.19: RSR equation

4. Evaluation of models

4.1. Selection of models, software and systems

Based on the information assembled from the literature review, set out in Chapter 2, it was decided to compare the SEWSAN, SWMM-EXTRAN and SWMM-TRANSPORT models. The three models were discussed in more detail in Chapter 3. The software packages used to analyse the models were SEWSAN and SWMM.

For the purposes of this study, two sewer systems were selected. Flow rate measurements were obtained on the sections chosen to be analysed. The two systems were large with the first serving 19 600 stands and the second serving 21 500 stands. The test cases highlighted how the three models handled the same flow scenario.

4.2. Procedure

Refer to Figure 1:1 and Figure 1:2 for a broad overview of the process to verify the models with the measured flow hydrographs. Boundary conditions for each longitudinal section were generated using a basic SEWSAN analysis of the entire system. The analysis gave each model the same initial conditions. If a SEWSAN analysis or an analysis with another model was not performed, inflow hydrographs would have had to be measured at each entry point into the longitudinal section. Such an approach was considered impractical and not cost effective.

An equivalent circular hydraulic radius for noncircular sections was calculated for each conduit to enable comparison, as the contributor hydrograph model used by SEWSAN assumes full flow. It was considered appropriate to generate results over 24 hours, because the period would also capture daily hydrograph peaks. The SEWSAN model was run over a 24-hour period, but SWMM-TRANSPORT and SWMM-EXTRAN had to be analysed over 48 hours in order to evaluate a 24h hydrograph. The longer time period was required to prime the system, which amounted to the model being given an initial flow when considering only the second 24-hour hydrograph. Due to the nature of the SEWSAN model, there was no change between the first 24-hour hydrograph and the second.

4.3. Summary of drainage systems

This section provides a basic description of the two drainage systems used to compare the three models. Both drainage systems are situated in South Africa; the first will be referred to as Drainage System A and the second as Drainage System B. Due to limitations in obtaining sufficient data for all the models only a single longitudinal section of each system was analysed within each system that could be analysed with enough detail.

The longitudinal section of Drainage System A which was analysed was 8.6 kilometres in length and the longitudinal section of Drainage System B which was analysed was 13.4 kilometres in length. Each system has a single calibration point near the end of their respective longitudinal sections. The measured flow data and positions of the flow loggers will be discussed under each specific drainage system.

4.4. Flow measurements

Flow data was obtained for seven consecutive dry-weather days at two measurement points. The first measurement point was near the lower reaches of the analysed Drainage System A longitudinal section, which shall be referred to as measurement point A. The second measurement point was near the lower reaches of the analysed Drainage System B longitudinal section, which shall be referred to as measurement point B

At measurement point A, flow hydrographs were measured at manhole 099 on a section with a long continuous slope: 90 metres before the measurement point and 190 metres after. The 280-metre stretch of constant slope helps reduce the hydraulic effect of upstream and downstream control structures. Figure 4:1 illustrates the constant continuous slope before and after manhole 099.

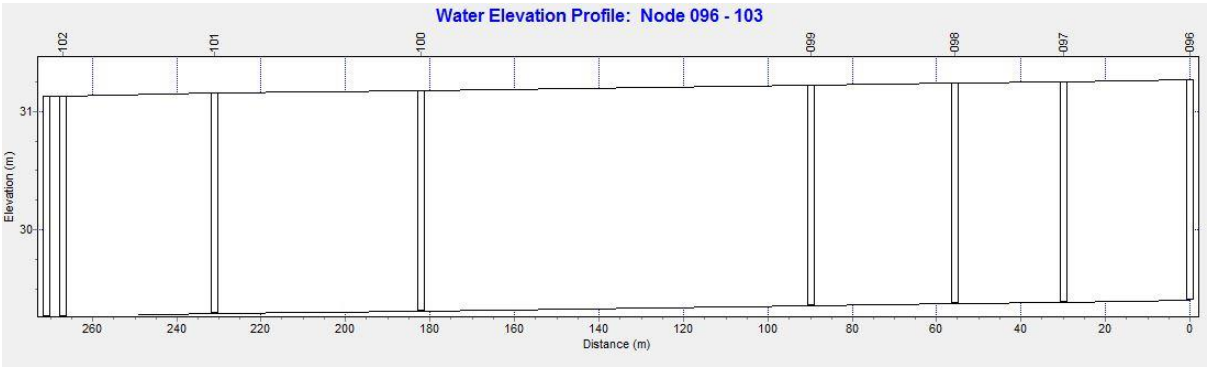

Figure 4:1: Measurement point A longitudinal section

At measurement point B, flow hydrographs were measured at manhole 198 on a section with a long continuous slope: 384 metres before the measurement point and over a kilometre after. The 1.3-kilometre stretch of constant slope helps to reduce the hydraulic effect of upstream and downstream control structures. Figure 4:2 illustrates the continuous slope before and after manhole 198.

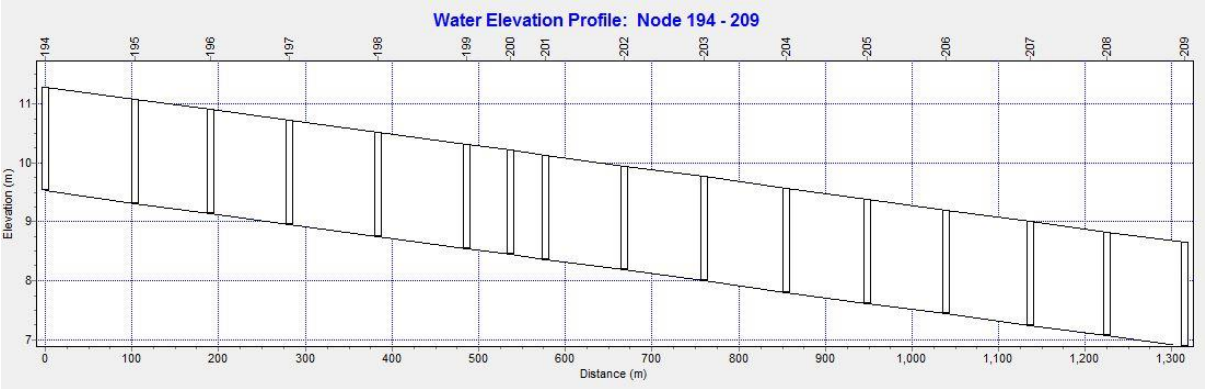

Figure 4:2: Measurement point B longitudinal section

Flow measurements were made with ultrasonic sensors to measure the flow depth. To calibrate the measurements, the flow velocity was measured at the same time as the flow depth. The combination of velocity and flow area enabled the flow rate to be determined. The Manning coefficient of roughness was determined once the flow rate, conduit area and conduit slope was known. The Manning coefficient from the calibration process was assumed to be constant and as such only the flow depths need to be measured after the initial calibration process.

Dry weather flow depths were measured at both measurement points once every hour from 11:25 on 1 July 2010 to the same time on 9 July 2010. Seven consecutive full days were measured with two half-days. The measurements included two weekend days. The difference between weekend flows and weekday flows are shown in Figure 4:3 and Figure 4:4. Since the boundary conditions of the simulated models included industrial and commercial flows, the weekend results were disregarded.

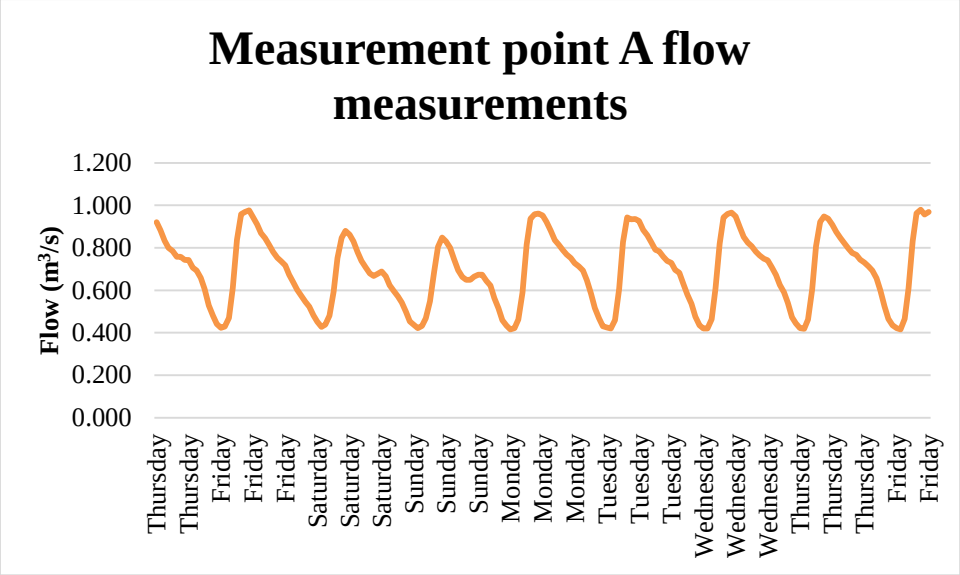

Figure 4:3: Measurement point A flow measurements

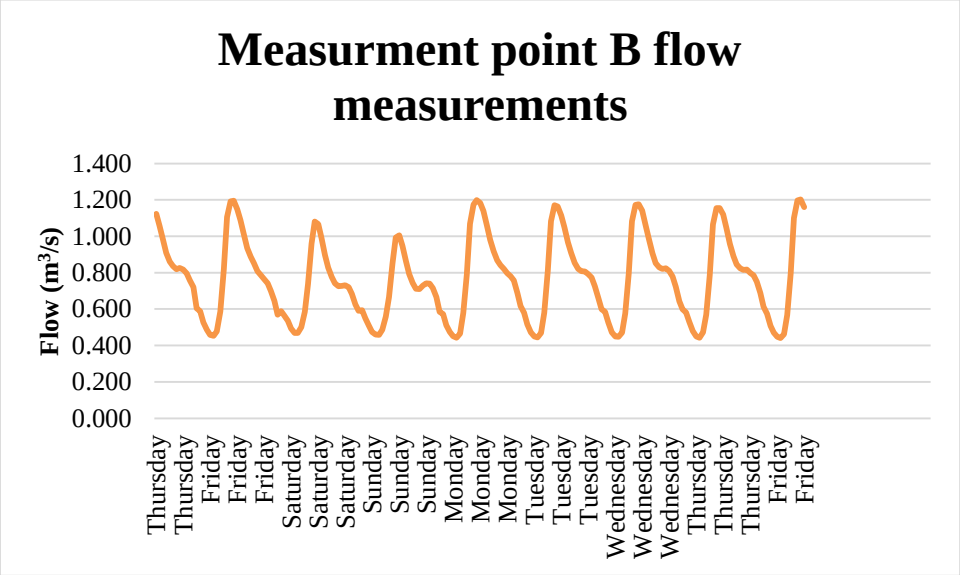

Figure 4:4: Measurement point B flow measurements

When calculating the average flow over a weekday period, only the days that flow depths were measured for a full day were used. Therefore, the partial days' measurements on Thursday the 01/07/2010 and Friday the 09/07/2010 were disregarded. The tables and the figures below show that the flows remained relatively similar over the five day period. The similarity between the measured days gives confidence that wet weather inflows did not affect the measured flow data. This is confirmed by weather reports for the period and the days before the flows were measured (Weather Online, 2013). As a result, the average flow

hydrograph for each of the two measurement points were derived from five dry weather week day flows.

Table 4.1: Measured flows at measurement point A

Measurement point A (flow in ℓ/s)						
Time	Day 1	Day 2	Day 3	Day 4	Day 5	Average
00:25	529.2	515.2	516.1	536.4	540.2	527.4
01:25	479.9	459.5	468.4	475.6	473.2	471.3
02:25	440.5	433.3	430.8	435.8	444.1	436.9
03:25	423.4	416.0	425.1	420.1	420.9	421.1
04:25	429.2	421.0	419.7	419.5	418.3	421.5
05:25	469.7	461.7	459.3	464.0	462.5	463.4
06:25	611.1	589.6	607.2	609.4	604.4	604.3
07:25	837.7	815.6	827.6	819.3	807.3	821.5
08:25	958.1	937.3	942.5	943.2	922.6	940.7
09:25	969.5	958.1	934.7	960.3	948.1	954.1
10:25	976.9	962.1	936.1	965.3	936.8	955.4
11:25	944.8	952.8	926.4	948.1	908.8	936.2
12:25	910.3	921.7	884.9	896.6	874.7	897.6
13:25	869.7	881.7	858.4	851.6	847.0	861.7
14:25	845.0	836.8	827.7	824.5	822.2	831.2
15:25	815.3	814.5	791.3	807.3	797.4	805.2
16:25	780.3	788.9	783.4	781.5	775.9	782.0
17:25	753.5	768.4	758.4	763.2	766.6	762.0
18:25	735.9	752.1	738.6	748.4	744.8	744.0
19:25	716.3	727.7	729.4	740.8	729.9	728.8
20:25	673.3	712.9	696.0	707.6	712.8	700.5
21:25	637.3	693.5	681.8	671.1	693.1	675.4
22:25	602.4	647.1	628.0	625.4	657.0	632.0
23:25	574.2	584.6	579.3	589.9	598.8	585.4

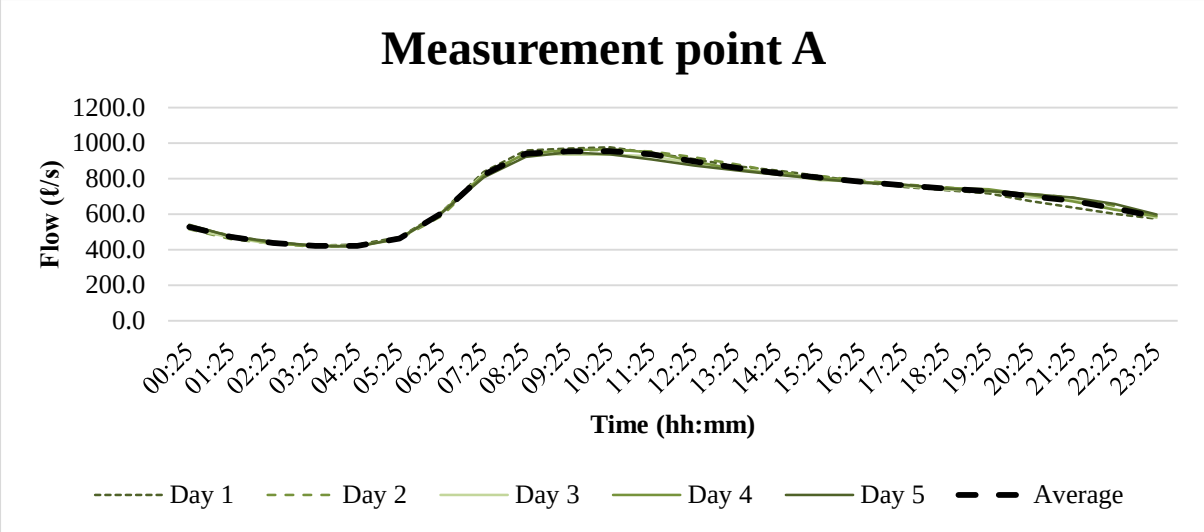

Figure 4:5: Measurement point A average flow hydrograph

Table 4.2: Measured flows at measurement point B

Measurement point B (Flow in ℓ/s)						
Time	Day 1	Day 2	Day 3	Day 4	Day 5	Average
00:25	588.9	573.5	579.5	584.3	581.9	581.6
01:25	526.1	511.5	517.1	527.5	531.3	522.7
02:25	487.0	473.6	472.5	472.7	478.7	476.9
03:25	458.7	450.8	450.0	449.0	449.6	451.6
04:25	452.6	442.5	444.4	447.9	442.2	445.9
05:25	478.1	464.9	468.6	471.2	471.7	470.9
06:25	586.8	578.1	579.9	575.5	569.5	578.0
07:25	819.8	788.8	809.5	796.3	785.9	800.1
08:25	1105.6	1069.6	1082.6	1083.3	1065.6	1081.3
09:25	1192.4	1173.6	1169.9	1173.0	1155.4	1172.9
10:25	1195.8	1199.0	1162.9	1175.6	1155.2	1177.7
11:25	1147.6	1182.3	1114.4	1141.0	1119.7	1141.0
12:25	1087.8	1138.8	1048.7	1064.8	1046.0	1077.2
13:25	1007.0	1058.9	967.4	984.0	958.4	995.1
14:25	935.3	980.4	908.7	907.0	890.4	924.4
15:25	887.2	918.1	854.7	851.6	844.9	871.3
16:25	853.1	868.9	820.9	830.1	824.3	839.5
17:25	808.9	841.4	808.2	821.4	815.9	819.2
18:25	784.9	821.4	806.2	824.6	816.4	810.7
19:25	764.7	797.6	792.8	811.1	799.2	793.1
20:25	741.6	779.8	772.7	777.9	785.7	771.5
21:25	699.2	757.6	725.7	721.8	750.2	730.9
22:25	645.6	692.6	663.4	648.0	692.8	668.5
23:25	578.4	622.1	606.5	603.6	619.9	606.1

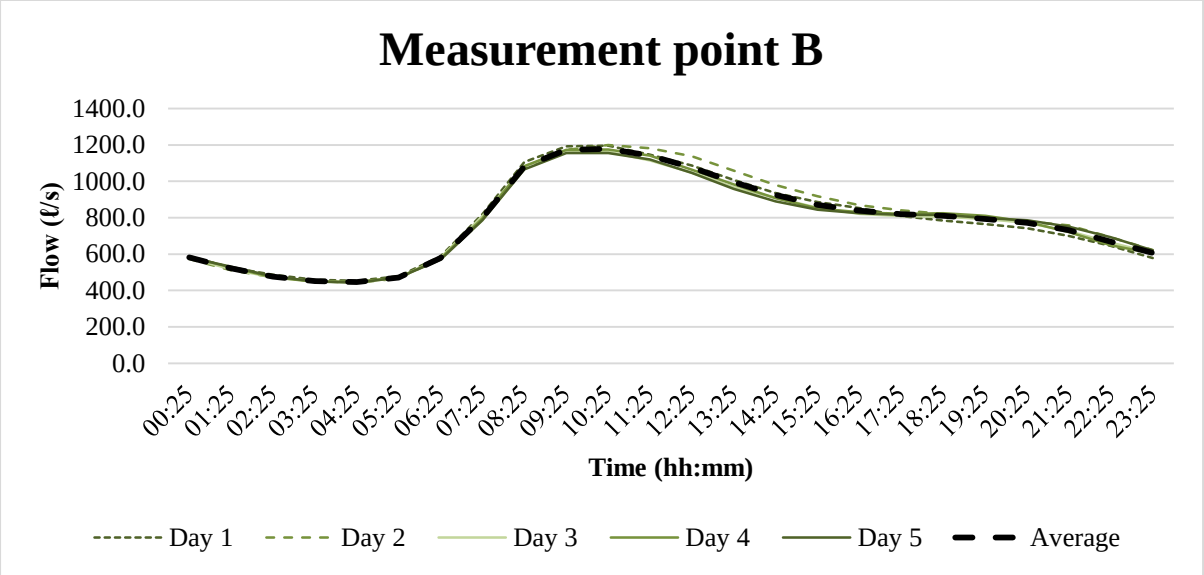

Figure 4:6: Measurement point B average flow hydrograph

4.5. Drainage System A

4.5.1. Drainage system description

The drainage system consists of approximately 600 kilometres of conventional gravity sewer conduits. The number and type of stands serviced by the drainage system are summarised in Table 4.3 as obtained from Treasury data.

Table 4.3: Drainage System A stands

Land use	No stands
Very-high-income residential	6 570
High-income residential	3 173
Medium-income residential	5 327
Low-income residential	0
Cluster	1 151
Flats	234
Business and commercial	1 242
Education	129
Government and institutes	16
Industry	303
Other	1 039
Farm	4
None	133
Unknown	4
Large	340

For the purposes of this study a single longitudinal section of connected conduits from the drainage system was analysed. The combined length of the conduits is approximately 8.6 kilometres in length and consists of 132 connected conduits, of which only one is circular; the other 131 are rectangular brick portal culverts.

4.5.2. Boundary conditions and system setup

Boundary conditions were created by making use of a Treasury database that contains the AADD, from water meters, and land use type of each stand serviced by the drainage system. The AADD together with the land use type of each stand was then linked to the nearest manhole. Stands with AADDs exceeding 20 kl/day were investigated to ensure that the demand was allocated to the correct manhole.

Each land use type has a predetermined unit hydrograph associated with it, refer to the Appendix C for a table of unit hydrographs used. These unit hydrographs were combined at each manhole and together with their AADDs, a unique inflow hydrograph was created at each manhole of the drainage system. This formed the boundary conditions for the drainage system.

With the boundary conditions known, a SEWSAN analysis was run on the entire drainage system. The analysis generated inflow hydrographs at various points along the longitudinal section that was used in the comparison. The inflow hydrographs at the entry points were taken and used as the boundary conditions for the chosen longitudinal sections.

If the boundary conditions were not created in the above manner then flows would have had to be measured at each entry point into the model and measurement point A at the same time. This was considered impractical and not cost effective.

4.5.3. Critical sections considered

After the three models had been used to simulate the longitudinal section, a single conduit (117) that lacked capacity was identified. The problem occurred where a 1.2-metre-diameter pipe, which bypassed an old brick tunnel, had been placed within the system. SEWSAN indicated that the conduit had -16% capacity, which meant that the conduit had exceeded its hydraulic capacity. SWMM-TRANSPORT (see Figure 4:7) also indicated that 100% of the conduit's capacity had been reached and that the conduit did not have spare capacity.

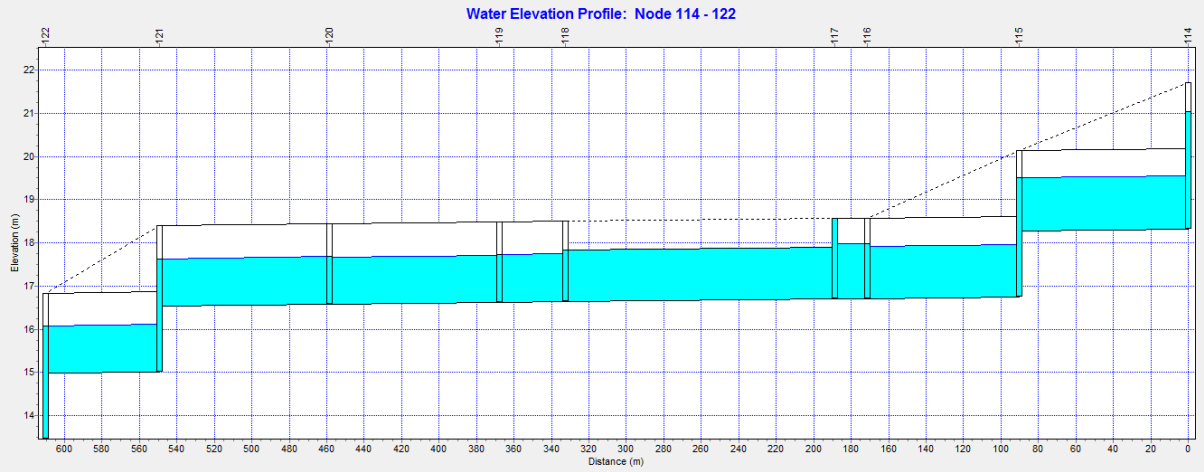

Figure 4:7: TRANSPORT peak flows (114 to 122)

There is a drop structure downstream from conduit 120 and another upstream of conduit 115. It has been discussed that SEWSAN and SWMM-TRANSPORT do not take hydraulic structures into account. SWMM-EXTRAN, shown in Figure 4:8, does take hydraulic structures into account and as a result calculated that only 75% of the conduit was being utilised. The flow between manhole 114 and 133 demonstrates how the three models react to rapidly varying flow conditions.

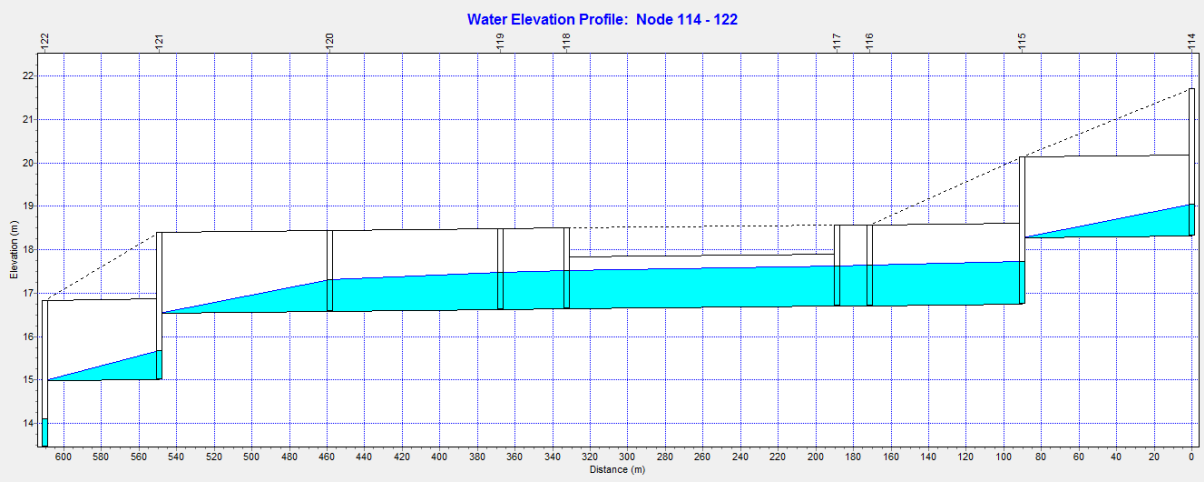

Figure 4:8: EXTRAN peak flows (114 to 122)

4.5.4. Results at measurement point

After each of the models had been used to simulate the longitudinal section, the following flow values were calculated for each time step at measurement point A. Table 4.4 contains the flows calculated at measurement point A as well as the average flow measurement at measurement point A. Figure 4:9 compares the hydrographs.

Table 4.4: Drainage System A modelled and measured flows

Sewage flow rates at measurement point A (ℓ/s)				
Time (h)	CALIBRATION	SEWSAN	EXTRAN	TRANSPORT
0	527	585	567	577
1	471	560	540	551
2	437	525	498	517
3	421	478	446	469
4	422	426	394	417
5	463	382	359	373
6	604	356	340	347
7	822	355	343	343
8	941	395	399	381
9	954	494	549	484
10	955	667	804	676
11	936	975	968	888
12	898	973	963	966
13	862	963	950	957
14	831	944	921	935
15	805	910	872	898
16	782	859	812	844
17	762	805	768	791
18	744	770	752	760
19	729	751	736	743
20	701	730	705	721
21	675	690	651	679
22	632	642	609	630
23	585	609	589	599

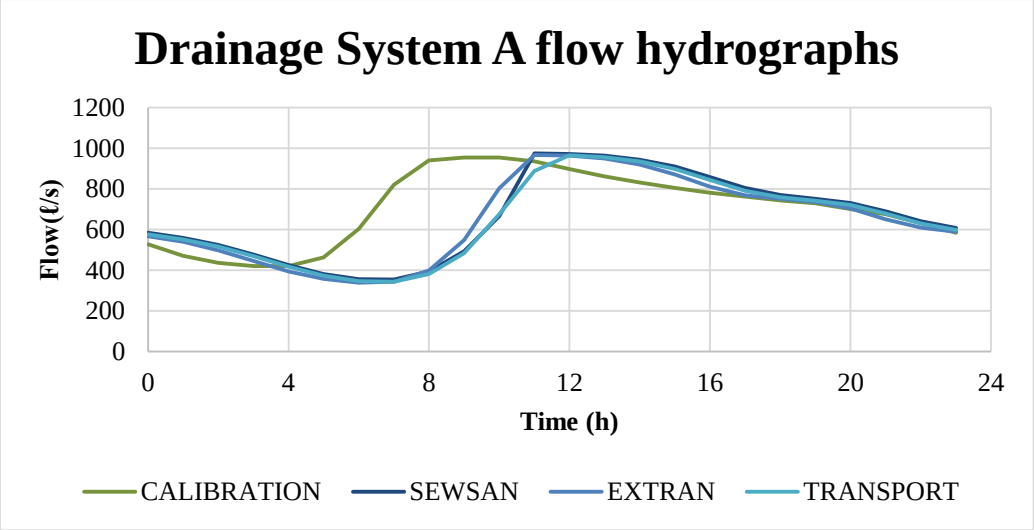

Figure 4:9: Drainage System A flow hydrographs

Table 4.5 shows the calculated verification values for Drainage System A, the calculations of which can be found in Appendix A. Acceptable values for RSR are between zero and one with zero being a perfect fit. None of the models is acceptable. Acceptable values for NSE are between one and zero with one being a perfect fit; again none of the models are within acceptable limits.

The peak flow and mean flow of SWMM-EXTRAN, SWMM-TRANSPORT and SEWSAN are within 10% of the measured data. The peak time is offset between one and two hours, which is much greater than the suggested 10 minutes. The factors combined suggest, as is confirmed by Figure 4:9, that the hydrographs are misaligned. The misalignment can be attributed to the boundary conditions of the models being incorrect.

Table 4.5: Statistical results of Drainage System A

	Drainage System A		
Verification	SEWSAN	EXTRAN	TRANSPORT
RSR	1.125	1.049	1.137
NSE	-0.290	-0.122	-0.318
PBIAS	6.585	8.406	8.335
Mean	-6.585%	-8.406%	-8.335%
Peak	2.03%	1.30%	1.10%
Time	1h	1h	2h

4.5.5. Shifted boundary conditions

Figure 4:9 shows that the flow hydrographs produced by the three models are similar to the measured hydrograph. The flow is, however, offset by between one and two hours. To obtain flow hydrographs that align better with the measured flow the boundary conditions were modified so that their flows occurred two hours earlier. Shifting the inflow hydrographs timewise in this manner will have no impact on the predicted peak flow, mean flow or PBIAS. Instead the shift will affect only the RSR, NSE and peak time.

Figure 4:10 shows the effect of the time shift on the results. The modelled hydrographs are visually a great deal closer to the measured flow hydrograph than the original modelled flow hydrographs.

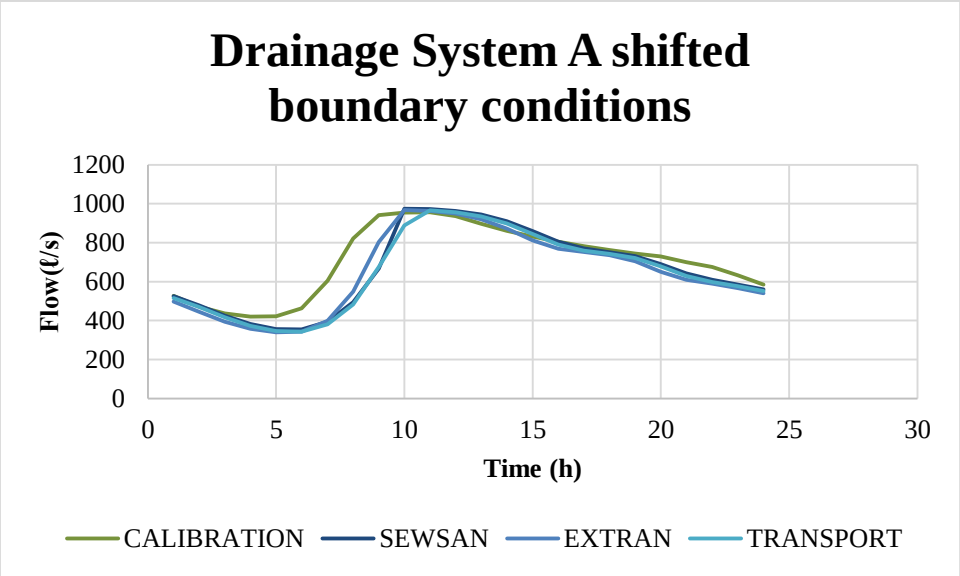

Figure 4:10: Drainage System A with shifted boundary conditions

Table 4.6 confirms that all three models now fall within acceptable RSR and NSE levels. The PBIAS and mean remains unchanged. The modelled peak flow times are now an hour earlier than the measured peak flow times in SEWSAN and SWMM-EXTRAN, but SWMM-TRANSPORT has the same peak flow time as measured. Even though the peak flow time remains outside acceptable bounds the other terms suggest a much better fit.

Table 4.6: Statistical results of Drainage System A with shifted boundary conditions

	Drainage System A		
Verification	SEWSAN	EXTRAN	TRANSPORT
RSR	0.591	0.512	0.613
NSE	0.643	0.733	0.616
PBIAS	6.585	8.406	8.335
Mean	-6.585%	-8.406%	-8.335%
Peak	2.03%	1.30%	1.10%
Time	1h	1h	0h

4.5.6. Comparison of models

The critical section investigated shows some major differences among the three models. SEWSAN and SWMM-TRANSPORT calculated that the conduit under investigation had no spare capacity while the hydraulically more detailed SWMM-EXTRAN calculated that there was still 25% spare capacity. The difference was due to rapidly varying changes upstream and downstream of the conduit causing flows to accelerate, resulting in a draw-down effect. Acceleration is a factor that is ignored by SWMM-TRANSPORT and SEWSAN.

The results were not within acceptable limits when comparing the flow hydrographs produced at the flow measurement point. The flow hydrographs were one hour late in the SEWSAN and SWMM-EXTRAN models and two hours late in SWMM-TRANSPORT. By modifying the boundary conditions by two hours, a much better correlation was achieved.

The PBIAS and mean flows from SEWSAN, SWMM-EXTRAN and SWMM-TRANSPORT indicate less flow than measured, but the values are still within acceptable limits. The peak flows are, however, greater than the measured peak flow.

The RSR and NSE values indicate that the initial, unadjusted flow hydrographs were not within acceptable limits. After modifying the boundary conditions, the fit becomes substantially better. SWMM-EXTRAN results in an RSR of 0.512 and an NSE of 0.733, which indicates a reasonable fit. SEWSAN results in an RSR 0.591 and an NSE of 0.643. The values indicate a reasonable fit, but not as good a fit as SWMM-EXTRAN. SWMM-TRANSPORT gives an RSR value of 0.613 and an NSE value of 0.616; the values still indicate a reasonable fit with results very similar to SEWSAN.

The fit of a model to actual measured data is largely dependent on the boundary conditions set by a modeller. By modifying the boundary conditions, the models provided a much better fit to measured flow hydrographs. The peak flow times do not correlate well with the measured flow hydrograph peak time.

4.6. Drainage System B

4.6.1. Drainage system description

The drainage system consists of approximately 1 000 kilometres of conventional gravity sewer conduits. The number and type of stands serviced by the drainage system are summarised in Table 4.7 as obtained from Treasury data.

Table 4.7: Drainage System B stands

Land use	No stands
Very-high-income residential	7 647
High-income residential	5 898
Medium-income residential	5 618
Low-income residential	17
Cluster	490
Flats	70
Business and commercial	596
Education	57
Government and institutes	19
Industry	0
Other	270
Farm	27
None	244
Unknown	400
Large	188

For the purposes of this study a single longitudinal section of connected conduits from the drainage system was analysed. The combined length of the conduits is approximately 13.4 kilometres in length and consists of 216 conduits, all of which are brick rectangular portal culverts.

4.6.2. Boundary conditions and system setup

Boundary conditions were created in a similar manner to Drainage System A.

4.6.3. Critical sections to consider

SEWSAN

The SEWSAN analysis shows that the capacities of conduits 078 to 087 and conduits 173 to 176 are less than zero. A spare capacity of less than zero from the SEWSAN analysis indicates that the flow through the conduit exceeds its full flow capacity.

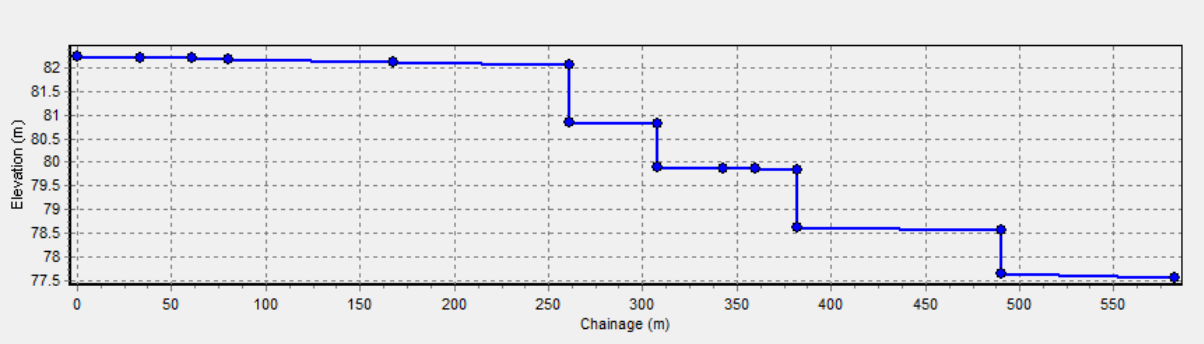

Figure 4:11: Invert levels (Conduits 078 to 088)

The invert levels in Figure 4:11 indicate that drop structures are present in the latter part of the longitudinal section. Drop structures should help to accelerate flow within the conduit and create extra capacity. SEWSAN does not take into account up- or downstream conditions, resulting in the drop structures being ignored in the hydraulic calculations.

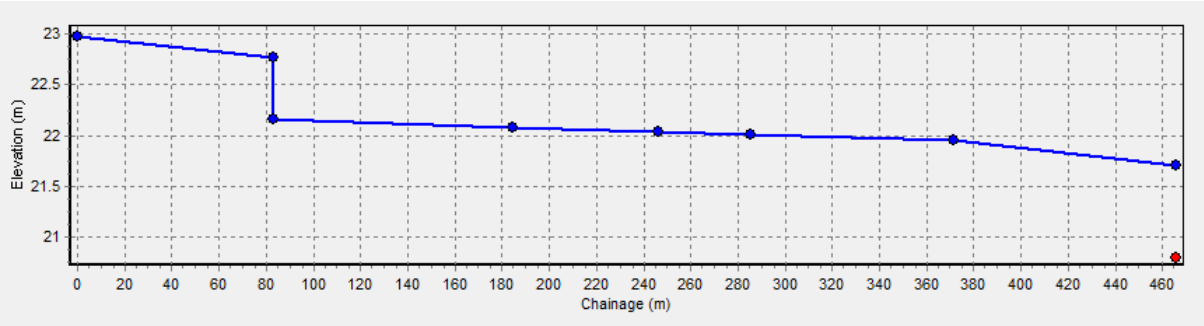

Figure 4:12: Invert levels (Conduits 172 to 177)

The invert levels in Figure 4:12, indicate that there is a drop structure just before the critical section. The drop should help to accelerate flows and improve downstream capacities. The slope of conduit 177 is also steeper than the conduits within the critical section and should improve upstream conditions as flow accelerates down the steeper incline.

SWMM-TRANSPORT

Figure 4:13 shows that the SWMM-TRANSPORT model does not take backwater effects into account, or not substantially. Unlike SEWSAN, SWMM-TRANSPORT results in a small amount of spare capacity. As most of the terms of the momentum equation have been dropped from SWMM-TRANSPORT's governing equation the effect of drop structures are not taken into account and do not contribute to improved conduit capacities.

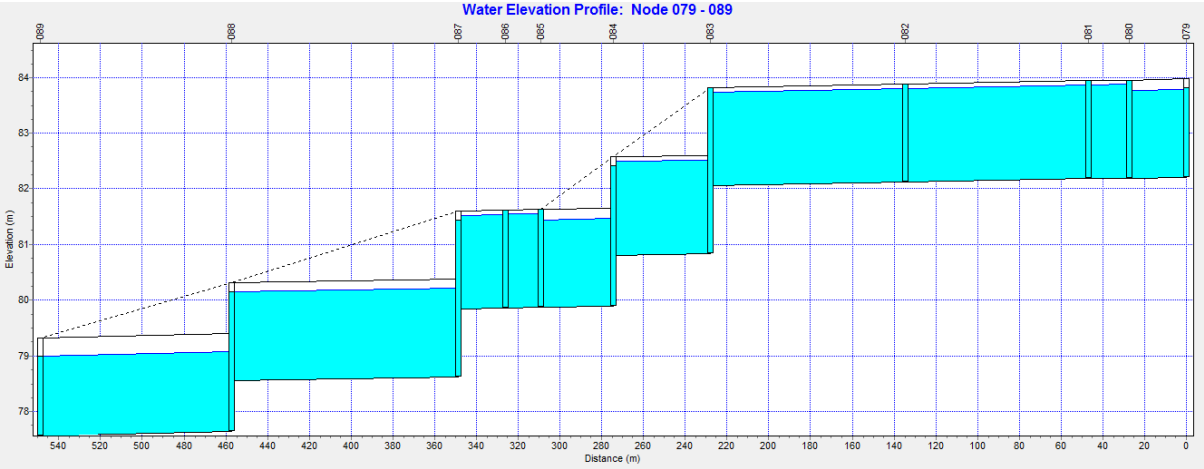

Figure 4:13: SWMM-TRANSPORT peak flow (079 to 089)

Figure 4:14 also shows that the SWMM-TRANSPORT model does not take backwater effects into account. Despite the drop structure at junction 173, the flows have not been accelerated and as a result, conduit 173 becomes surcharged. Such conditions are not ideal for SWMM-TRANSPORT as the model does not handle surcharging.

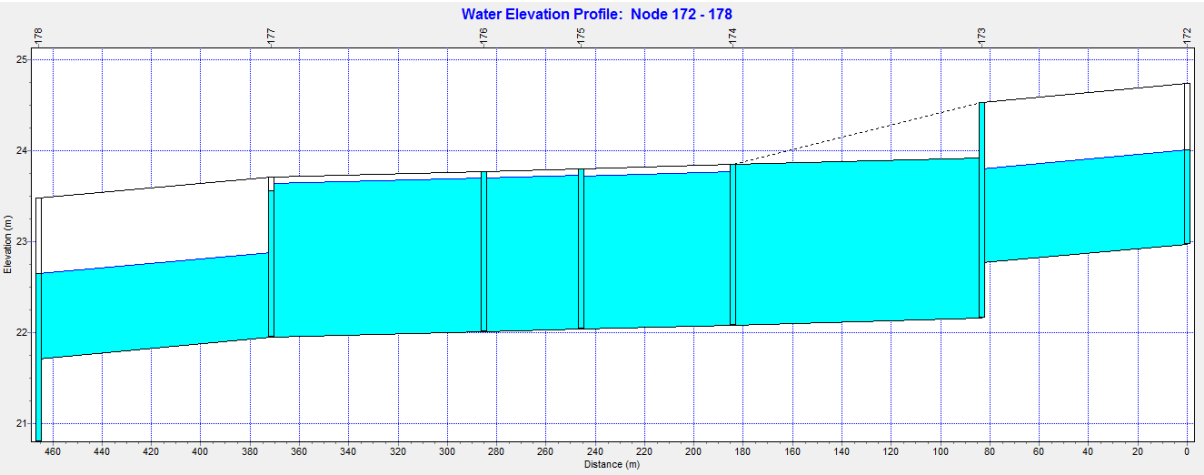

Figure 4:14: SWMM-TRANSPORT peak flow (172 to 178)

The flow hydrograph upstream of conduit 173 is shown in Figure 4:15 below. The effect of surcharge conditions in the conduit is displayed in Figure 4:16. The peak flow has been capped, and downstream flow is limited by the capacity of conduit 173.

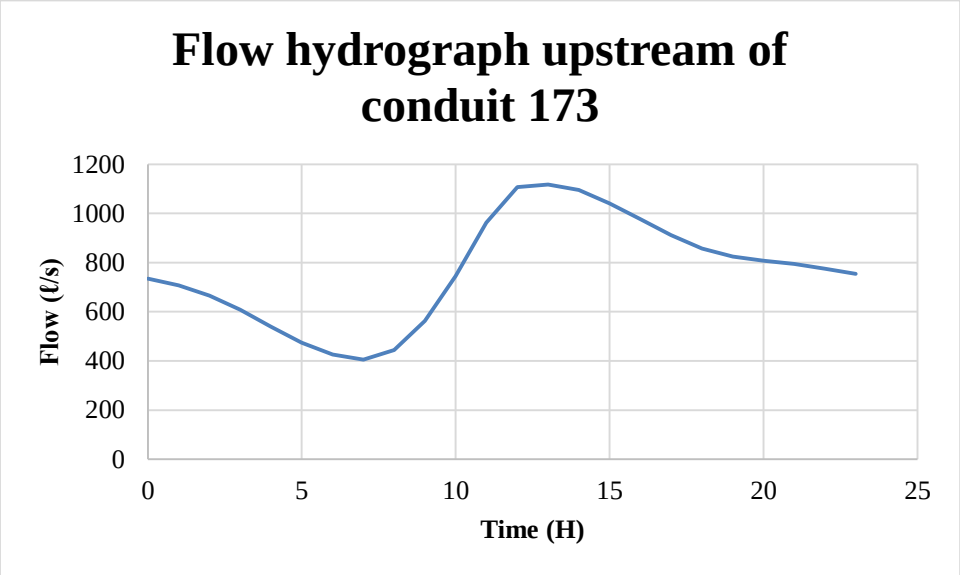

Figure 4:15: Flow hydrograph upstream of conduit 173 (SWMM-TRANSPORT)

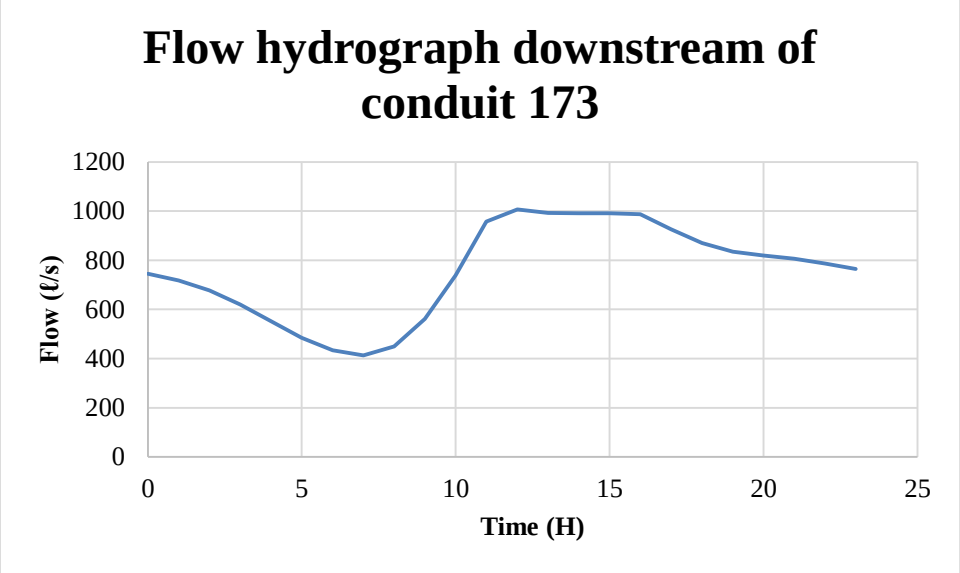

Figure 4:16: Flow hydrograph downstream of conduit 173 (SWMM-TRANSPORT)

The steeper slope of conduit 177 greatly improves the capacity of the conduit, but a lack of backwater and other missing factors from the momentum equation mean that upstream conduits remain unaffected.

SWMM-EXTRAN

The effect of the fully dynamic wave momentum equation is illustrated in Figure 4:17. The drop structures accelerate flow, thereby decreasing flow depths upstream. The draw-down effect spans multiple conduits as flow velocities are gradually increased. The difference between SWMM-EXTRAN compared to SEWSAN and SWMM-TRANSPORT is pronounced.

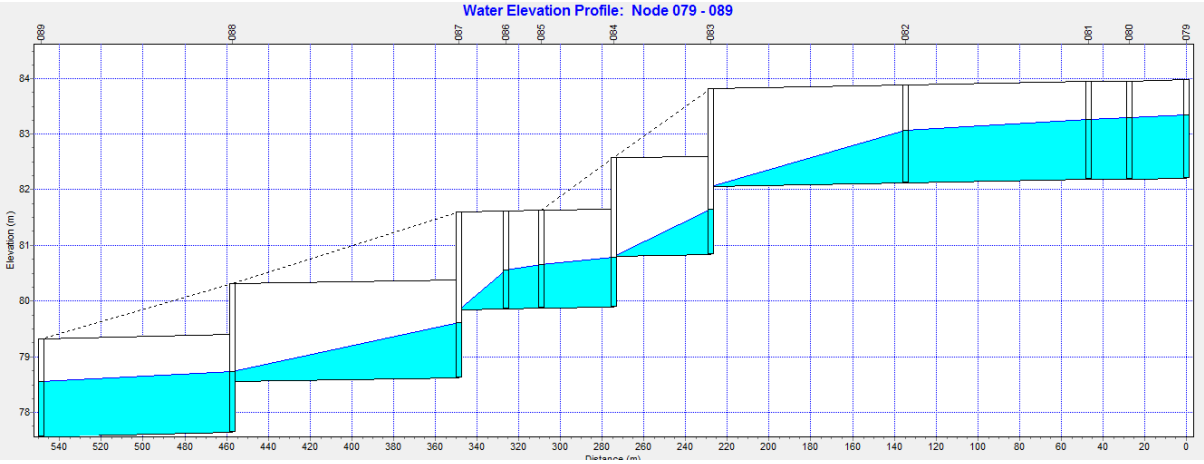

Figure 4:17: SWMM-EXTRAN peak flow (079 to 089)

The effect of the fully dynamic wave momentum equation is also shown in Figure 4:18. The drop structure accelerates flow, thereby decreasing flow depths upstream. More importantly, the steeper slope of conduit 177 draws down the flows from the four upstream conduits, which greatly improves the capacity of the system.

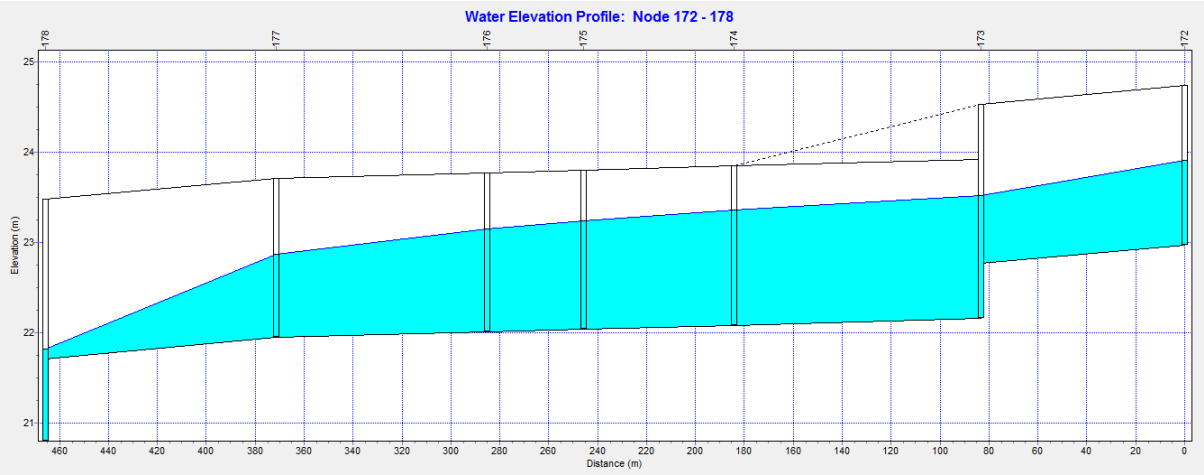

Figure 4:18: SWMM-EXTRAN peak flow (172 to 178)

4.6.4. Results at measurement point

After each of the models had been run, flow values were calculated for each time step at measurement point B. Table 4.8 contains the flows calculated at measurement point B as well as the average flow measured at measurement point B. Figure 4:19 compares the hydrographs.

Table 4.8: Drainage System B modelled and measured flows

Sewage flow rates measurement point B (ℓ/s)				
Time (h)	CALIBRATION	SEWSAN	EXTRAN	TRANSPORT
0	582	764	747	761
1	523	738	715	735
2	477	701	666	697
3	452	650	597	644
4	446	585	525	577
5	471	517	464	507
6	578	460	424	451
7	800	432	412	424
8	1081	460	457	447
9	1173	567	623	541
10	1178	711	912	702
11	1141	889	1128	926
12	1077	1182	1183	1022
13	995	1176	1153	1025
14	924	1144	1104	1007
15	871	1095	1036	1006
16	839	1035	961	1006
17	819	971	897	955
18	811	909	858	893
19	793	863	840	852
20	772	839	826	834
21	731	825	807	822
22	668	808	785	804
23	606	786	767	781

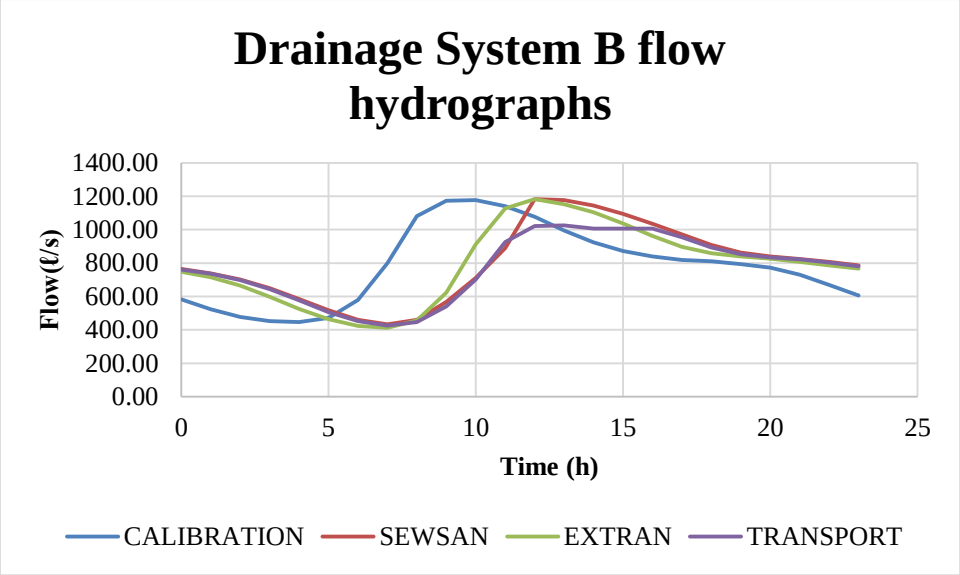

Figure 4:19: Drainage System B hydrographs

Table 4.9 shows the calculated verification values for Drainage System B, the calculations of which can be found in Appendix A. Acceptable values for RSR are between zero and one with zero being a perfect fit; only SWMM-EXTRAN is below one. Acceptable values for NSE are between one and zero with one being a perfect fit; again only SWMM-EXTRAN falls within the required limits.

The peak flow and mean flow of SWMM-EXTRAN and SEWSAN are similar to the measured flows, but the peak time is offset by two hours. The offset is much greater than the suggested 10 minutes. The combined factors suggest, and is confirmed by Figure 4:19, that the hydrographs are misaligned. The misalignment can be attributed to the boundary conditions of the models being incorrect. SWMM-TRANSPORT shows only a slightly lower mean flow since flows stored in manhole 173 from the surcharged conduit (173) are released back into the system once there is capacity in conduit 173. The flattened flow hydrograph results in a peak flow that is inaccurate.

Table 4.9: Drainage System B statistical results

	Drainage System B		
Verification	SEWSAN	EXTRAN	TRANSPORT
RSR	1.129	0.974	1.094
NSE	-0.305	0.028	-0.227
PBIAS	-1.592	-0.418	2.061
Mean	1.592%	0.418%	-2.061%
Peak	0.40%	0.42%	-12.99%
Time	2h	2h	3h

4.6.5. Shifted boundary conditions

The boundary condition were modified in a similar manner as in Drainage System A. Figure 4:20 shows that the shape of the flow hydrographs produced by the three models are similar to the measured flow hydrograph.

Shifting the boundary conditions timewise will have no impact on the predicted peak flow, mean flow or PBIAS. Instead, the shift will affect the RSR, NSE and peak time. The effect of the time shift is shown in Figure 4:20. The modelled hydrographs are visually a great deal closer to the actual measured flow hydrograph than the original hydrographs.

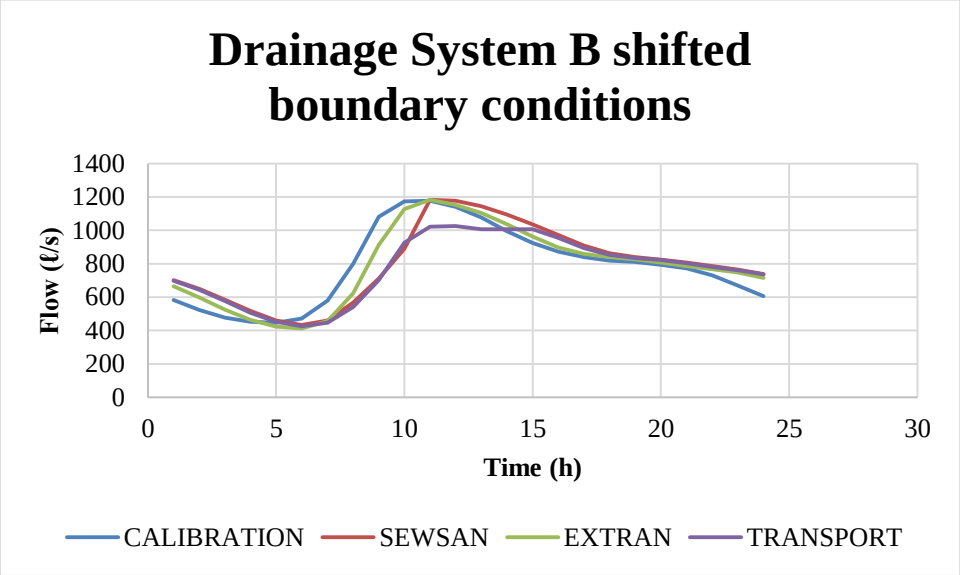

Figure 4:20: Drainage System B shifted boundary conditions

Table 4.10 confirms that all three models now fall within acceptable RSR and NSE levels. The PBIAS and mean remains unchanged. The peak flow times are now the same as the measured peak flow times in SEWSAN and SWMM-EXTRAN, but

SWMM-TRANSPORT's peak flow time remains one hour behind. Even though the peak flow hour remains outside acceptable bounds for SWMM-TRANSPORT the other terms suggest a much better fit.

Table 4.10: Drainage System B shifted boundary conditions statistical results

	Drainage System B		
Verification	SEWSAN	EXTRAN	TRANSPORT
RSR	0.563	0.305	0.570
NSE	0.676	0.905	0.667
PBIAS	-1.592	-0.418	2.061
Mean	1.592%	0.418%	-2.061%
Peak	0.40%	0.42%	-12.99%
Time	0h	0h	1h

4.6.6. Comparison of models

The results of SWMM-EXTRAN are barely acceptable when verifying the flow hydrographs produced at the flow measurement point. SWMM-TRANSPORT and SEWSAN, however, fall outside acceptable limits. Peak flows from SEWSAN and SWMM-EXTRAN are within a percent of the measured data. The difference between SWMM-TRANSPORT and measured flows is 13%, which is unacceptable.

The reason for SWMM-TRANSPORT being inaccurate in System B is due to the model being unable to handle surcharge conditions. The peak flow was capped by a single upstream conduit (173) that had insufficient capacity to route the entire flow downstream. SWMM-EXTRAN, which uses momentum equations, allows flows to accelerate, hence giving a conduit greater capacity. Full use of dynamic wave equations allows SWMM-EXTRAN to route the entire flow downstream without affecting the flow hydrograph. SEWSAN, though showing negative capacities between conduits 078 to 087 and conduits 173 to 176, still routed the entire flow hydrograph downstream.

The PBIAS and mean flow results indicate that both SEWSAN and SWMM-EXTRAN routed a larger amount of flow than recorded by the flow measurements, with SEWSAN being overly conservative. SWMM-EXTRAN produced results that were very similar to the measured data. SWMM-TRANPORT routed considerably less flow than recorded by the flow measurements. This can be attributed to upstream surcharge conditions that result into manholes storing excess flows temporarily.

The RSR and NSE values indicate that the initial, unadjusted flow hydrographs are not within acceptable limits. By shifting the boundary conditions by two hours, the fit becomes better. SWMM-EXTRAN gives an RSR of 0.305 and an NSE of 0.905, which indicates a good fit. SEWSAN gives an RSR 0.563 and an NSE of 0.676, which indicates a reasonable fit, even if performance is poorer than SWMM-EXTRAN. Despite the chopped peak of SWMM-TRANSPORT, the model still gives an RSR of 0.570 and an NSE of 0.667; the values still indicate a reasonable fit to the measured data.

The fact that the RSR and NSE values of SWMM-TRANSPORT indicate a reasonable fit while the peak flows differ by 13% shows that all factors should be viewed together in order to judge whether a model has produced satisfactory results. The peak flow times do not correlate well with the measured peak flow time. The verification criteria stated that models should be within 10 minutes. Such a target is very difficult to achieve since the time steps are one hour in length.

4.7. Summary of model evaluation

The results from both Drainage System A and B indicate that the models did not perform within reasonable limits. Adjusting the boundary conditions by two hours improved the correlation between the measured flow hydrographs and the modelled flow hydrographs. The only model that did not perform within reasonable limits was the SWMM-TRANSPORT in the System B where the peak flow was substantially reduced due to upstream limits caused by surcharge. SEWSAN and SWMM-EXTRAN managed to route the flow hydrographs intact downstream. SEWSAN creates an undisturbed flow hydrograph by ignoring the lack of capacity in conduits and reporting negative absolute flow capacities. SWMM-EXTRAN, making use of fully dynamic flow equations, is able to take into account hydraulic structures such as drop structures and also backwater effects.

The major issue found was that the flow hydrographs from the simulations were between one and three hours behind. Due to the difference, the models gave unacceptable results in terms of RSR and NSE. The time difference did not affect the peak flow, mean flow or the PBIAS values. By shifting the boundary conditions, a much better fit was made in both Systems A and B.

In System A, SEWSAN gave the highest peak flow as was expected since no dampening of flows takes place within the model as the peaks are merely shifted downstream and are never

lost. However, in System B, SEWSAN and SWMM-EXTRAN resulted in almost identical peak flows: 1 182.4 ℓ/s and 1 182.6 ℓ/s respectively.

The SEWSAN and SWMM-TRANSPORT models indicated sections with zero capacity. The indicated sections contain drop structures and conduits with steeper gradients. Since neither SEWSAN nor SWMM-TRANSPORT take momentum nor other hydraulic factors into account, the hydraulic structures cannot contribute positively to the hydraulic capacity of the conduit. SWMM-EXTRAN, by making use of local acceleration and convective acceleration and by taking into account the water surface gradient, can make use of hydraulic structures to increase the flow capacity of a conduit. The effects can often span multiple conduits, as shown in Figure 4:18 where the backwater effects span for more than four conduits.

If there are sections along the system that become surcharged, use of SWMM-TRANSPORT is not recommended as peak flows can be reduced. When investigating problem areas in a system where hydraulic structures exist or where there are varying conduit slopes SWMM-EXTRAN would be the best model to use.

The RSR and NSE values were easily improved by shifting the boundary conditions by two hours. Though the shift in boundary conditions did not impact the peak or mean flows, the shift still resulted in hydrographs with a much better fit to the measured flow hydrographs. The change in RSR and NSE values emphasises the importance of boundary conditions. Without proper boundary conditions, even the most sophisticated model will be unable to produce acceptable results.

5. Sensitivity analysis

The longitudinal section from Drainage System A was used for the sensitivity analysis because there were no upstream flow constraints as is the case with Drainage System B. The sensitivity analysis compared how modelled flow hydrographs at measurement point A differ with variations in parameters. The Manning equation of flow is a function of flow area (hydraulic radius), slope and surface roughness. The sensitivity analysis focused on these three parameters. The resultant flow hydrographs produced for each scenario can be found in Appendix B.

5.1. Variation in conduit slope

For each simulation, the conduit slopes were increased in increments of 5% from a minimum of -10% to a maximum of +10% of the value used in the initial model setup. The results from each model were then compared with the original flow hydrographs of the same model. The resultant hydrographs would show how sensitive the specific model was to a variation in slope.

5.1.1. RSR values

Table 5.1 and Figure 5:1 below show the variation in RSR values when the variation in slopes from the original model analysis is compared. The results vary in a linear fashion, radiating away from the original analysis. SWMM-TRANSPORT is the most sensitive to changes in slope while SWMM-EXTRAN is the least sensitive.

Table 5.1: Variation in slope (RSR)

	-10%	-5%	0%	5%	10%
SEWSAN	0.0180	0.0090	0.0000	0.0087	0.0166
TRANSPORT	0.0235	0.0119	0.0000	0.0115	0.0223
EXTRAN	0.0013	0.0007	0.0000	0.0007	0.0015

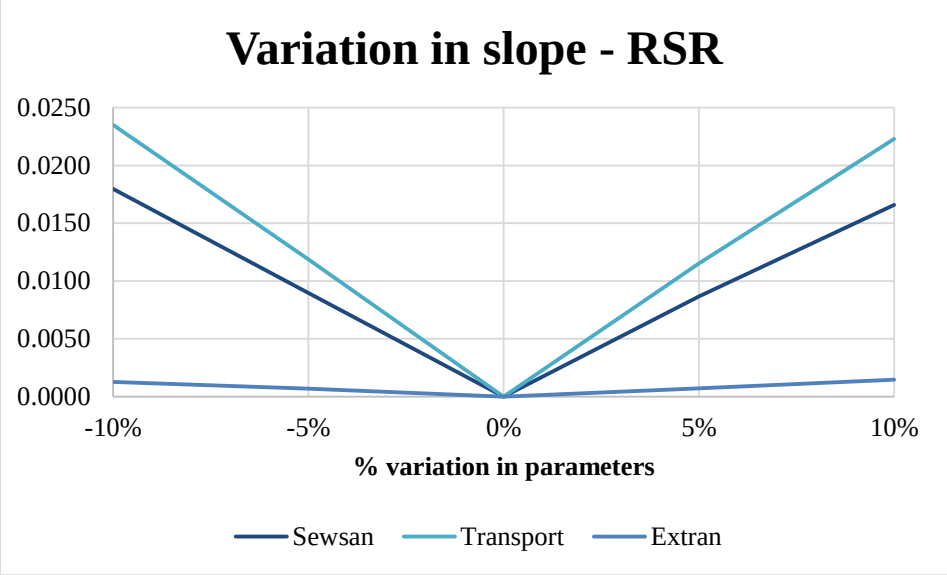

Figure 5:1: Variation in slope - RSR

5.1.2. NSE values

Table 5.2 and Figure 5:2 below show the variation in NSE values when differing slopes from the original model analysis are compared. The results vary in a nonlinear manner. SWMM-TRANSPORT is the most sensitive to changes in slope while SWMM-EXTRAN is the least sensitive, with almost no variation from the original flow hydrograph.

Table 5.2: Variation in slope (NSE)

	-10%	-5%	0%	5%	10%
SEWSAN	0.9997	0.9999	1.0000	0.9999	0.9997
TRANSPORT	0.9994	0.9999	1.0000	0.9999	0.9995
EXTRAN	1.0000	1.0000	1.0000	1.0000	1.0000

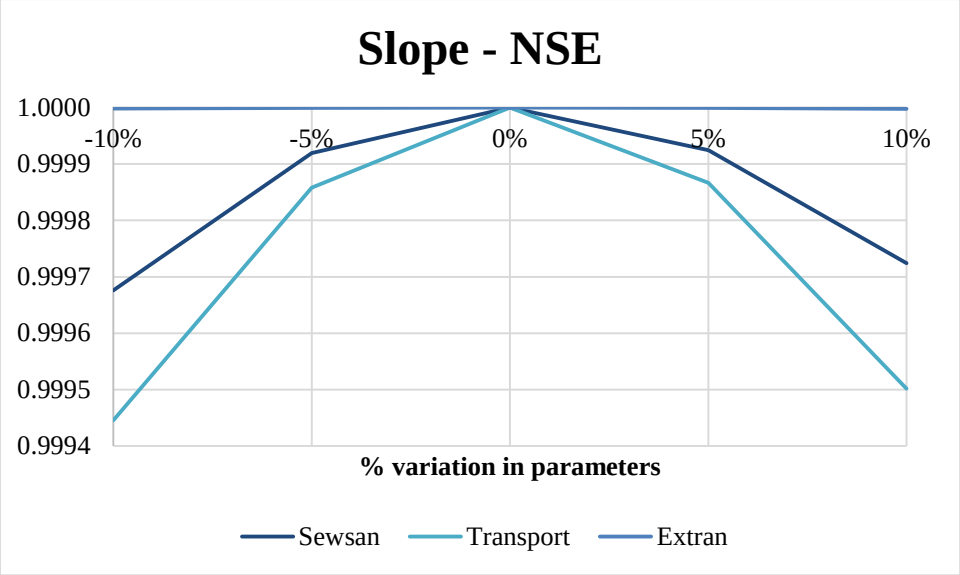

Figure 5:2: Variation in slope - NSE

5.1.3. PBIAS values

Table 5.3 and Figure 5:3 below show the variation in PBIAS values when differing slopes from the original model analysis are compared. The results vary in a fairly linear fashion. SEWSAN is the most sensitive to changes in slope while SWMM-EXTRAN is the least sensitive.

Table 5.3: Variation in slope (PBIAS)

	-10%	-5%	0%	5%	10%
SEWSAN	-0.1371	-0.0723	0.0000	0.0723	0.1400
TRANSPORT	0.0137	0.0068	0.0000	-0.0065	-0.0124
EXTRAN	-0.0036	-0.0019	0.0000	0.0019	0.0038

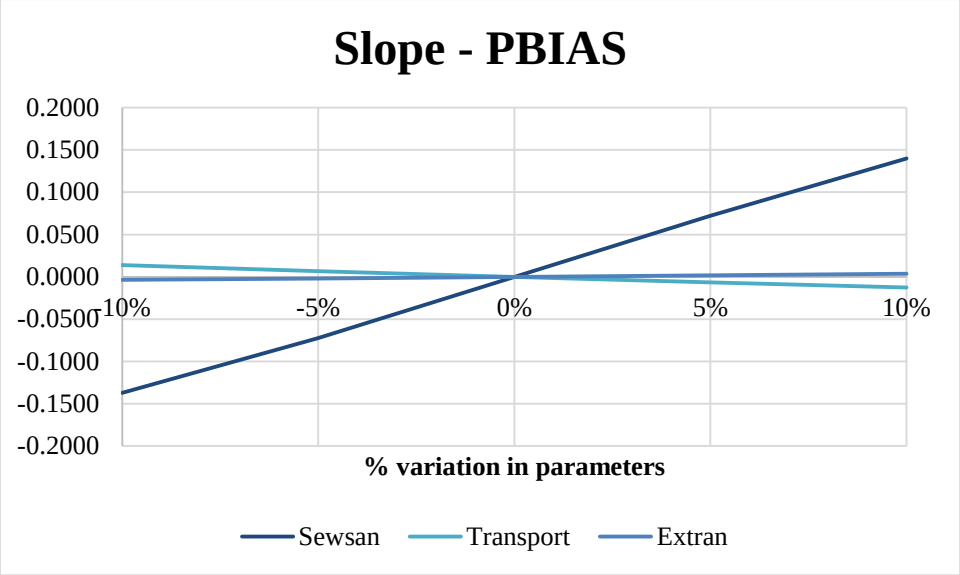

Figure 5:3: Variation in slope - PBIAS

5.1.4. Peak flow values

Table 5.4 and Figure 5:4 below show the variation in peak flow values when differing slopes from the original model analysis are compared. The SWMM-EXTRAN and SWMM-TRANSPORT results vary in a linear fashion. SEWSAN, however, has a large deviation at 10% due to peak flow shifting. SWMM-TRANSPORT is the most sensitive to changes in slope if the peak shift in SEWSAN is ignored while SWMM-EXTRAN is the least sensitive.

Table 5.4: Variation in slope (peak %)

	-10%	-5%	0%	5%	10%
SEWSAN	0.008%	0.004%	0.000%	0.003%	0.020%
TRANSPORT	0.015%	0.007%	0.000%	-0.007%	-0.014%
EXTRAN	-0.002%	-0.001%	0.000%	0.001%	0.002%

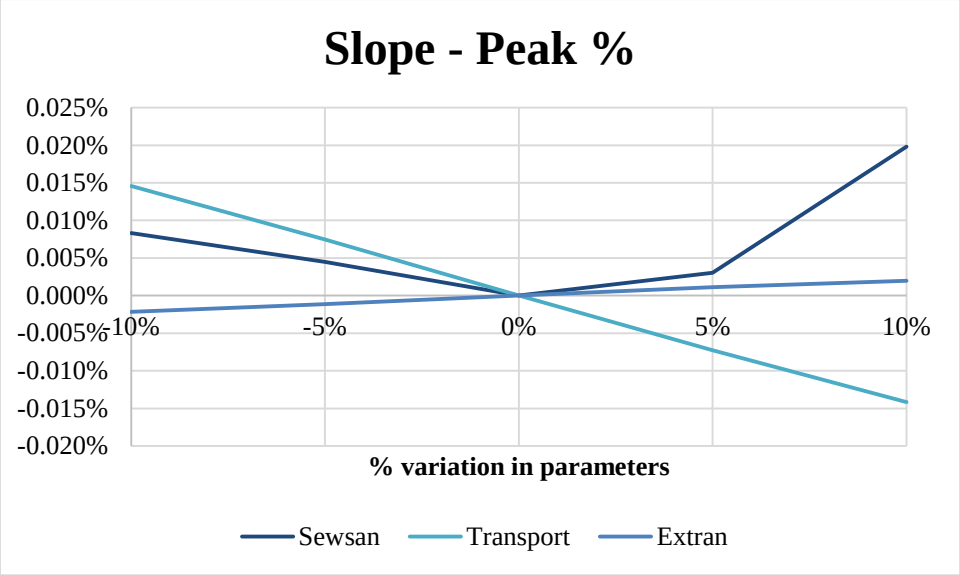

Figure 5:4: Variation in slope m- Peak %

5.1.5. Summary

The results indicate that SEWSAN is the most sensitive to changes when comparing PBIAS values. SWMM-TRANSPORT is affected the most when comparing RSR and NSE values. The peak flow of SWMM-TRANSPORT varies the most, but SEWSAN deviates a lot when the slope is increased by 10%. The sudden change can be attributed to peak flow shifting. The flow shift ensures that SEWSAN is the most sensitive. SWMM-EXTRAN is the most resilient to changes in slope when comparing the resultant hydrograph.

5.2. Variation in flow area

The flow area of each conduit was modified so that for each simulation the conduit area would be decreased by 10% and 5% as well as increased by 5% and 10%. The results from each model were then compared with the original flow hydrographs of the same model. The resultant flow hydrographs would show how sensitive the specific model was to a variation in flow area.

5.2.1. RSR values

Table 5.5 and Figure 5:5 below show the variation in RSR values when differing flow areas from the original model analysis are compared. That the results vary linearly radiating away from the original analysis. SEWSAN is the most sensitive to changes in flow area while SWMM-EXTRAN is the least sensitive.

Table 5.5: Variation in flow area (RSR)

	-10%	-5%	0%	5%	10%
SEWSAN	0.0129	0.0063	0.0000	0.0058	0.0110
TRANSPORT	0.0114	0.0054	0.0000	0.0050	0.0095
EXTRAN	0.0009	0.0005	0.0000	0.0005	0.0010

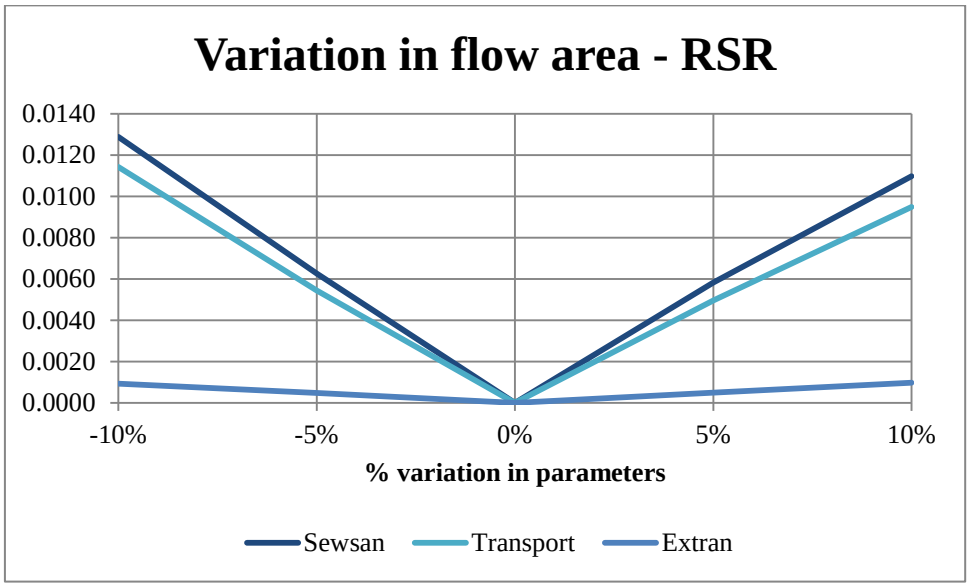

Figure 5:5: Variation in flow area - RSR

5.2.2. NSE values

Table 5.6 and Figure 5:6 below show the variation in NSE values when differing flow areas from the original model analysis are compared. The results vary in a nonlinear manner. SEWSAN is the most sensitive to changes in flow area while SWMM-EXTRAN is the least sensitive, with almost no variation from the original flow hydrograph.

Table 5.6: Variation in flow area (NSE)

	-10%	-5%	0%	5%	10%
SEWSAN	0.9998	1.0000	1.0000	1.0000	0.9999
TRANSPORT	0.9999	1.0000	1.0000	1.0000	0.9999
EXTRAN	1.0000	1.0000	1.0000	1.0000	1.0000

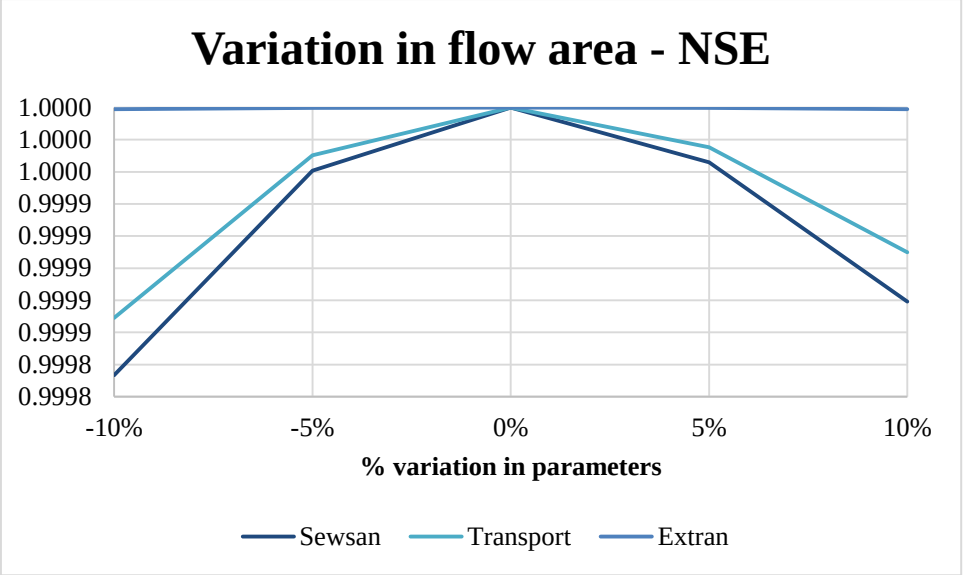

Figure 5:6: Variation in flow area - NSE

5.2.3. PBIAS values

Table 5.7 and Figure 5:7 below show the variation in PBIAS values when differing flow areas from the original model analysis are compared. The results vary in a fairly linear fashion. SEWSAN is the most sensitive to changes in flow area while SWMM-EXTRAN is the least sensitive.

Table 5.7: Variation in flow area (PBIAS)

	-10%	-5%	0%	5%	10%
SEWSAN	-0.0473	-0.0256	0.0000	0.0231	0.0437
TRANSPORT	0.0064	0.0032	0.0000	-0.0031	-0.0061
EXTRAN	0.0005	0.0003	0.0000	-0.0004	-0.0011

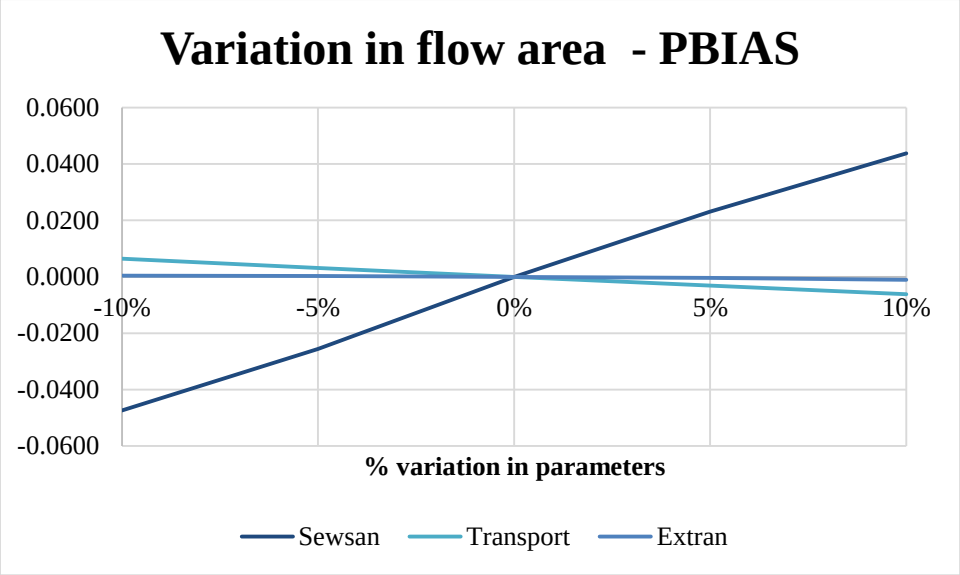

Figure 5:7: Variation in flow area - PBIAS

5.2.4. Peak flow values

Table 5.8 and Figure 5:8 below show the variation in peak flow values when differing flow areas from the original model analysis are compared. The SWMM-EXTRAN and SWMM-TRANSPORT results vary in a linear fashion. SEWSAN shows a bit more variation, but the changes are not pronounced. SEWSAN is the most sensitive to changes in flow area while SWMM-EXTRAN is the least sensitive.

Table 5.8: Variation in flow area (peak %)

	-10%	-5%	0%	5%	10%
SEWSAN	-0.030%	-0.015%	0.000%	0.022%	0.036%
TRANSPORT	0.008%	0.004%	0.000%	-0.004%	-0.007%
EXTRAN	-0.002%	-0.001%	0.000%	0.001%	0.002%

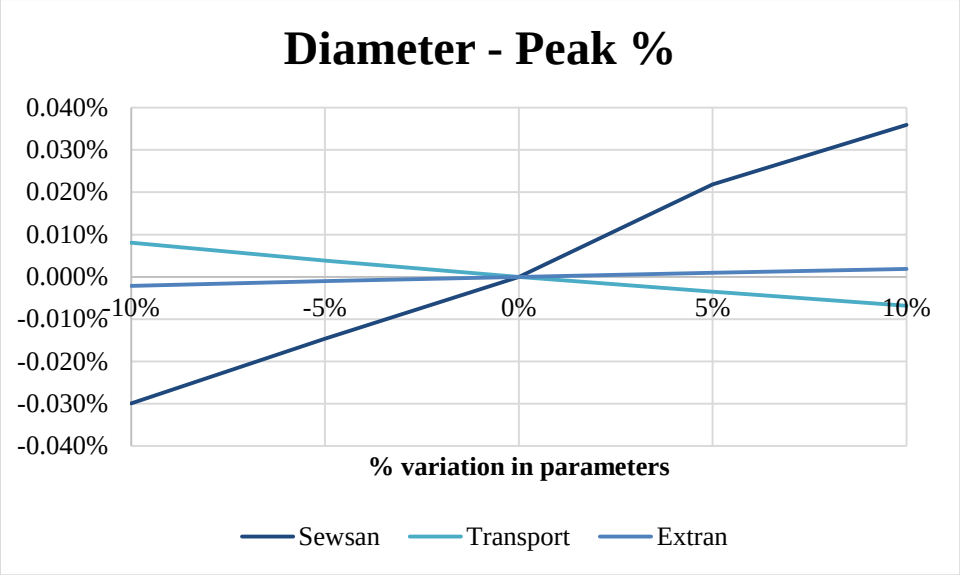

Figure 5:8: Variation in flow area - Peak %

5.2.5. Summary

The results indicate that SEWSAN is the most sensitive to changes in flow area. The peak flow is affected by a change in flow area and begins to show some signs of peak flow shifting. SWMM-TRANSPORT is affected less by a change in flow area. SWMM-EXTRAN is the most resilient to changes in flow area when comparing changes to the resultant hydrograph.

5.3. Variation in conduit roughness

5.3.1. RSR values

Table 5.9 and Figure 5:9 below show the variation in RSR values when differing conduit roughnesses from the original model analysis are compared. The results vary in a linear fashion, radiating away from the original analysis. SWMM-TRANSPORT is marginally more sensitive than SEWSAN. While SEWSAN is not the most sensitive to changes in roughness, a pronounced deviation occurs when the roughness is 10% less than normal. SWMM-EXTRAN is the least sensitive.

Table 5.9: Variation in roughness (RSR)

	-10%	-5%	0%	5%	10%
SEWSAN	0.3091	0.0178	0.0000	0.0185	0.0378
TRANSPORT	0.0478	0.0274	0.0000	0.0241	0.0443
EXTRAN	0.0150	0.0074	0.0000	0.0052	0.0141

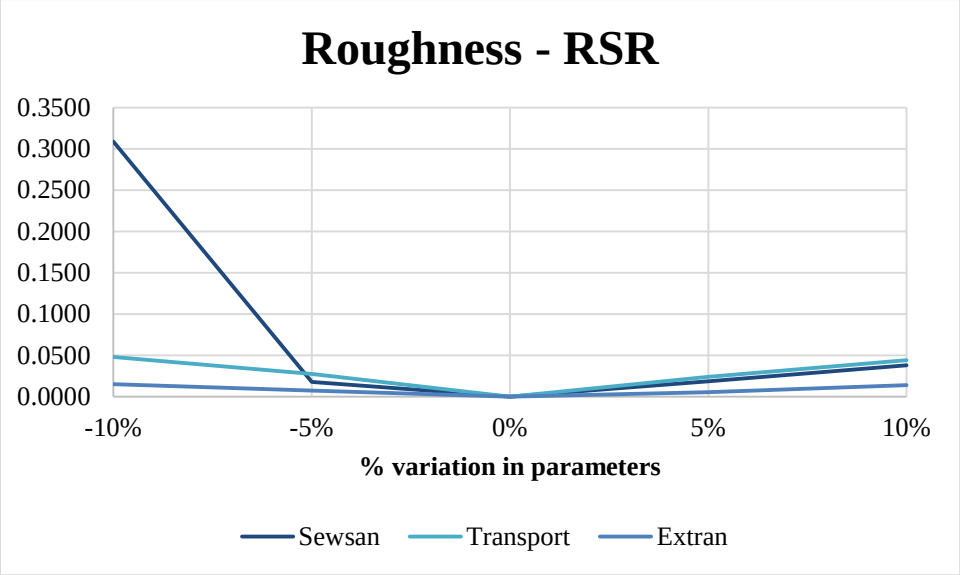

Figure 5:9: Variation in roughness - RSR

5.3.2. NSE values

Table 5.10 and Figure 5:10 below show the variation in NSE values when differing conduit roughnesses from the original model analysis are compared. The results vary in a nonlinear manner. SWMM-TRANSPORT is the most sensitive to changes. SEWSAN, however, shows a pronounced deviation when the roughness is 10% less than normal. SWMM-EXTRAN is the least sensitive to the conduit roughness with almost no variation from the original flow hydrograph.

Table 5.10: Variation in roughness (NSE)

	-10%	-5%	0%	5%	10%
SEWSAN	0.9042	0.9997	1.0000	0.9997	0.9986
TRANSPORT	0.9977	0.9992	1.0000	0.9994	0.9980
EXTRAN	0.9998	0.9999	1.0000	1.0000	0.9998

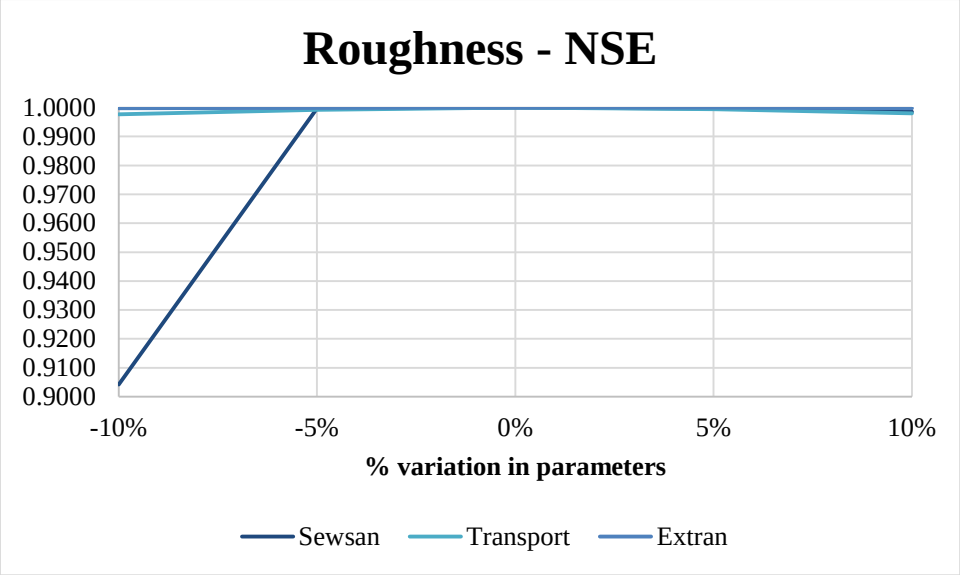

Figure 5:10: Variation in roughness - NSE

5.3.3. PBIAS values

Table 5.11 and Figure 5:11 below show the variation in PBIAS values when differing conduit roughnesses from the original model analysis are compared. The results vary in a linear fashion. SEWSAN is the most sensitive to changes in roughness and also has a pronounced variation when the roughness is 10% less than normal. SWMM-EXTRAN is the least sensitive.

Table 5.11: Variation in roughness (PBIAS)

	-10%	-5%	0%	5%	10%
SEWSAN	-1.5082	0.1503	0.0000	-0.1411	-0.2749
TRANSPORT	-0.0264	-0.0148	0.0000	0.0141	0.0269
EXTRAN	-0.0003	-0.0002	0.0000	0.0001	0.0003

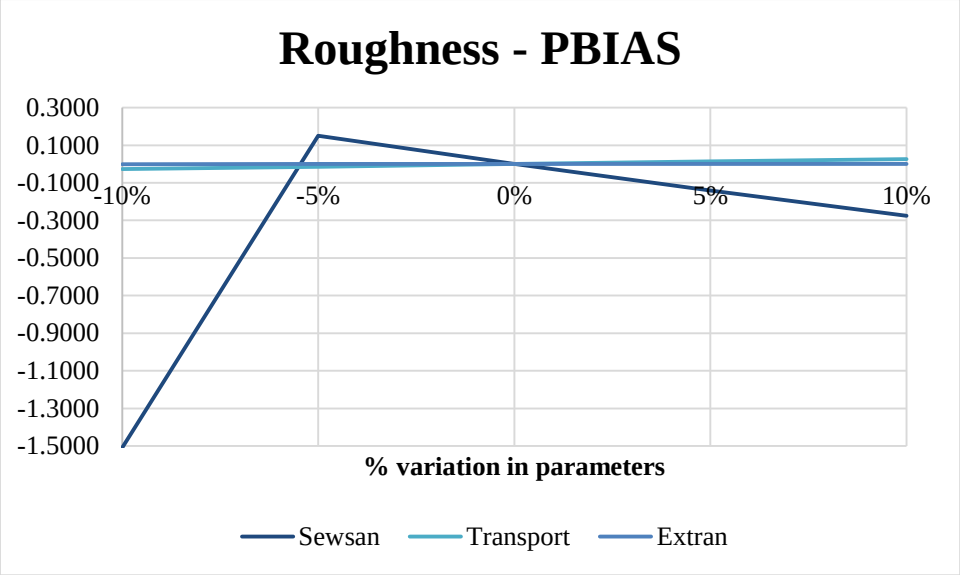

Figure 5:11: Variation in roughness - PBIAS

5.3.4. Peak flow values

Table 5.12 and Figure 5:12 below show the variation in peak flow values when differing conduit roughnesses from the original model analysis are compared. SWMM-TRANSPORT results vary in a fairly linear fashion. SEWSAN shows a great deal of variation, with pronounced differences. SWMM-EXTRAN varies quadratically with the deviation increasing more rapidly the greater the deviation in roughness is.

Table 5.12: Variation in roughness (peak %)

	-10%	-5%	0%	5%	10%
SEWSAN	0.074%	0.019%	0.000%	0.008%	0.016%
TRANSPORT	-0.031%	-0.019%	0.000%	0.015%	0.026%
EXTRAN	0.005%	0.004%	0.000%	-0.010%	-0.033%

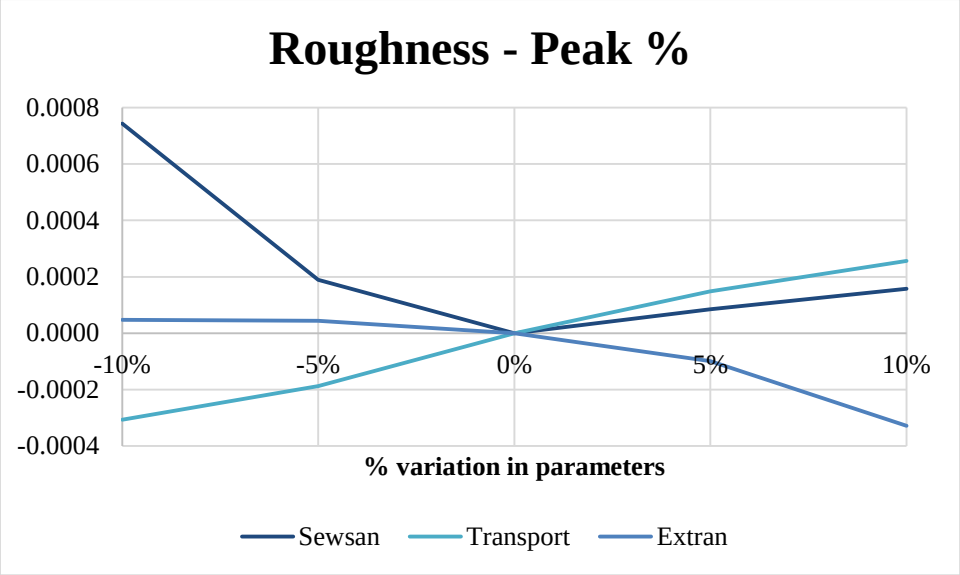

Figure 5:12: Variation in roughness - Peak %

5.3.5. Summary

The results indicate that SWMM-TRANSPORT is the most sensitive to changes in roughness, though SEWSAN does have a large jump when roughnesses were reduced by 10%. The sudden change is due to peak flow shifting that causes a shift in peak flows by one hour (see Figure 5:13). The flow area of the hydrograph is affected the most in SEWSAN. SWMM-EXTRAN is the most resilient to changes in roughness comparing with the resultant hydrographs.

Figure 5:13 displays the peak shift that occurs in the SEWSAN model when the roughness is varied. The hydrographs of the other models are not shown since they do not deviate much from the original modelled flow hydrograph.

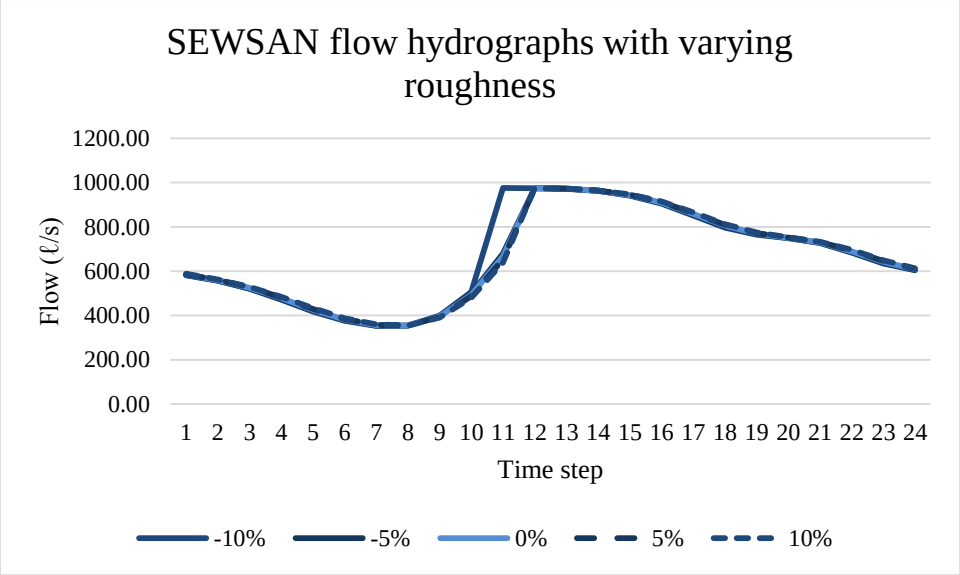

Figure 5:13: SEWSAN flow hydrographs with varying roughness

5.4. Summary of sensitivity analysis

Figure 5:14 shows the varying RSR values for the SEWSAN model. The results show that SEWSAN, like the other models, is affected the most by variations in roughness and the least by variations in flow area.

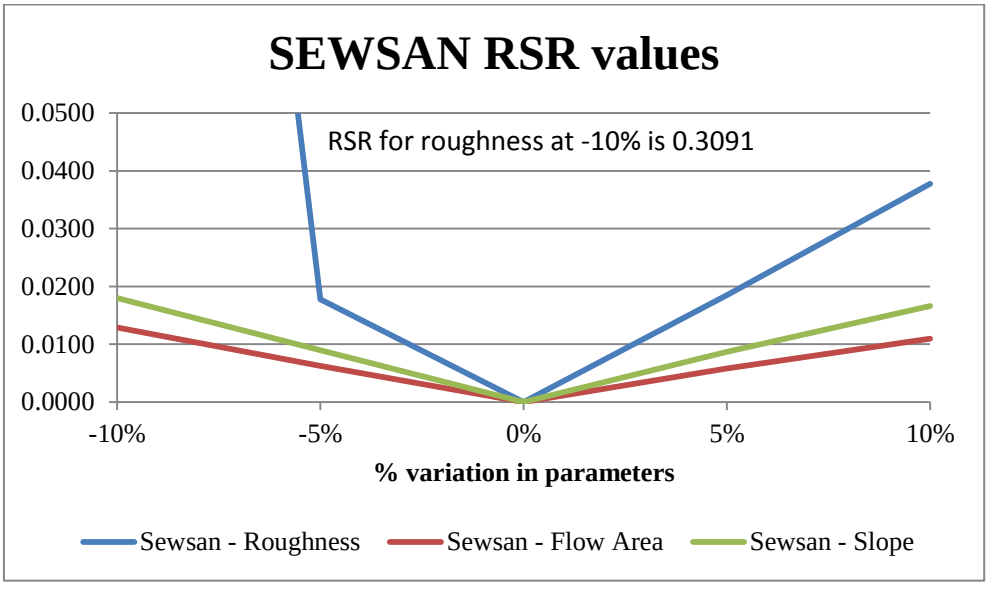

Figure 5:14: SEWSAN RSR values

Figure 5:15 shows the varying RSR values for the SWMM-TRANSPORT model. The results show that SWMM-TRANSPORT is affected the most by variation in roughness and the least by variation in flow area. While sensitivity to flow area is less than in SEWSAN,

SWMM-TRANSPORT shows a greater sensitivity to changes in roughness and slope than SEWSAN if the peak shift is excluded.

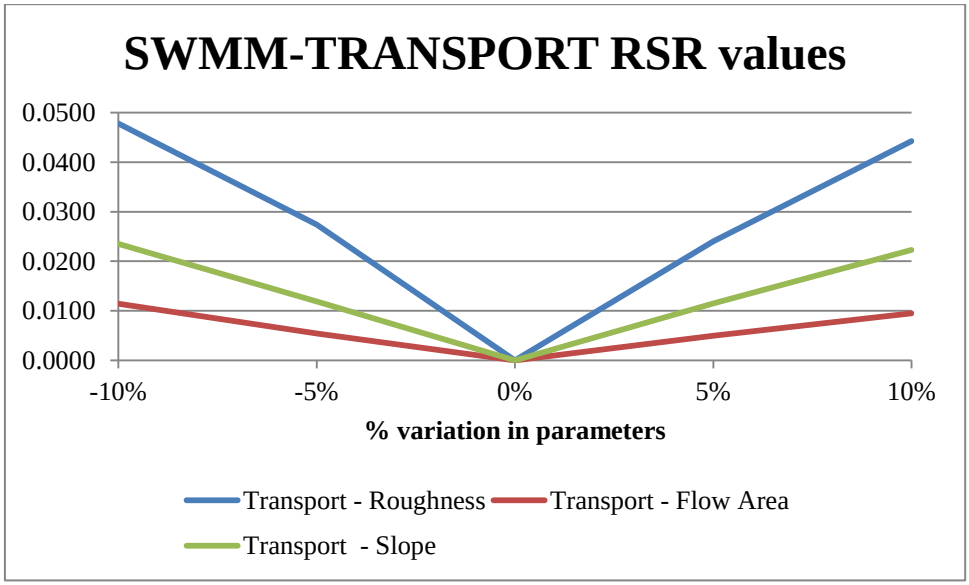

Figure 5:15: SWMM-TRANSPORT RSR values

Figure 5:16 shows that varying RSR values for the SWMM-EXTRAN model. SWMM-EXTRAN is the least sensitive to variations in the parameters. With the system used the model shows almost no effect due to the change in slope and flow area.

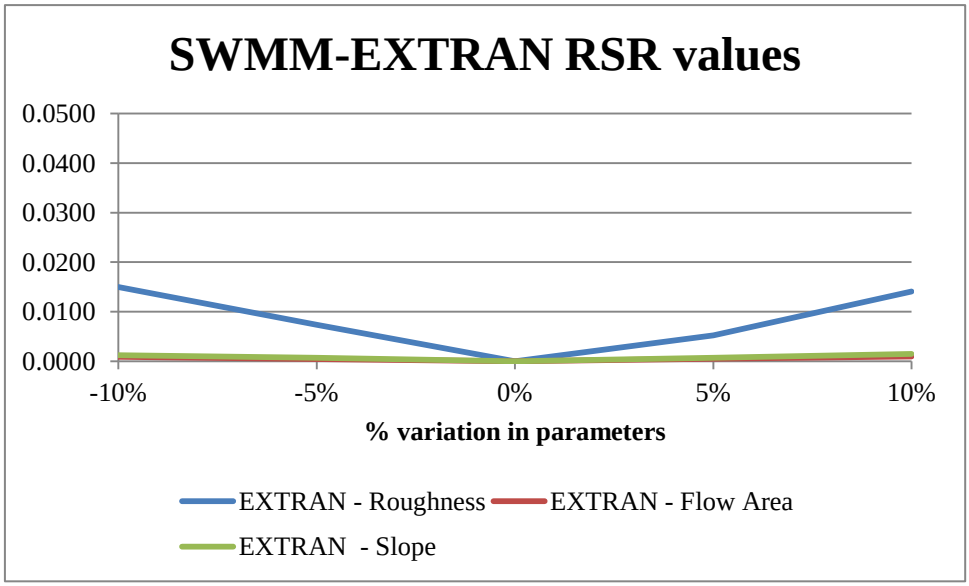

Figure 5:16: SWMM-EXTRAN RSR values

The RSR results indicate that the models are less sensitive to variations in flow area and slope while being the most sensitive to conduit roughness. SEWSAN and SWMM-TRANSPORT show similar sensitivity to variations in flow area and slope while SWMM-EXTRAN remains relatively unaffected.

Table 5.13 shows how the models rank in terms of sensitivity, with one being the least sensitive. SEWSAN can be very sensitive to changes due to peak shifting. It should be noted that any parameter change could cause a peak shift, making SEWSAN relatively unstable when considering the shape of a flow hydrograph. SWMM-EXTRAN is the most stable model. SWMM-TRANSPORT can be more sensitive to variations in slope but reacts in a more predicable manner than SEWSAN.

Table 5.13: Sensitivity rank according to the RSR values

Parameter	SEWSAN	SWMM-TRANSPORT	SWMM-EXTRAN
Slope	2	3	1
Flow area	3	2	1
Roughness	3	2	1

6. Discussion

It has been discussed that a sewer system analysis has three primary objectives; planning, design and evaluation, each having different requirements. Three models were chosen to evaluate Drainage System A and B, each being of different hydraulic sophistication. SWMM-EXTRAN, being a fully dynamic wave model, has the greatest hydraulic sophistication. SWMM-TRANSPORT, being a simplified kinematic wave model, has less sophistication. SEWSAN is the most basic model and relies on full flow velocities and peak flow shifting.

The analysis of the two longitudinal sections, Drainage System A and B, showed that SWMM-EXTRAN provided the most consistent results and correlated the best to the measured flow hydrograph. The results from SWMM-TRANSPORT and SEWSAN were similar in Drainage System A. SWMM-TRANSPORT, however, failed to provide accurate peak flows, being incorrect by 13%, when surcharge conditions occurred within Drainage System B.

The sensitivity analyses, however, showed that the flow hydrograph calculated by SEWSAN was vulnerable to peak shifting, which notably impacted the simulation results in terms of mean flows and peak flow times. The shift only occurred when the roughness was varied, but the shift in peak flow could occur with a variation in any of the parameters and is determined by the calculated lag time. The analysis showed that SWMM-TRANSPORT was more stable than SEWSAN as long as surcharge conditions did not occur within the system. The resultant SWMM-TRANSPORT hydrograph was shown to be almost as sensitive to changes in the three parameters as SEWSAN. SWMM-EXTRAN, however, proved to be the most stable when the three parameters were adjusted, with changes in slope and flow area having an almost negligible effect on the results.

7. Conclusions

7.1. Discussion

Sewer drainage systems can be simulated with a variety of models, which range from detailed models making use of fully dynamic flow equations to basic models that assume full flow conditions. If a designer is aware of the simplifications and assumptions made by models, the best model can be chosen for a specific drainage system and objective (design, planning or evaluation).

In Drainage System A, the contributor hydrograph model and kinematic wave model provided results that were similar to those of the fully dynamic wave model. The fully dynamic wave model correlated the best with measured flow hydrographs under all conditions. The sensitivity analyses also indicated that the fully dynamic wave model was the least affected by parameter changes.

The contributor hydrograph and kinematic wave models failed to provide accurate results when rapidly varying flow conditions or surcharge conditions occurred within the model, the most prominent being surcharge conditions in Drainage System B. The kinematic wave model, not taking backwater effects into account and being unable to handle surcharge conditions, failed to accurately model peak flows downstream from conduit 173. The contributor hydrograph model handled surcharge conditions by ignoring surcharge conditions by routing the full hydrograph downstream while reporting negative spare capacities. The fully dynamic wave model, taking considerably more hydraulic factors into account, managed to efficiently route flows downstream.

The boundary conditions used to initially populate the models resulted in peak flows that were offset by two hours when compared to measured flows. After the boundary conditions were adjusted by two hours, to provide better correlation with the measured flows, a much better correlation between simulated and measured hydrographs was obtained. The improved verification values obtained from the adjusted boundary conditions emphasised the importance of boundary conditions and the effect that they have on the accuracy of a model.

The RSR, NSE and PBIAS equations used to compare computed flow hydrographs with the measured flow hydrographs provided a means to determine whether a model provided accurate results. The kinematic wave results in Drainage System B highlighted a shortcoming of the RSR, NSE and PBIAS equations when only looking at the results of the three

equations. The peak flow was 13% below the measured hydrograph, but the RSR, NSE and PBIAS values were still within acceptable limits. When viewing any one of the values, RSR, NSE, PBIAS, peak flow, mean flow and peak time, on its own can lead to misleading confidence. All six values should be considered together, and only when all of them combined are within acceptable limits should the modelled results be considered acceptable. The only exception would be the peak time as time steps in sewer models are often quite large. The difference between measured peak times and modelled peak times may vary greatly without drastically affecting the overall accuracy of a model.

When using the kinematic wave model underestimated peak flows with accurate NSE and RSR values occurred. The scenario indicated that the kinematic wave model experienced limitations during surcharge conditions. The negative flow capacities reported in the contributor hydrograph model, which are not hydraulically possible, should not be overlooked and indicates a need for a more sophisticated model.

Figure 2:10 showed that an evaluation analysis requires high levels of model sophistication and that a planning analysis requires low levels of model sophistication. Figure 2:10 can be summarised in Table 7.1. It was also shown in the results from Chapter 4 that the contributor hydrograph model is able provide results that are very similar to a kinematic wave model.

Table 7.1: Required model sophistication for each model type

Analysis	Model		
	Fully Dynamic	Kinematic	Contributor hydrograph
Planning	X	X	X
Design	X	X	X
Evaluation	X		

The sensitivity analysis showed that the fully dynamic wave model was the least sensitive to variations in the three parameters while the contributor hydrograph model was the most sensitive. Table 7.2 shows that basic models require high levels of parameter confidence in order to produce accurate results. The results from Table 7.2 indicate that a design analysis should only be performed with the contributor hydrograph model if enough confidence exists in the available parameter set.

Table 7.2: Required parameter confidence for each model type

Parameter Confidence	Model		
	Fully dynamic	Kinematic	Contributor hydrograph
High	X	X	X
Medium	X	X	
Low	X		

Furthermore, when performing an evaluation analysis confidence should exist in the parameter set. Required parameter confidence is lower for a design analysis than an evaluation analysis as parameters, such as diameter, could still be changed. There often exists little confidence in parameters when performing a planning analysis as some parameters, such as inverts, are often estimated. Table 7.3 illustrates these needs.

Table 7.3: Required parameter confidence for an analysis type

Parameter Confidence	Analysis		
	Evaluation	Design	Planning
High	X	X	X
Medium		X	X
Low			X

There exists a contradiction in requirements between Table 7.2 and Table 7.3. Table 7.2 indicates that the contributor hydrograph model requires confidence in a parameter set to be accurate while Table 7.3 indicates a planning analysis, which is coupled with the contributor hydrograph from Table 7.1, does not require much confidence in the parameter set. Since the results from a planning analysis are not always required to be as accurate as for a design or evaluation analysis the results are accurate enough as long as the inaccuracies in the parameter set are noted.

The contributor hydrograph model is not capable of analysing gradually varying flow as full flow conditions are always assumed. When drop structures are present in a drainage system or when surcharge conditions occur then the fully dynamic wave model provides the most accurate results. The kinematic wave model can take gradually varying flows into account. The more rapid the change in flow conditions within a drainage system the less accurate the kinematic wave model becomes. The contributor hydrograph model is only suited to analyse

constant flows. The contributor hydrograph model is also not capable of analysing gradually varying flow, since full flow is always assumed.

Table 7.4: Model type required for differing flow conditions

System Topology	Model		
	Fully dynamic	Kinematic	Contributor hydrograph
Surcharge conditions	X		
Flow through hydraulic structures	X		
Rapidly varying flow	X	Limited	
Gradually varying flow	X	X	
Constant flow in conduit	X	X	X

When performing an evaluation analysis all hydraulic factors need to be accounted for. Surcharge should not be considered in a design analysis as the drainage system design should be improved. A design analysis, however, might need to take areas of rapidly varying flow conditions into account. A planning analysis will rarely need to take hydraulic structures or rapidly varying flow conditions into account. The contributor hydrograph model should not be used for a design analysis when hydraulic structures are present in a drainage system since the contributor hydrograph model does not take flow through hydraulic structures into account.

Table 7.5: System topology versus analysis type

System Topology	Analysis		
	Evaluation	Design	Planning
Surcharge conditions	X		
Hydraulic structures	X	X	
Rapidly varying flow	X	Partially	
Gradually varying flow	X	X	X

A fully dynamic wave model such as SWMM-EXTRAN can be used in all scenarios. A kinematic wave model such as SWMM-TRANSPORT can be used for a design analysis if no hydraulic structures are in the system. A contributor hydrograph model such as SEWSAN should not be used for evaluation designs. A contributor hydrograph model can, however, be used for a design analysis if a high level of confidence in the parameter set exists and no areas of rapidly varying flow or hydraulic structures exist within the system.

Therefore, if the objective of an analysis is known and a known confidence in the parameter set of a drainage system exists a model that will provide reasonable results can be chosen.

7.2. Further research

This study focused on comparing three modelling models, each with different levels of hydraulic sophistication. Further studies can be done with models with the same design philosophy, for example SWMM-EXTRAN compared to MOUSE, SWMM-TRANSPORT compared to HydroSim and SEWSAN compared to SWMM-RUNOFF.

This study was based on actual field measurements in two sewers with no diversion structures, pumps or siphons along the selected longitudinal sections. Further studies can be done to determine how each of the models perform when hydraulic structures are present in a drainage system.

Flows were initially measured at one hour intervals. The analyses, however, indicated that shorter intervals would be required to test peak flow times with greater accuracy. Unfortunately, shorter measurements periods could not be obtained for this study. Further studies could be performed where flows could be measured at shorter intervals.

This study highlighted the importance of boundary conditions. By adjusting the drainage system boundary conditions without modifying the hydrograph shape a much better fit with measured data in both the test drainage systems were obtained. Further studies could investigate the formulation of unit hydrographs associated with land use types so that modelled flow hydrographs correlate with measured flow hydrographs.

Reference list

Argaman, , Shamir, U. and Spivak, E. (1973) 'Design of Opitmal Sewerage Systems', *Journal of the Environmental Engineering Division*.

ASCE (1993) 'Criteria for evaluation of watershed models', *Journal of Irrigation Drainage Engineering*, vol. 119(3), pp. 429-442.

Ashley , R.J., Wotherspoon, D.J.J. and Coghlan, B.P. (1992) 'The Erosion and Movement of Sediments and Associated Pollutants in Combined Sewers', *Water Science and Technology*, vol. 25(8), pp. 101-114.

Beven, K. (2006) 'On Undermining the Science?', *Hydrological Processes*, vol. 20, pp. 3131-3146.

Blandford, G.E. and Ormsbee, L.E. (1993) 'A Diffusion Wave Finite Element Model for Channel Networks', *Journal of Hydrology*, vol. 142, pp. 99-120.

Butler, D. and Graham, N.J..D. (1995) 'Modelling Dry Weather Wastewater Flow in Sewer Networks', *Journal of Environmental Engineering*, February, pp. 161-173.

Chadwick, A., Morfett, J. and Borthwick, M. (2006) *Hydraulics in Civil and Environmental Engineering*, Bodmin: Spon Press.

Chow, V.T. (1959) *Open Channel Hydraulics*, New York: McGraw-Hill Book Co.

Clemmens, A.J. and Strelkoff, T. (2011) 'Zero-Inertial Recession for Kinematic-Wave Model', *Journal of Irrigation and Drainage Engineering*, pp. 263-266.

Clift, M.A. (1968) 'Experiance with Pressure Sewerage', *Journal of Sanitary Engineering*, vol. 94(5), p. 865.

Colebrook, C.F. (1938) 'Turbulent Flow in Pipes with Particular Reference to the Transistion Region Between the Smooth and Rough Pipe Laws', *Journal Institution of Civil Engineers*, vol. 11, pp. 133-156.

Deletic, A., Dotto, C.B., McCarthy, D.T., Kleidorfer, M., Freni, G., Mannina, G., Uhl, M., Henrichs, M., Fletcher, T.D., Rauch, W., Bertrand-Krejewski, J.L. and Tait, S. (2012) 'Assessing Uncertainties in Urban Drainage Models', *Physic and Chemistry of the Earth*.

DHI Software (n.d) 'Mouse Pipe Flow'.

Fair, K. (2008 a) 'Contributor Hydrograph Theory Course on Water and Sewer Networks', Stellenbosch.

Fair, K. (2008 b) 'Estimating Sewer Flow', Stellenbosch.

Gaume, E., Villeneuve, J.P. and Desbordes, M. (1998) 'Uncertainty Assesment and Analysis of the Calibrated Parameter Values of an Urban Storm Water Quality Model', *Journal of Hydrology*, vol. 210, pp. 38-50.

GLS Software (2013) *GLS Software*, [Online], Available: http://www.gls.co.za/software/ [01 Dec 2013].

Green, M.J. and Drinkwater, A. (1985) 'Guide to Sewer Flow Surveys'.

Guo, Q. and Song, C.C.S. (1989) 'Surging in Urban Storm Drainage Systems', *Journal of Hydraulic Engineering*, vol. 116 (12), pp. 1523-1537.

Huber, W.C. and Dickinson, R.E. (1998) 'Storm Water Management Model, Version 4: User's Manual'.

Hydrosim CC (2001) 'Hydrosim V for Windows: User's Guide'.

Jain, S.K., Singh, V.P. and Bhunya, P.K. (2006) 'Development of Optimal and Physical Realizable Unit Hydrograph', *Journal of Hydrologic Engineering*, vol. 11, no. 6, pp. 612-66.

Johnson, P.A. (1996) 'Uncertainty of Hydraulic Parameters', *Journal of Hydraulic Engineering*, February, pp. 112-114.

Joliffe, I.B. (1984) 'Computation of Dynamic Waves in Channel Networks', *Journal of Hydraulic Engineering*, vol. 110(10), pp. 1358-1370.

Killen, J.M. and Anderson, A.G. (1969) 'A Study of the Air-Water Interface in Air-Entrained Flow in Open-Channels', Proceedings of the 13th Congress of the International Association of Hydraulic Research, Tokyo, Japan, 339-348.

Kuczera, G. and Parent, E. (1998) 'Monte Carlo Assesment of Parameter Uncertainty in Conceptual Cachment Models: The Metropolis Algorithm.', *Journal of Hydrology* , vol. 211, pp. 69-85.

Little, C.J. (2004) 'A comparison of sewer reticulation system design standards gravity, vacuum and small bore sewers', *Water SA*, vol. 30, no. 5, pp. 137-144.

Manenti, S., Sibilla, S., Gallati, M., Agate, G. and Roberto, G. (2012) 'SPH Simulation of Sediment Flushing Induced by a Rapid Water Flow', *Journal of Hydraulic Engineering*, vol. 138(3), pp. 272-284.

Mays, L.W. (2001) *Stormwater Collection Systems Design Handbook*, New York: McGraw-Hill.

Moriasi, D.N., Arnold, J.G., Van Liew, M.W., Binger, R.L., Harmel, R.D. and Veith, T.L. (2006) 'Model evaluation guidelines for systematic quantification of accuracy in watershed simulations', *American Societ of Agricultural and Biological Engineers*, vol. 50(3), pp. 885-900.

Mourad, M., Bertrand-Krajewski, J.L. and Chebbo, G. (2005) 'Stormwater Quality Models: Sensitivity to Calibration Data', *Water Science and Technology*, vol. 52, no. 5, pp. 61-68.

Ota, J.J. and Nalluri, C. (2003) 'Urban Storm Sewer Design: Approach in Consideration of Sediments', *Journal of Hydraulic Engineering*, vol. 129(4), pp. 291-297.

Roesner, L.A. and Aldrich, J.A. (1992) *Storm Water Management Model User's Manual Version 4: EXTRAN Addendum*, Orlando, Florida: US Envirnomental Protection Agency.

Rossman, L.A. (2006) 'Storm water Management Model Quality Assurance Report: Dynamic Wave Flow Routine'.

Rossman, L.A. (2007) 'Storm Water Management Model Quality Assurance Report: Dynamic Wave Flow Routing'.

Rouse, H. (1965) 'Critical Analysis of Open-Channel Resistance', *Journal of the Hydraulics Division*, vol. 91, pp. 1-25.

Schaarup-Jensen, K., Johansen, C. and Thornadal, S. (2005) 'Uncertainties related to extreme event statistics of sewer system surcharge and overflow', 10th International Conference on Urban Drainage, Copenhagen, 21-26.

Shaw, V.A. (1963) 'The Development of Contributory Hydrographs for Sanitary Sewers and their use in Sewer Design '.

Silberstein, R.P. (2006) 'Hydrological Models Are So Good, Do We Still Need Data?', *Environmental Modelling & Software*, vol. 21, no. 9, pp. 1340-1352.

Singh, J., Knapp, H.V. and Demissie, M. (2004-08) 'Hydrologic modeling of the Iroquois River watershed using HSPF and SWAT.'.

Song, C.C.S., Cardle, J.A. and Leung, K.S. (1983) 'Transient Mixed-Flow Models for Storm Sewers', *Journal of Hydraulic Engineering*, vol. 109(11), pp. 1487-1504.

Stephenson, D. and Hine, A.E. (1982) 'Computor Analysis of Johannesburg Sewers'.

Thorndahl, S., Beven, K.J., Jensen, J.B. and Schaarup-Jensen, K. (2008) 'Event based uncertainty assessment in urban drainage modelling, applying the GLUE methodologhy', *Journal of Hydrology*, pp. 421-437.

Water Environment Federation (1999) 'Alternative Sewer Systems FD-12', in *Overview of Wastewater Collection Systems*, New York: McGraw-Hill.

Weather Online (2013) *Weather Online*, [Online], Available: http://www.weatheronline.co.uk/ [28 Nov 2013].

Willems, P. (2012) 'Model uncertainty analysis by variance decomposition', *Physics and Chemistry of the Earth*, pp. 21-30.

Yen, B.C. (1978) 'Hydraulic Instabilities of Storm Sewer Flows', Urban Storm Drainage, Proceedings of the 1st International Conferance, New York, 282-293.

Yen, B.C. (1980) 'Surcharge of Sewer Systems'.

Yen, B.C. (1986) *Advances in Hydroscience*, Orlando, FL: Academic Press.

Yen, B.C. (1991) 'Hydraulic Resistance in Open Channels', Channel Flow Resistance: Centinnial of Manning's Formula, Highlands Ranch, 1-135.

Yen, B.C. (2004) *Hydraulic Design Handbook*, New York: McGraw-Hill.

Yen, B.C. and Sevuk, A.S. (1975) 'Design of Storm Sewer Networks', *Journal of Enivornmental Engineering Division*, vol. 101, pp. 535-553.

Zhong, J. (1998) 'General hydrodynamic Model for Sewer/Channel Network Systems', *Journal of Hydraulic Engineering*, pp. 307-215.

Appendix A: Evaluation of models

A = $(Calibration_t - Model_t)^2$

B = $(Calibration_t - Calibration_{avg})^2$

C = $(Calibration_t - Model_t)$

Drainage System A results: SEWSAN

Time	CALIBRATION	SEWSAN	A	B	C
1	527.420	584.833	3296.306	32126.380	-57.413
2	471.320	559.600	7793.406	55384.131	-88.280
3	436.900	524.972	7756.737	72769.558	-88.072
4	421.100	478.149	3254.595	81543.562	-57.049
5	421.540	425.653	16.915	81292.464	-4.113
6	463.440	381.908	6647.399	59155.158	81.532
7	604.340	356.165	61590.662	10469.041	248.175
8	821.500	354.526	218064.879	13188.608	466.974
9	940.740	394.830	298017.451	54794.227	545.910
10	954.140	493.608	212090.181	61247.175	460.532
11	955.440	666.776	83326.648	61892.318	288.664
12	936.180	974.813	1492.474	52680.195	-38.633
13	897.640	972.521	5607.233	36473.997	-74.881
14	861.680	963.455	10358.077	24031.717	-101.775
15	831.240	944.096	12736.402	15520.592	-112.856
16	805.160	910.069	11005.855	9702.578	-104.909
17	782.000	858.723	5886.474	5676.367	-76.723
18	762.020	805.310	1873.982	3064.914	-43.290
19	743.960	770.350	696.420	1391.414	-26.390
20	728.820	751.026	493.128	491.139	-22.206
21	700.520	730.468	896.887	37.679	-29.948
22	675.360	690.254	221.837	979.586	-14.894
23	631.980	642.143	103.278	5576.853	-10.163
24	585.360	608.761	547.627	14713.286	-23.401
		RSR	**1.125**		
		NSE	**-0.290**		
		PBIAS	**6.585**		
		Mean	**-0.066**		
		Peak	**0.020**		

Drainage System A results: SWMM-EXTRAN

Time	CALIBRATION	EXTRAN	A	B	C
1	527.420	566.670	1540.581	32126.380	-39.250
2	471.320	539.949	4710.005	55384.131	-68.629
3	436.900	498.071	3741.919	72769.558	-61.171
4	421.100	445.865	613.301	81543.562	-24.765
5	421.540	394.194	747.790	81292.464	27.346
6	463.440	358.659	10979.152	59155.158	104.781
7	604.340	339.525	70127.245	10469.041	264.815
8	821.500	343.219	228752.732	13188.608	478.281
9	940.740	399.121	293351.027	54794.227	541.619
10	954.140	549.016	164125.263	61247.175	405.124
11	955.440	803.528	23077.216	61892.318	151.912
12	936.180	967.826	1001.440	52680.195	-31.646
13	897.640	963.466	4333.069	36473.997	-65.826
14	861.680	949.696	7746.828	24031.717	-88.016
15	831.240	920.807	8022.205	15520.592	-89.567
16	805.160	872.003	4467.925	9702.578	-66.843
17	782.000	811.747	884.910	5676.367	-29.747
18	762.020	768.409	40.819	3064.914	-6.389
19	743.960	751.846	62.194	1391.414	-7.886
20	728.820	736.366	56.936	491.139	-7.546
21	700.520	704.932	19.467	37.679	-4.412
22	675.360	650.982	594.303	979.586	24.378
23	631.980	609.195	519.146	5576.853	22.785
24	585.360	589.022	13.412	14713.286	-3.662
		RSR	**1.049**		
		NSE	**-0.122**		
		PBIAS	**8.406**		
		Mean	**-0.084**		
		Peak	**0.013**		

Drainage System A results: SWMM-TRANSPORT

Time	CALIBRATION	TRANSPORT	A	B	C
1	527.420	576.920	2450.212	32126.380	-49.500
2	471.320	551.482	6425.931	55384.131	-80.162
3	436.900	516.511	6337.877	72769.558	-79.611
4	421.100	469.187	2312.330	81543.562	-48.087
5	421.540	417.226	18.611	81292.464	4.314
6	463.440	373.478	8093.130	59155.158	89.962
7	604.340	347.266	66086.986	10469.041	257.074
8	821.500	343.157	228811.832	13188.608	478.343
9	940.740	381.336	312933.131	54794.227	559.404
10	954.140	483.697	221316.254	61247.175	470.443
11	955.440	675.551	78337.654	61892.318	279.889
12	936.180	888.228	2299.366	52680.195	47.952
13	897.640	965.940	4664.906	36473.997	-68.300
14	861.680	956.560	9002.229	24031.717	-94.880
15	831.240	935.350	10838.967	15520.592	-104.110
16	805.160	898.143	8645.859	9702.578	-92.983
17	782.000	843.996	3843.458	5676.367	-61.996
18	762.020	790.898	833.923	3064.914	-28.878
19	743.960	759.814	251.352	1391.414	-15.854
20	728.820	742.625	190.570	491.139	-13.805
21	700.520	721.182	426.915	37.679	-20.662
22	675.360	679.159	14.432	979.586	-3.799
23	631.980	629.903	4.316	5576.853	2.077
24	585.360	598.604	175.399	14713.286	-13.244
		RSR	**1.137**		
		NSE	**-0.318**		
		PBIAS	**8.335**		
		Mean	**-0.083**		
		Peak	**0.011**		

Drainage System A results (Shifted boundary conditions): Sewsan

Time	CALIBRATION	SEWSAN	A	B	C
1	527.420	524.972	5.991	32126.380	2.448
2	471.320	478.149	46.636	55384.131	-6.829
3	436.900	425.653	126.501	72769.558	11.247
4	421.100	381.908	1535.980	81543.562	39.192
5	421.540	356.165	4273.846	81292.464	65.375
6	463.440	354.526	11862.297	59155.158	108.914
7	604.340	394.830	43894.334	10469.041	209.510
8	821.500	493.608	107513.490	13188.608	327.892
9	940.740	666.776	75056.029	54794.227	273.964
10	954.140	974.813	427.354	61247.175	-20.673
11	955.440	972.521	291.776	61892.318	-17.081
12	936.180	963.455	743.906	52680.195	-27.275
13	897.640	944.096	2158.129	36473.997	-46.456
14	861.680	910.069	2341.475	24031.717	-48.389
15	831.240	858.723	755.335	15520.592	-27.483
16	805.160	805.310	0.022	9702.578	-0.150
17	782.000	770.350	135.728	5676.367	11.650
18	762.020	751.026	120.857	3064.914	10.994
19	743.960	730.468	182.032	1391.414	13.492
20	728.820	690.254	1487.323	491.139	38.566
21	700.520	642.143	3407.921	37.679	58.377
22	675.360	608.761	4435.369	979.586	66.599
23	631.980	584.833	2222.795	5576.853	47.147
24	585.360	559.600	663.564	14713.286	25.760
		RSR	**0.591**		
		NSE	**0.643**		
		PBIAS	**6.585**		
		Mean	**-0.066**		
		Peak	**0.020**		

Drainage System A results (Shifted boundary conditions): SWMM-EXTRAN

Time	CALIBRATION	EXTRAN	A	B	C
1	527.420	498.071	861.351	32126.380	29.349
2	471.320	445.865	647.961	55384.131	25.455
3	436.900	394.194	1823.781	72769.558	42.706
4	421.100	358.659	3898.934	81543.562	62.441
5	421.540	339.525	6726.541	81292.464	82.015
6	463.440	343.219	14453.093	59155.158	120.221
7	604.340	399.121	42114.795	10469.041	205.219
8	821.500	549.016	74247.401	13188.608	272.484
9	940.740	803.528	18827.097	54794.227	137.212
10	954.140	967.826	187.294	61247.175	-13.686
11	955.440	963.466	64.417	61892.318	-8.026
12	936.180	949.696	182.684	52680.195	-13.516
13	897.640	920.807	536.699	36473.997	-23.167
14	861.680	872.003	106.555	24031.717	-10.323
15	831.240	811.747	379.960	15520.592	19.493
16	805.160	768.409	1350.639	9702.578	36.751
17	782.000	751.846	909.245	5676.367	30.154
18	762.020	736.366	658.147	3064.914	25.654
19	743.960	704.932	1523.177	1391.414	39.028
20	728.820	650.982	6058.806	491.139	77.838
21	700.520	609.195	8340.213	37.679	91.325
22	675.360	589.022	7454.202	979.586	86.338
23	631.980	566.670	4265.365	5576.853	65.310
24	585.360	539.949	2062.116	14713.286	45.411
		RSR	**0.512**		
		NSE	**0.733**		
		PBIAS	**8.406**		
		Mean	**-0.084**		
		Peak	**0.013**		

Drainage System A results (Shifted boundary conditions): SWMM-TRANSPORT

Time	CALIBRATION	TRANSPORT	A	B	C
1	527.420	516.511	119.011	32126.380	10.909
2	471.320	469.187	4.551	55384.131	2.133
3	436.900	417.226	387.070	72769.558	19.674
4	421.100	373.478	2267.838	81543.562	47.622
5	421.540	347.266	5516.611	81292.464	74.274
6	463.440	343.157	14467.951	59155.158	120.283
7	604.340	381.336	49730.902	10469.041	223.004
8	821.500	483.697	114110.607	13188.608	337.803
9	940.740	675.551	70325.017	54794.227	265.189
10	954.140	888.228	4344.353	61247.175	65.912
11	955.440	965.940	110.252	61892.318	-10.500
12	936.180	956.560	415.347	52680.195	-20.380
13	897.640	935.350	1422.071	36473.997	-37.710
14	861.680	898.143	1329.559	24031.717	-36.463
15	831.240	843.996	162.706	15520.592	-12.756
16	805.160	790.898	203.412	9702.578	14.262
17	782.000	759.814	492.215	5676.367	22.186
18	762.020	742.625	376.178	3064.914	19.395
19	743.960	721.182	518.841	1391.414	22.778
20	728.820	679.159	2466.216	491.139	49.661
21	700.520	629.903	4986.817	37.679	70.617
22	675.360	598.604	5891.507	979.586	76.756
23	631.980	576.920	3031.646	5576.853	55.060
24	585.360	551.482	1147.725	14713.286	33.878
		RSR	**0.613**		
		NSE	**0.616**		
		PBIAS	**8.335**		
		Mean	**-0.083**		
		Peak	**0.011**		

Drainage System B results: SEWSAN

Time	CALIBRATION	SEWSAN	A	B	C
1	581.620	764.080	33291.572	40823.192	-182.460
2	522.700	738.180	46431.642	68104.036	-215.480
3	476.900	701.205	50312.575	94106.299	-224.305
4	451.620	650.245	39451.999	110255.542	-198.625
5	445.920	585.388	19451.381	114073.374	-139.468
6	470.900	516.498	2079.208	97823.509	-45.598
7	577.960	459.702	13985.029	42315.576	118.258
8	800.060	432.224	135303.311	268.714	367.836
9	1081.340	460.210	385802.080	88608.917	621.130
10	1172.860	566.600	367551.714	151470.802	606.260
11	1177.700	710.969	217838.055	155261.611	466.731
12	1141.000	888.672	63669.636	127686.516	252.328
13	1077.220	1182.448	11072.917	86173.070	-105.228
14	995.140	1176.011	32714.293	44720.618	-180.871
15	924.360	1144.494	48459.104	19794.380	-220.134
16	871.300	1095.231	50144.968	7679.455	-223.931
17	839.460	1034.975	38225.972	3112.803	-195.515
18	819.160	971.141	23098.327	1259.718	-151.981
19	810.700	908.991	9661.146	730.756	-98.291
20	793.080	863.175	4913.321	88.595	-70.095
21	771.540	838.574	4493.598	147.076	-67.034
22	730.900	824.805	8818.175	2784.409	-93.905
23	668.480	807.769	19401.333	13268.160	-139.289
24	606.100	785.816	32298.013	31530.217	-179.716

RSR	**1.129**
NSE	**-0.305**
PBIAS	**-1.592**
Mean	**1.592%**
Peak	**0.403%**

Drainage System B results: SWMM-EXTRAN

Time	CALIBRATION	EXTRAN	A	B	C
1	581.620	747.424	27491.028	40823.192	-165.804
2	522.700	715.302	37095.573	68104.036	-192.602
3	476.900	665.798	35682.322	94106.299	-188.898
4	451.620	597.323	21229.503	110255.542	-145.703
5	445.920	524.548	6182.436	114073.374	-78.628
6	470.900	464.260	44.094	97823.509	6.640
7	577.960	424.250	23626.890	42315.576	153.710
8	800.060	411.497	150980.999	268.714	388.563
9	1081.340	456.527	390390.994	88608.917	624.813
10	1172.860	622.863	302497.165	151470.802	549.997
11	1177.700	912.363	70403.917	155261.611	265.337
12	1141.000	1127.548	180.950	127686.516	13.452
13	1077.220	1182.603	11105.477	86173.070	-105.383
14	995.140	1152.679	24818.526	44720.618	-157.539
15	924.360	1103.768	32187.142	19794.380	-179.408
16	871.300	1036.028	27135.284	7679.455	-164.728
17	839.460	961.406	14870.825	3112.803	-121.946
18	819.160	897.336	6111.507	1259.718	-78.176
19	810.700	858.371	2272.549	730.756	-47.671
20	793.080	840.209	2221.121	88.595	-47.129
21	771.540	825.577	2919.967	147.076	-54.037
22	730.900	806.982	5788.468	2784.409	-76.082
23	668.480	784.963	13568.195	13268.160	-116.483
24	606.100	767.068	25910.745	31530.217	-160.968
		RSR	**0.974**		
		NSE	**0.028**		
		PBIAS	**-0.418**		
		Mean	**0.418%**		
		Peak	**0.416%**		

Drainage System B results: SWMM-TRANSPORT

Time	CALIBRATION	TRANSPORT	A	B	C
1	581.620	761.056	32197.451	40823.192	-179.436
2	522.700	735.356	45222.690	68104.036	-212.656
3	476.900	696.944	48419.414	94106.299	-220.044
4	451.620	644.242	37103.162	110255.542	-192.622
5	445.920	576.632	17085.524	114073.374	-130.712
6	470.900	506.825	1290.633	97823.509	-35.925
7	577.960	451.402	16017.046	42315.576	126.558
8	800.060	424.430	141098.044	268.714	375.630
9	1081.340	447.379	401905.992	88608.917	633.961
10	1172.860	541.070	399158.172	151470.802	631.790
11	1177.700	702.062	226231.950	155261.611	475.638
12	1141.000	925.942	46249.967	127686.516	215.058
13	1077.220	1021.892	3061.167	86173.070	55.328
14	995.140	1024.774	878.178	44720.618	-29.634
15	924.360	1007.086	6843.657	19794.380	-82.726
16	871.300	1005.713	18066.787	7679.455	-134.413
17	839.460	1006.148	27785.042	3112.803	-166.688
18	819.160	955.477	18582.276	1259.718	-136.317
19	810.700	893.065	6783.989	730.756	-82.365
20	793.080	852.477	3527.984	88.595	-59.397
21	771.540	833.967	3897.149	147.076	-62.427
22	730.900	821.843	8270.656	2784.409	-90.943
23	668.480	803.667	18275.608	13268.160	-135.187
24	606.100	780.923	30563.230	31530.217	-174.823
		RSR	**1.094**		
		NSE	**-0.227**		
		PBIAS	**2.061**		
		Mean	**-2.061%**		
		Peak	**-12.985%**		

Drainage System B results (Shifted boundary conditions): SEWSAN

Time	CALIBRATION	SEWSAN	A	B	C
1	581.620	701.205	14300.488	40823.192	-119.585
2	522.700	650.245	16267.797	68104.036	-127.545
3	476.900	585.388	11769.691	94106.299	-108.488
4	451.620	516.498	4209.197	110255.542	-64.878
5	445.920	459.702	189.935	114073.374	-13.782
6	470.900	432.224	1495.832	97823.509	38.676
7	577.960	460.210	13864.987	42315.576	117.750
8	800.060	566.600	54503.774	268.714	233.460
9	1081.340	710.969	137174.859	88608.917	370.371
10	1172.860	888.672	80763.063	151470.802	284.188
11	1177.700	1182.448	22.543	155261.611	-4.748
12	1141.000	1176.011	1225.765	127686.516	-35.011
13	1077.220	1144.494	4525.830	86173.070	-67.274
14	995.140	1095.231	10018.152	44720.618	-100.091
15	924.360	1034.975	12235.597	19794.380	-110.615
16	871.300	971.141	9968.292	7679.455	-99.841
17	839.460	908.991	4834.578	3112.803	-69.531
18	819.160	863.175	1937.328	1259.718	-44.015
19	810.700	838.574	776.977	730.756	-27.874
20	793.080	824.805	1006.484	88.595	-31.725
21	771.540	807.769	1312.516	147.076	-36.229
22	730.900	785.816	3015.820	2784.409	-54.916
23	668.480	764.080	9139.319	13268.160	-95.600
24	606.100	738.180	17445.133	31530.217	-132.080
		RSR	**0.563**		
		NSE	**0.676**		
		PBIAS	**-1.592**		
		Mean	**1.592%**		
		Peak	**0.403%**		

Drainage System B results (Shifted boundary conditions): SWMM-EXTRAN

Time	CALIBRATION	EXTRAN	A	B	C
1	581.620	665.798	7085.877	40823.192	-84.178
2	522.700	597.323	5568.663	68104.036	-74.623
3	476.900	524.548	2270.377	94106.299	-47.648
4	451.620	464.260	159.762	110255.542	-12.640
5	445.920	424.250	469.607	114073.374	21.670
6	470.900	411.497	3528.685	97823.509	59.403
7	577.960	456.527	14745.917	42315.576	121.433
8	800.060	622.863	31398.927	268.714	177.197
9	1081.340	912.363	28553.350	88608.917	168.977
10	1172.860	1127.548	2053.158	151470.802	45.312
11	1177.700	1182.603	24.035	155261.611	-4.903
12	1141.000	1152.679	136.398	127686.516	-11.679
13	1077.220	1103.768	704.783	86173.070	-26.548
14	995.140	1036.028	1671.821	44720.618	-40.888
15	924.360	961.406	1372.406	19794.380	-37.046
16	871.300	897.336	677.880	7679.455	-26.036
17	839.460	858.371	357.636	3112.803	-18.911
18	819.160	840.209	443.051	1259.718	-21.049
19	810.700	825.577	221.317	730.756	-14.877
20	793.080	806.982	193.265	88.595	-13.902
21	771.540	784.963	180.166	147.076	-13.423
22	730.900	767.068	1308.135	2784.409	-36.168
23	668.480	747.424	6232.184	13268.160	-78.944
24	606.100	715.302	11925.101	31530.217	-109.202
		RSR	**0.305**		
		NSE	**0.905**		
		PBIAS	**-0.418**		
		Mean	**0.418%**		
		Peak	**0.416%**		

Drainage System B results (Shifted boundary conditions): SWMM-TRANSPORT

Time	CALIBRATION	TRANSPORT	A	B	C
1	581.620	696.944	13299.652	40823.192	-115.324
2	522.700	644.242	14772.412	68104.036	-121.542
3	476.900	576.632	9946.393	94106.299	-99.732
4	451.620	506.825	3047.635	110255.542	-55.205
5	445.920	451.402	30.047	114073.374	-5.482
6	470.900	424.430	2159.479	97823.509	46.470
7	577.960	447.379	17051.283	42315.576	130.581
8	800.060	541.070	67075.643	268.714	258.990
9	1081.340	702.062	143852.155	88608.917	379.278
10	1172.860	925.942	60968.526	151470.802	246.918
11	1177.700	1021.892	24276.074	155261.611	155.808
12	1141.000	1024.774	13508.466	127686.516	116.226
13	1077.220	1007.086	4918.722	86173.070	70.134
14	995.140	1005.713	111.783	44720.618	-10.573
15	924.360	1006.148	6689.352	19794.380	-81.788
16	871.300	955.477	7085.737	7679.455	-84.177
17	839.460	893.065	2873.493	3112.803	-53.605
18	819.160	852.477	1110.012	1259.718	-33.317
19	810.700	833.967	541.360	730.756	-23.267
20	793.080	821.843	827.319	88.595	-28.763
21	771.540	803.667	1032.164	147.076	-32.127
22	730.900	780.923	2502.343	2784.409	-50.023
23	668.480	761.056	8570.405	13268.160	-92.576
24	606.100	735.356	16707.184	31530.217	-129.256
		RSR	**0.570**		
		NSE	**0.667**		
		PBIAS	**2.061**		
		Mean	**-2.061%**		
		Peak	**-12.985%**		

Appendix B: Sensitivity analysis

SEWSAN variation in slope

Time (h)	-10%	-5%	0%	5%	10%
0	586.33	585.59	584.83	584.09	583.40
1	561.21	560.42	559.60	558.80	558.06
2	527.27	526.12	524.97	523.86	522.85
3	481.45	479.81	478.15	476.53	475.04
4	429.43	427.56	425.65	423.78	422.03
5	384.95	383.46	381.91	380.35	378.88
6	357.89	357.05	356.17	355.27	354.40
7	354.66	354.60	354.53	354.41	354.27
8	393.00	394.11	394.83	395.49	396.06
9	487.59	490.72	493.61	496.34	498.78
10	653.88	660.34	666.78	672.97	678.59
11	974.89	974.86	974.81	974.84	975.01
12	972.69	972.60	972.52	972.47	972.49
13	964.01	963.73	963.45	963.20	962.97
14	945.21	944.65	944.10	943.56	943.07
15	912.29	911.17	910.07	909.01	908.05
16	862.50	860.62	858.72	856.92	855.30
17	809.26	807.32	805.31	803.33	801.50
18	772.58	771.50	770.35	769.17	768.02
19	751.87	751.46	751.03	750.59	750.17
20	731.71	731.10	730.47	729.87	729.33
21	693.41	691.83	690.25	688.75	687.39
22	645.75	643.98	642.14	640.32	638.60
23	610.91	609.87	608.76	607.64	606.55

RSR	**0.018**	**0.009**	**0.000**	**0.009**	**0.017**
NSE	**1.000**	**1.000**	**1.000**	**1.000**	**1.000**
PBIAS	**-0.137**	**-0.072**	**0.000**	**0.072**	**0.140**
Peak %	**0.008%**	**0.004%**	**0.000%**	**0.003%**	**0.020%**

SWMM-EXTRAN variation in slope

Time (h)	-10%	-5%	0%	5%	10%
0	566.76	566.72	566.67	566.62	566.57
1	540.07	540.02	539.95	539.88	539.81
2	498.26	498.17	498.07	497.96	497.85
3	446.12	446.00	445.86	445.71	445.56
4	394.50	394.36	394.19	394.03	393.85
5	358.88	358.78	358.66	358.53	358.40
6	339.65	339.59	339.52	339.45	339.38
7	343.19	343.20	343.22	343.24	343.25
8	398.79	398.95	399.12	399.31	399.50
9	548.21	548.58	549.02	549.49	549.96
10	802.89	803.18	803.53	803.90	804.28
11	967.80	967.81	967.83	967.84	967.84
12	963.48	963.48	963.47	963.46	963.45
13	949.74	949.72	949.70	949.68	949.66
14	920.90	920.86	920.81	920.76	920.71
15	872.15	872.09	872.00	871.92	871.84
16	811.88	811.82	811.75	811.67	811.59
17	768.47	768.44	768.41	768.37	768.34
18	751.87	751.86	751.85	751.83	751.82
19	736.43	736.40	736.37	736.33	736.29
20	705.08	705.01	704.93	704.85	704.76
21	651.14	651.07	650.98	650.89	650.80
22	609.31	609.25	609.20	609.13	609.07
23	589.10	589.06	589.02	588.98	588.94

RSR	**0.001**	**0.001**	**0.000**	**0.001**	**0.001**
NSE	**1.000**	**1.000**	**1.000**	**1.000**	**1.000**
PBIAS	**-0.004**	**-0.002**	**0.000**	**0.002**	**0.004**
Peak %	**-0.002%**	**-0.001%**	**0.000%**	**0.001%**	**0.002%**

SWMM-TRANSPORT variation in slope

Time (h)	-10%	-5%	0%	5%	10%
0	578.15	577.54	576.92	576.31	575.74
1	552.80	552.15	551.48	550.83	550.22
2	518.79	517.66	516.51	515.39	514.34
3	472.26	470.74	469.19	467.68	466.26
4	420.43	418.85	417.23	415.65	414.18
5	375.61	374.56	373.48	372.43	371.45
6	348.42	347.85	347.27	346.70	346.17
7	343.31	343.23	343.16	343.10	343.05
8	378.95	380.12	381.34	382.53	383.67
9	475.71	479.66	483.70	487.60	491.24
10	660.72	668.06	675.55	682.81	689.57
11	875.74	881.91	888.23	894.36	900.09
12	966.08	966.01	965.94	965.87	965.80
13	957.12	956.85	956.56	956.28	956.02
14	936.46	935.92	935.35	934.80	934.28
15	900.52	899.35	898.14	896.98	895.89
16	847.71	845.87	844.00	842.17	840.47
17	793.87	792.40	790.90	789.44	788.07
18	760.85	760.34	759.81	759.30	758.83
19	743.10	742.87	742.62	742.39	742.17
20	722.59	721.90	721.18	720.49	719.84
21	682.56	680.88	679.16	677.49	675.92
22	632.58	631.26	629.90	628.58	627.35
23	599.75	599.18	598.60	598.04	597.51

RSR	**0.024**	**0.012**	**0.000**	**0.012**	**0.022**
NSE	**0.999**	**1.000**	**1.000**	**1.000**	**1.000**
PBIAS	**0.014**	**0.007**	**0.000**	**-0.006**	**-0.012**
Peak %	**0.015%**	**0.007%**	**0.000%**	**-0.007%**	**-0.014%**

SEWSAN variation in flow area

Time (h)	-10%	-5%	0%	5%	10%
0	585.58	585.20	584.83	584.49	584.20
1	560.43	560.01	559.60	559.22	558.89
2	526.31	525.62	524.97	524.37	523.86
3	480.22	479.17	478.15	477.20	476.38
4	428.08	426.85	425.65	424.53	423.54
5	383.80	382.85	381.91	381.02	380.22
6	357.10	356.63	356.17	355.72	355.33
7	354.30	354.42	354.53	354.62	354.70
8	393.07	394.14	394.83	395.47	396.04
9	488.80	491.36	493.61	495.69	497.52
10	656.98	661.99	666.78	671.24	675.18
11	974.52	974.67	974.81	975.03	975.16
12	972.29	972.41	972.52	972.66	972.78
13	963.51	963.48	963.45	963.44	963.45
14	944.56	944.32	944.10	943.89	943.73
15	911.34	910.69	910.07	909.50	909.02
16	861.14	859.91	858.72	857.65	856.69
17	807.87	806.58	805.31	804.13	803.06
18	771.65	771.00	770.35	769.72	769.15
19	751.30	751.16	751.03	750.90	750.79
20	731.01	730.75	730.47	730.22	730.02
21	692.20	691.21	690.25	689.38	688.63
22	644.45	643.29	642.14	641.06	640.10
23	610.00	609.38	608.76	608.17	607.63

RSR	**0.013**	**0.006**	**0.000**	**0.006**	**0.011**
NSE	**1.000**	**1.000**	**1.000**	**1.000**	**1.000**
PBIAS	**-0.047**	**-0.026**	**0.000**	**0.023**	**0.044**
Peak %	**-0.030%**	**-0.015%**	**0.000%**	**0.022%**	**0.036%**

SWMM-EXTRAN variation in flow area

Time (h)	-10%	-5%	0%	5%	10%
0	566.62	566.64	566.67	566.70	566.73
1	539.85	539.90	539.95	540.00	540.05
2	497.94	498.00	498.07	498.14	498.22
3	445.71	445.78	445.86	445.95	446.03
4	394.04	394.11	394.19	394.28	394.36
5	358.54	358.60	358.66	358.72	358.79
6	339.46	339.49	339.52	339.56	339.60
7	343.25	343.23	343.22	343.20	343.19
8	399.37	399.25	399.12	399.00	398.87
9	549.73	549.38	549.02	548.65	548.27
10	803.91	803.72	803.53	803.32	803.13
11	967.80	967.82	967.83	967.83	967.84
12	963.45	963.46	963.47	963.47	963.48
13	949.67	949.68	949.70	949.71	949.73
14	920.75	920.78	920.81	920.84	920.88
15	871.91	871.96	872.00	872.06	872.12
16	811.66	811.71	811.75	811.79	811.83
17	768.39	768.40	768.41	768.42	768.44
18	751.84	751.84	751.85	751.85	751.86
19	736.31	736.34	736.37	736.39	736.42
20	704.81	704.87	704.93	704.99	705.06
21	650.89	650.94	650.98	651.03	651.08
22	609.16	609.18	609.20	609.22	609.24
23	588.98	589.00	589.02	589.05	589.07

RSR	**0.001**	**0.000**	**0.000**	**0.000**	**0.001**
NSE	**1.000**	**1.000**	**1.000**	**1.000**	**1.000**
PBIAS	**0.000**	**0.000**	**0.000**	**0.000**	**-0.001**
Peak %	**-0.002%**	**-0.001%**	**0.000%**	**0.001%**	**0.002%**

SWMM-TRANSPORT variation in flow area

Time (h)	-10%	-5%	0%	5%	10%
0	577.48	577.19	576.92	576.68	576.46
1	552.07	551.76	551.48	551.23	551.00
2	517.50	516.98	516.51	516.09	515.71
3	470.45	469.78	469.19	468.65	468.17
4	418.44	417.80	417.23	416.72	416.26
5	374.22	373.83	373.48	373.17	372.90
6	347.64	347.44	347.27	347.11	346.97
7	343.21	343.18	343.16	343.14	343.12
8	380.58	380.98	381.34	381.65	381.93
9	480.65	482.26	483.70	484.99	486.15
10	668.48	672.19	675.55	678.61	681.41
11	881.42	884.98	888.23	891.20	893.94
12	966.02	965.98	965.94	965.91	965.87
13	956.87	956.71	956.56	956.42	956.30
14	935.97	935.65	935.35	935.08	934.83
15	899.45	898.77	898.14	897.57	897.05
16	846.00	844.95	844.00	843.12	842.33
17	792.47	791.65	790.90	790.22	789.59
18	760.35	760.07	759.81	759.58	759.37
19	742.87	742.74	742.62	742.52	742.42
20	721.90	721.52	721.18	720.87	720.59
21	680.85	679.96	679.16	678.43	677.77
22	631.19	630.51	629.90	629.35	628.85
23	599.14	598.86	598.60	598.37	598.17

RSR	**0.011**	**0.005**	**0.000**	**0.005**	**0.009**
NSE	**1.000**	**1.000**	**1.000**	**1.000**	**1.000**
PBIAS	**0.006**	**0.003**	**0.000**	**-0.003**	**-0.006**
Peak %	**0.008%**	**0.004%**	**0.000%**	**-0.004%**	**-0.007%**

SEWSAN variation in roughness

Time (h)	-10%	-5%	0%	5%	10%
0	581.78	583.30	584.83	586.38	587.91
1	556.18	557.95	559.60	561.26	562.89
2	520.30	522.70	524.97	527.34	529.80
3	471.46	474.83	478.15	481.55	485.04
4	418.03	421.77	425.65	429.54	433.45
5	375.54	378.66	381.91	385.04	388.05
6	352.49	354.28	356.17	357.94	359.59
7	354.91	354.24	354.53	354.67	354.80
8	398.79	396.15	394.83	392.96	391.20
9	505.74	499.14	493.61	487.41	480.84
10	975.54	679.42	666.78	653.48	639.34
11	975.14	975.00	974.81	974.90	974.97
12	972.27	972.48	972.52	972.69	972.87
13	962.36	962.93	963.45	964.03	964.62
14	941.73	943.00	944.10	945.24	946.44
15	905.53	907.91	910.07	912.35	914.77
16	851.38	855.06	858.72	862.62	866.67
17	797.36	801.23	805.31	809.37	813.34
18	765.45	767.85	770.35	772.64	774.70
19	749.12	750.11	751.03	751.89	752.68
20	727.79	729.25	730.47	731.74	733.14
21	684.25	687.19	690.25	693.50	696.98
22	634.79	638.35	642.14	645.86	649.48
23	604.02	606.39	608.76	610.97	613.00

RSR	**0.309**	**0.018**	**0.000**	**0.019**	**0.038**
NSE	**0.904**	**1.000**	**1.000**	**1.000**	**0.999**
PBIAS	**-1.508**	**0.150**	**0.000**	**-0.141**	**-0.275**
Peak %	**0.074%**	**0.019%**	**0.000%**	**0.008%**	**0.016%**

SWMM-EXTRAN variation in roughness

Time (h)	-10%	-5%	0%	5%	10%
0	565.73	566.20	566.67	567.00	567.59
1	538.50	539.25	539.95	540.41	541.23
2	495.99	497.06	498.07	498.77	499.99
3	443.36	444.63	445.86	446.76	448.28
4	391.62	392.91	394.19	395.16	396.75
5	356.83	357.75	358.66	359.35	360.46
6	338.53	339.03	339.52	339.91	340.51
7	343.45	343.33	343.22	343.23	343.06
8	401.93	400.47	399.12	398.31	396.57
9	558.68	553.62	549.02	545.92	540.79
10	812.26	807.93	803.53	800.25	794.67
11	967.87	967.87	967.83	967.73	967.51
12	963.18	963.32	963.47	963.56	963.74
13	949.10	949.40	949.70	949.90	950.29
14	919.38	920.10	920.81	921.30	922.20
15	869.73	870.87	872.00	872.81	874.21
16	809.84	810.79	811.75	812.45	813.66
17	767.68	768.03	768.41	768.71	769.26
18	751.55	751.69	751.85	751.96	752.18
19	735.45	735.92	736.37	736.65	737.19
20	702.79	703.88	704.93	705.65	706.87
21	649.06	650.01	650.98	651.71	652.95
22	608.13	608.64	609.20	609.65	610.45
23	588.17	588.60	589.02	589.20	589.85

RSR	**0.015**	**0.007**	**0.000**	**0.005**	**0.014**
NSE	**1.000**	**1.000**	**1.000**	**1.000**	**1.000**
PBIAS	**0.034**	**0.018**	**0.000**	**-0.014**	**-0.040**
Peak %	**0.005%**	**0.004%**	**0.000%**	**-0.010%**	**-0.033%**

SWMM-TRANSPORT variation in roughness

Time (h)	-10%	-5%	0%	5%	10%
0	574.38	575.45	576.92	578.17	579.19
1	548.76	549.88	551.48	552.83	553.89
2	511.84	513.79	516.51	518.84	520.72
3	462.90	465.56	469.19	472.33	474.92
4	410.68	413.47	417.23	420.50	423.22
5	369.11	370.97	373.48	375.66	377.48
6	344.92	345.93	347.27	348.45	349.45
7	343.00	343.13	343.16	343.31	343.57
8	386.42	384.47	381.34	378.90	377.19
9	499.86	493.13	483.70	475.53	468.86
10	705.61	692.73	675.55	660.37	647.56
11	913.70	902.65	888.23	875.45	864.58
12	965.64	965.76	965.94	966.08	966.19
13	955.39	955.86	956.56	957.14	957.57
14	933.05	933.98	935.35	936.49	937.36
15	893.30	895.33	898.14	900.57	902.57
16	836.42	839.67	844.00	847.79	850.99
17	784.82	787.44	790.90	793.94	796.51
18	757.69	758.59	759.81	760.87	761.75
19	741.65	742.01	742.62	743.11	743.44
20	718.30	719.50	721.18	722.62	723.80
21	672.20	675.19	679.16	682.64	685.55
22	624.41	626.76	629.90	632.64	634.93
23	596.25	597.25	598.60	599.78	600.75

RSR	**0.048**	**0.027**	**0.000**	**0.024**	**0.044**
NSE	**0.998**	**0.999**	**1.000**	**0.999**	**0.998**
PBIAS	**-0.026**	**-0.015**	**0.000**	**0.014**	**0.027**
Peak %	**-0.031%**	**-0.019%**	**0.000%**	**0.015%**	**0.026%**

Appendix C: Unit hydrographs

Used with permission from GLS Consulting.

	Land use(s) following typical UH pattern														
	Very high Inc. Res.	High Inc. Res.	Medium Inc. Res.	Low Inc. Res.	Cluster	Flats	Bus_Comm	Educational	Gov_Inst	Industrial	Other	Farm_AH	None (eg. P.O.S)	Unknown	Large (per kl AADD)
Hour	Dimensionless flow ordinates (relative to hydrograph peak)														
1	0.15	0.17	0.15	0.09	0.15	0.15	0.08	0.08	0.08	0.09	0.08	0.17	0.00	0.09	0.09
2	0.08	0.10	0.09	0.05	0.09	0.09	0.07	0.07	0.07	0.07	0.07	0.10	0.00	0.07	0.07
3	0.06	0.05	0.07	0.06	0.07	0.07	0.06	0.06	0.06	0.06	0.06	0.05	0.00	0.06	0.06
4	0.05	0.05	0.05	0.19	0.05	0.05	0.05	0.05	0.05	0.05	0.05	0.05	0.00	0.05	0.05
5	0.05	0.05	0.15	0.49	0.15	0.15	0.06	0.06	0.06	0.06	0.06	0.05	0.00	0.08	0.08
6	0.11	0.44	0.77	0.80	0.77	0.77	0.08	0.08	0.08	0.10	0.08	0.44	0.00	0.25	0.25
7	0.67	1.00	1.00	0.83	1.00	1.00	0.15	0.15	0.15	0.47	0.15	1.00	0.00	0.69	0.69
8	1.00	0.91	0.98	0.93	0.98	0.98	0.34	0.34	0.34	0.68	0.34	0.91	0.00	0.95	0.95
9	0.87	0.94	0.73	1.00	0.73	0.73	0.83	0.83	0.83	0.84	0.83	0.94	0.00	1.00	1.00
10	0.85	0.84	0.66	0.96	0.66	0.66	0.94	0.94	0.94	0.93	0.94	0.84	0.00	0.89	0.89
11	0.82	0.74	0.72	0.89	0.72	0.72	1.00	1.00	1.00	0.94	1.00	0.74	0.00	0.87	0.87
12	0.71	0.59	0.65	0.75	0.65	0.65	0.98	0.98	0.98	0.89	0.98	0.59	0.00	0.83	0.83
13	0.56	0.48	0.61	0.71	0.61	0.61	0.94	0.94	0.94	0.75	0.94	0.48	0.00	0.60	0.60
14	0.50	0.41	0.57	0.74	0.57	0.57	0.89	0.89	0.89	0.81	0.89	0.41	0.00	0.59	0.59
15	0.46	0.40	0.63	0.76	0.63	0.63	0.88	0.88	0.88	0.95	0.88	0.40	0.00	0.53	0.53
16	0.44	0.38	0.66	0.73	0.66	0.66	0.92	0.92	0.92	1.00	0.92	0.38	0.00	0.53	0.53
17	0.41	0.39	0.70	0.70	0.70	0.70	0.84	0.84	0.84	0.89	0.84	0.39	0.00	0.47	0.47
18	0.38	0.48	0.68	0.66	0.68	0.68	0.35	0.35	0.35	0.66	0.35	0.48	0.00	0.37	0.37
19	0.45	0.53	0.72	0.59	0.72	0.72	0.22	0.22	0.22	0.35	0.22	0.53	0.00	0.28	0.28
20	0.49	0.52	0.70	0.51	0.70	0.70	0.15	0.15	0.15	0.22	0.15	0.52	0.00	0.24	0.24
21	0.45	0.51	0.68	0.38	0.68	0.68	0.12	0.12	0.12	0.17	0.12	0.51	0.00	0.20	0.20
22	0.50	0.49	0.57	0.26	0.57	0.57	0.11	0.11	0.11	0.14	0.11	0.49	0.00	0.16	0.16
23	0.40	0.42	0.44	0.18	0.44	0.44	0.10	0.10	0.10	0.12	0.10	0.42	0.00	0.15	0.15
24	0.29	0.28	0.22	0.13	0.22	0.22	0.09	0.09	0.09	0.10	0.09	0.28	0.00	0.13	0.13
	Unit hydrograph parameters (l ℓ/min)														
Hydrograph Peak	1.69	1.04	0.64	0.39	0.37	0.30	2.46	4.97	1.93	2.19	1.75	0.59	0.00	0.55	2.00
% of AADD	50%	55%	60%	75%	65%	75%	55%	55%	55%	55%	55%	60%	0%	55%	60%
Leakage & base flow	0.26	0.21	0.19	0.15	0.14	0.11	1.05	2.12	0.83	1.04	0.75	0.15	0.00	0.23	0.21

	Land use(s) following typical UH pattern														
	Very high Inc. Res.	High Inc. Res.	Medium Inc. Res.	Low Inc. Res.	Cluster	Flats	Bus_Comm	Educational	Gov_Inst	Industrial	Other	Farm_AH	None (eg. P.O.S)	Unknown	Large (per kl AADD)
Hour	Flows (ℓ /min)														
1	0.51	0.39	0.29	0.19	0.20	0.16	1.25	2.52	0.98	1.24	0.89	0.25	0	0.28	0.39
2	0.40	0.31	0.25	0.17	0.17	0.14	1.22	2.47	0.97	1.19	0.87	0.21	0	0.27	0.35
3	0.36	0.26	0.23	0.17	0.17	0.13	1.20	2.42	0.95	1.17	0.86	0.18	0	0.26	0.33
4	0.34	0.26	0.22	0.22	0.16	0.13	1.17	2.37	0.93	1.15	0.84	0.18	0	0.26	0.31
5	0.34	0.26	0.29	0.34	0.20	0.16	1.20	2.42	0.95	1.17	0.86	0.18	0	0.27	0.37
6	0.45	0.67	0.68	0.46	0.42	0.34	1.25	2.52	0.98	1.26	0.89	0.41	0	0.37	0.71
7	1.39	1.25	0.83	0.47	0.51	0.41	1.42	2.87	1.12	2.07	1.01	0.74	0	0.61	1.59
8	1.95	1.16	0.82	0.51	0.50	0.40	1.89	3.81	1.49	2.53	1.35	0.69	0	0.75	2.11
9	1.73	1.19	0.66	0.54	0.41	0.33	3.09	6.25	2.43	2.88	2.20	0.70	0	0.78	2.21
10	1.70	1.08	0.61	0.52	0.38	0.31	3.36	6.79	2.64	3.08	2.40	0.65	0	0.72	1.99
11	1.65	0.98	0.65	0.50	0.41	0.33	3.51	7.09	2.76	3.10	2.50	0.59	0	0.71	1.95
12	1.46	0.82	0.61	0.44	0.38	0.31	3.46	6.99	2.72	2.99	2.47	0.50	0	0.69	1.87
13	1.21	0.71	0.58	0.43	0.37	0.29	3.36	6.79	2.64	2.68	2.40	0.43	0	0.56	1.41
14	1.11	0.64	0.55	0.44	0.35	0.28	3.24	6.54	2.55	2.81	2.31	0.39	0	0.55	1.39
15	1.04	0.63	0.59	0.45	0.37	0.30	3.21	6.49	2.53	3.12	2.29	0.39	0	0.52	1.27
16	1.00	0.61	0.61	0.43	0.38	0.31	3.31	6.69	2.61	3.23	2.36	0.37	0	0.52	1.27
17	0.95	0.62	0.64	0.42	0.40	0.32	3.12	6.29	2.45	2.99	2.22	0.38	0	0.49	1.15
18	0.90	0.71	0.63	0.41	0.39	0.31	1.91	3.86	1.51	2.49	1.36	0.43	0	0.43	0.95
19	1.02	0.76	0.65	0.38	0.41	0.33	1.59	3.21	1.25	1.81	1.14	0.46	0	0.38	0.77
20	1.09	0.75	0.64	0.35	0.40	0.32	1.42	2.87	1.12	1.52	1.01	0.46	0	0.36	0.69
21	1.02	0.74	0.63	0.30	0.39	0.31	1.35	2.72	1.06	1.41	0.96	0.45	0	0.34	0.61
22	1.11	0.72	0.55	0.25	0.35	0.28	1.32	2.67	1.04	1.35	0.94	0.44	0	0.32	0.53
23	0.94	0.65	0.47	0.22	0.30	0.24	1.30	2.62	1.02	1.30	0.93	0.40	0	0.31	0.51
24	0.75	0.50	0.33	0.20	0.22	0.18	1.27	2.57	1.00	1.26	0.91	0.32	0	0.30	0.47
	Flow hydrograph volumes (ℓ/d)														
Regular flow	1090	697	507	313	293	238	1513	3057	1187	1490	1076	395	0	333	1210
Leakage & base flow	374	302	274	216	202	158	1512	3053	1195	1498	1080	216	0	331	302
TOTAL FLOW	1464	999	780	529	495	396	3025	6109	2382	2988	2156	611	0	664	1512
AADD	2929	1817	1301	706	761	528	5500	11108	4331	5432	3920	1019	0	1207	2520